AN ABSTRACT OF THE THESIS OF

Daniel L. Rowell for the degree of Master of Science in Wood Science presented on May 10, 2005.

Title: An Investigation into the Dynamics of RF LVL Pressing.

Abstract approved: Redacted for Privacy

Philip E. Humphrey

The dynamics of radio frequency (RF) laminated veneer lumber (LVL) pressing are explored for the purpose of optimizing this process. The RF LVL press at the Albany Trus Joist plant is the focus of this investigation. The investigation first focuses on bond strength development characteristics of the Georgia Pacific adhesive formula in use at the subject plant. The automated bonding evaluation system (ABES) developed by Dr. P. E. Humphrey is used in this study to determine the bond strength development rate of this adhesive. The second focus of the investigation is the development of a spreadsheet based, deterministic model of temperature, bond strength and vapor pressure development within the LVL veneer assembly during the pressing cycle. This tool may be used to conduct sensitivity studies to investigate changes that may effect the efficiency of the RF LVL pressing processing. The final focus of the investigation is capturing actual data from the subject press during operation in order to evaluate the deterministic model. The goal of this investigation is to provide information and tools to maximize the productivity of the RF LVL pressing process.

The study concludes that the deterministic model usefully predicts temperature and bond strength development within the veneer assembly over the course of the RF pressing cycle. It demonstrates that a spreadsheet format may be successfully employed for one dimensional deterministic modeling of the RF LVL pressing process.

An Investigation into the Dynamics of RF LVL Pressing

by

Daniel L. Rowell

A THESIS

submitted to

Oregon State University

in partial fulfillment of
the requirements for the
degree of

Master of Science

Presented May 10, 2005

Commencement June 2006

Master of Science thesis of Daniel L. Rowell presented on May 10, 2005

APPROVED:

Redacted for Privacy

Major Professor, representing Wood Science & Engineering

Redacted for Privacy

Head of the Department of Wood Science & Engineering

Redacted for Privacy

Dean of the Graduate School

I understand that my thesis will become part of the permanent collection of Oregon State University libraries. My signature below authorizes release of my thesis to any reader upon request.

Redacted for Privacy

Daniel L. Rowell, Author

ACKNOWLEDGMENTS

I owe a great debt of gratitude to Phil Humphrey, my advisor, for his guidance, encouragement, patience and friendship. If it were not for his creative approaches and encouragement, I would have been severely tempted to abandon this work.

I wish to express my sincere appreciation for the cooperation and assistance of the former Willamette Industries, Inc. and the new owners, Weyerhaeuser Co. I am also grateful to my fellow Associates at the Albany plant for their encouragement and assistance in obtaining the mill data for this research.

I am indebted to John Fiutak, my former supervisor and friend, for encouraging me to undertake this research.

Finally, I wish to express my deep appreciation to my wife, Jean, for her love, patience, self sacrifice, and encouragement.

TABLE OF CONTENTS

TABLE OF CONTENTS (Continued)

TABLE OF CONTENTS (Continued)

LIST OF FIGURES

LIST OF FIGURES (Continued)

LIST OF TABLES

APPENDIX TABLES

To my father, who taught me perseverance by example.

AN INVESTIGATION INTO THE DYNAMICS OF RF LVL PRESSING

CHAPTER 1
INTRODUCTION

The importance of engineered wood products has increased as the size and quality of logs from our nation's forests has decreased. The harvesting of old growth forests has, over the last half century, given way to fiber from second, third and even fourth growth forests (Schuler 2001). High quality engineered wood products can be produced by utilizing these forests of smaller diameter trees and their correspondingly lower quality fiber (Vlosky 1993).

Laminated veneer lumber (LVL) was first used to make propellers for World War II aircraft and other high strength wooden parts for aircraft (Baldwin 1995). Weyerhaeuser Corporation was the first to commercially market LVL in the early 1960's but the venture was very limited and did not succeed past the pilot operation and was later discontinued (Nelson 1997). Trus Joist Company began producing the Microllam® brand of LVL in 1968 using a proprietary (US Patent office 1973) continuous pressing process (Leichti 1989, Nelson 1997, Vlosky 1993). Trus Joist used LVL as high strength flange material for wooden I-joists. This was an improvement over the solid sawn flange material because it had a significantly lower coefficient of variation and it solved the problem of the short supply of high quality machine stress-rated lumber (Kunesh 1976). They also began selling LVL as beam and header product. Later on, LVL scaffold plank and concrete formwork were also successfully marketed (Kunesh 1976). Although Trus Joist continues to be the world's leader in the production of LVL, several other producers are marketing the product in the US and world wide (Nelson 1997). In 2000, it was reported that annual production of LVL had grown to 52 million cubic feet in North America (Schuler 2000).

The use of engineered wood products continues to increase in structural applications in world markets for several reasons as noted by Schuler (2001). He states that on an installed cost-value basis, engineered wood products are becoming more economically attractive in the face of increasing prices for high quality lumber from large diameter logs. Schuler (2001) further notes that the worldwide movement to performance-based building codes makes it easier to introduce new engineered lumber building products. Schuler also comments that the usage of engineered lumber products results in labor saving construction technologies which become increasingly important with the rising average age of the labor force in North America, Europe and Japan. Additionally, Schuler suggests that the superior performance and predictability of engineered lumber products is leading to the growing popularity of LVL with architects and builders when specifying construction materials. Use of these products helps them to avoid costly litigation, no doubt due to the high quality standards and techniques employed in the production of these products. A final reason Schuler gives for the increase in the use of engineered wood products is the rising world wide demand for clean air and water and for healthy, sustainable forests, as the world's standard of living increases. For these reasons Schuler has an optimistic outlook for the future of engineered wood products.

The present study concerns the manufacture of LVL using radio frequency (RF) hot pressing technology. Traditionally, LVL is formed by gluing uniaxially oriented veneers together using a thermosetting resin. Consolidation and heating are usually effected in a hot press. Most hot presses have heated platens that press against the veneer assembly. The mechanisms of thermal conduction and, to a much lesser degree, migration of thermally generated within-void vapor (convection) are mainly responsible for the transfer of heat to the resin lying at interfaces of the veneers throughout the veneer assembly. Such heat transfer within the veneer assembly is a relatively slow and inefficient process however, especially since wood veneers have low fluid permeability compared to that of particulate panel products (such as MDF, OSB and the like). The convective component therefore contributes relatively little to the heating of veneer-based panels. The conventional hot pressing process is, however, widely used and produces consistent results and valuable products.

Considerable attention has been devoted to the dynamics of hot pressing wood based composite panels (Humphrey 1982, 1997, Humphrey and Bolton 1989, Zavala 1987, Zavala and Humphrey 1996, Bolton and Humphrey 1988, 1989a, 1989b, 1994, Wellons 1982). These studies have shown that there is a complex spatial and time-based interaction of physical processes, including the following:

1) Heat and moisture transfer
2) Bond strength development, and
3) Rheology (change in form, density, and residual micro-stress).

An alternative method of transferring heat to glue lines is by the use of dielectric heating. This technology is not new, though it now is being used in new applications. The dielectric heating method works on a fundamentally different principle than that of conventional hot pressing. The application of electromagnetic energy to the veneer assemblies in the form of radio frequency waves (or microwaves) can result in heating throughout the veneer assembly's cross-section.

The dynamics of the dielectric heating and curing process are not as well understood as are the dynamics of the conventional hot pressing method. Dielectric heating involves all the physical processes of hot pressing plus the electromagnetic transfer of energy to the load. An objective of the present study is to explore these physical processes and their interaction in order to gain a better understanding of the dielectric LVL pressing process. This is done with a view toward maximizing production efficiency. The study will be confined to RF. Microwave heating is also being used in some presses but it is beyond the scope of this study; the subject plant is of the RF type.

The study will focus on the LVL RF press in operation at the Weyerhaeuser Trus Joist facility in Albany, Oregon, referred to hereafter as "the subject plant". A better understanding of the dynamics of the RF pressing process may lead to more efficient operation of this production press. There may be opportunities to reduce press cycle times and possibly reduce the amount of defective product produced.

This study will focus on three main tasks:

- Quantify the isothermal bond strength development characteristics of the adhesive currently in use at the subject mill.

- Develop a spread sheet-based, deterministic model to estimate temperature, vapor pressure and bond strength development over time as the veneer assembly is being consolidated in the press. This deterministic model will incorporate RF heating as well as simultaneous heating from the hot platens. The main purpose of the model is to provide a tool that helps in understanding the effect that diverse process and raw material parameters have on production efficiency. Of particular interest at the outset will be the effects that veneer moisture content, platen temperature, and RF power have on temperature rise, within-void vapor pressure development, and bond strength development within the veneer assembly throughout the pressing process.
- Verify the accuracy of the deterministic model by taking actual measurements of temperature and vapor pressure during the industrial pressing process.

Before addressing the above, relevant literature is reviewed in Chapter 2.

CHAPTER 2
A CRITICAL LITERATURE SURVEY

2.0 INTRODUCTION

The discussion that follows emphasizes aspects of the LVL production process that are relevant to the goals of the project – principally material behavior and internal conditions that are generated during the RF pressing process. Included, therefore, are discussions of the characteristics of veneer and adhesive that makes them suitable for use in LVL production, and of the mechanical processes used to produce LVL. Literature is also surveyed which discusses the use of RF heating in general theory and specifically in wood heating applications. The physical pressing mechanisms are surveyed with attention to heat transfer, vapor generation and movement, adhesive considerations, and veneer assembly consolidation. This will be followed by a review of numerical modeling of the physical pressing mechanisms. Some of the characteristics of the finished product will be summarized.

2.1 LVL MANUFACTURE

This section addresses veneer, adhesive, and mechanical processes used in the manufacture of LVL.

2.1.1 Veneer

Rotary peeled veneer is the major component of LVL, and its structure and properties influence its response to conditions generated in the RF pressing process, as well as product properties. There are a number of general works that provide a broad overview of rotary peeled veneer production (Baldwin 1995, Haygreen 1996, Tsoumis 1991).

Most veneer used in LVL is peeled from preconditioned peeler blocks. Baldwin explains that preconditioning with heat and moisture softens the peeler block and this aids peeling. This is due to the combined effects that heat and sorbed moisture have on the visco-elastic properties of cell wall material (Thömen 2002). Of special interest is the advantage of smoother peel and finer checking. Baldwin (1995) cites the work of Resch and Parker (1979) who noted that smoother veneer allows adhesive spreads to be reduced, presumably because the smoother surfaces make better intimate contact and there are fewer voids for the adhesive to fill.

Tsoumis (1991) notes that almost all softwood veneer, including that for LVL, is produced by means of the rotary cutting method. The production of good quality veneer is a result of setting up the lathe properly, including the peripheral cutting speed, knife geometry and sharpness, knife angle, spacing between knife and pressure bar, and the shape of the nose bar and the pressure applied. Research by Cade and Choong (1968) concluded that the faster the cutting speed, the lower the tensile strength across the grain. They determined that this effect is related to the depth of lathe checks generated in the veneer. This effect may be due in part to the viscous component of the material's mechanical properties; rapid application of stress at the knife decreases the opportunity for stress dissipation and increases stress intensity at the advancing crack front. Counteracting this effect is the increased localized frictional heat generation which can result in softening of the wood material at the knife edge (particularly when the cell wall material is water saturated.)

Surface roughness of softwood veneer has been demonstrated to have a significant effect on gluability. The research of Collett (1972) and Faust and Rice (1986) revealed that rough veneer is difficult to bond because of the difficulty in achieving intimate contact between the veneers. They also found that rough veneer surfaces promote adhesive over-penetration and associated "dry-out".

Drying of the veneer is another aspect that has an effect on the quality of veneer used in LVL manufacture. Tsoumis (1991) indicates that the typical target oven dry moisture content for veneer is 2% - 8%. He notes that high moisture content can result in weak joints as well as delaminations due to the generation of excessive within-pore vapor

pressure during the pressing process. Conversely, over drying the veneer inhibits wettability of the veneer, preventing the entrance of the adhesive into the veneer's cellular substructure.

One other aspect of veneer drying that may effect the gluability is surface inactivation. This is the thermally induced chemical modification of veneer surfaces (or indeed, the whole structure) which reduces the availability of reactive sites for adhesive wetting and subsequent bonding. Surface inactivation is usually induced when drying veneer. Tsoumis (1991) comments that veneer dried above 160°C results in surface inactivation. Wellons (1979) studied this issue and noted that previous studies did not focus on the behavior of phenolic adhesives at elevated temperatures. In his study, he concludes that poor wettability did not inhibit the gluability of the veneer with phenolic adhesive under hot-press conditions. However, he did note that on very dry veneer, over penetration produced dry-out. Both authors seem to agree that over-dried veneer can be a source of poor bonding in hot-pressing. The chemical nature, kinetics, and consequences of this phenomenon seem to be poorly understood. Much reported work is of an empirical nature. There is a need to adopt an analytical approach in which the nature of the chemical changes is identified and the effect that time, temperature, and moisture have on them is quantified.

In his discussion of veneer used in LVL, Baldwin (1995) describes how it is graded for maximum efficiency of utilization. Veneer is visually graded as it leaves the dryer. It is visually graded in compliance with the C and D veneer grades described in Product Standard PS-1-74 for softwood plywood (Kunesh 1976). The current standard (PS 1-95 US Product Standards 1995) differs little from that used in the earlier publication. The standard sets the maximum size and types of defects allowed in the veneer. Until recently, this visual grading was done manually. Optical scanning technology has now been successfully, and widely, introduced to accomplish the visual grading of the veneer (Logan 2000).

In addition to visual grading, veneer used in LVL production is electronically graded to estimate strength characteristics of each sheet of veneer. It has been demonstrated that it is possible to sort veneer sheets into strength categories using ultrasonic

propagation time (UPT) as an indicator of strength and stiffness (Kunesh 1978). Metriguard, Inc. of Pullman, WA has developed technology for measuring the UPT of veneer leaving driers at production speeds. Logan (2000) explains that the machine has a wheel which contains a transmitter and another wheel containing a receiver. As the veneer travels under the wheels an ultrasonic pulse is sent between the wheels which are at a pre-determined distance from each other. The sound waves travel longitudinally through the veneer and are timed to determine their velocity. Sound pulses are sent at the rate of 120 to 200 pulses/sec. The strength category is determined by averaging the sound velocity of the pulses timed for each sheet. The sheets can then be marked according to their strength category. Jung (1979) realized that if the veneer could be pre-sorted by its strength properties, a manufacturer could have significant control over the strength properties of the finished LVL and thereby more efficiently use the veneer resource. Baldwin (1995) reported that this method of veneer grading is widely utilized among LVL producers.

Recent research has been conducted to use UPT grading prior to drying. If this can be done there may be opportunities to improve productivity at the driers by drying veneers of similar strength and stiffness together (Bradshaw et al. 2002), and potentially discarding deficient pieces.

Metriguard, Inc. in recent years had taken the UPT grading process one step further. Based on the work of Finnish research (Vainikainen et al. 1987), Metriguard has developed the technology using Radio waves to determine oven dry moisture content and density of the veneer. By compensating for veneer temperature they are able to compute Modulus of Elasticity (MOE) in addition to UPT, density, and moisture content (Logan 2000). This method could significantly enhance the pre-grading of veneer used for LVL production.

Another method of nondestructive evaluation of the quality of veneer focusing on lathe check depth and knots has been explored by Wang et al. (1998). They experimented with impact-induced stress wave techniques and an ultrasonic method. By taking measurements parallel and perpendicular to the grain in the orthogonal direction, they found a correlation between the presence of knots and lathe check depth ranging from an

r^2 value of 0.39 to 0.50 in their regression models. They recognized that conducting these measurements under production conditions would be difficult and further research would be needed to make it practical. Since lathe check depth and the presence of knots are major factors in the performance of veneer in LVL this method may, however, hold promise as an improved grading method in the future.

Scanning the dielectric properties of wood for defects as a grading method has been explored by Forrer and Funk (1998). They demonstrated that it is possible to detect defects such as knots, pitch pockets, open holes etc. using this method. Further development will be required to determine if this could be implemented successfully in production settings.

To sum up, high quality LVL veneer is carefully rotary peeled, dried and graded both visually and electronically, in order to produce LVL that consistently meets strength and stiffness requirements and makes efficient use of the veneer supply.

2.1.2 LVL Adhesive

Phenol-formaldehyde adhesives are the principle bonding agents used in LVL pressing (Baldwin 1995, Haygreen 1989). Such an adhesive is used in the plant which is the subject of the present investigation. This is due to its strength, durability, low formaldehyde emissions rate and relatively low cost (Zavala 1986, Johnson 2000).

Pure phenolic resins produce bonds that are stronger than is necessary for the wood being bonded. Therefore, less costly fillers and extenders are added to reduce the cost of the adhesive. Fillers serve mainly as a bulking agent to control adhesive viscosity. The main purpose of extenders is to build and maintain a uniform viscosity and to hold the adhesive on the surface of the wood (Neese 1997, Stone 1977).

In order to reduce curing time, caustic soda catalyst is normally added to liquid PF resins. The proportion of caustic soda varies between 0.1% and 1.0% of the weight of the phenol (Whitehouse 1955). Caustic soda has a strong ionic charge. Therefore, it has a significant impact on adhesive performance in radio frequency LVL pressing. This will

be discussed more fully later in this present study. Similarly, bond strength development kinetics will be discussed in 2.4.3.

2.1.3 The LVL Pressing Process

The purpose of this section is to review literature pertaining to the processes used in LVL production. Pressing mechanisms of heat transfer, vapor generation, adhesive curing and consolidation of the LVL veneers will be discussed in Section 2.4

In his discussion of LVL assembly systems, Baldwin (1995) identifies two major categories: batch systems and continuous systems. He describes batch systems as those in which end-glued veneers of a specified length up to 18.3 m are coated with adhesive and stacked in layers and then placed in a pre-press as a complete unit. Later, they are loaded into the hot press for curing. Continuous LVL systems are described as those in which adhesive-coated sheets are delivered to a mechanism that extends and retracts as it places the veneer in alignment with the previously laid sheets and overlapping the veneer ends a set distance.

There is no distinction made by Baldwin (1995) between continuous presses that are continuously moving forward (Graf 1999) or are moving forward in short time intervals (U. S. Patent Office 1973), and those which move forward the full length of the press platens after the cure of that section is completed. This is the case with the subject press. Perhaps this type of press should be called a "continuous-batch" press since it has features of both types of presses.

The methods for obtaining the required temperature for curing thermosetting adhesives include: hot platens only, hot platens and microwave energy, hot platens and radio frequency energy. Some experimentation with steam injection techniques (Annett 1991, Baldwin 1995, Graf 1999 Troughton 1999) has also been completed.

The use of hot platens has long been the main method of heating the veneer in plywood and much of early LVL pressing. The platens may be heated with hot oil or high pressure steam circulating through the platens. Some presses also use electrically heated platens. The heat must migrate from the hot platens through the plies of the ve-

neer to the middle of the veneer assembly. Wood is a relatively poor conductor of heat (typically in the order of 0.1 W/m/°C). Therefore, this method is the slowest method of providing the required heat to the core of the veneer assembly (Annett 1991, Troughton 1999).

The Dieffenbacher GmbH & Co. of Germany has developed an LVL pressing system incorporating microwave pre-heating. It is reported that this system achieves a 40% to 50% reduction in pressing time over conventional hot platen pressing (Graf 1999). The microwave energy is applied to the LVL veneer assembly just before it enters the press. The microwave applicator is designed to focus most of the microwave energy into the middle of the veneer assembly, raising the core temperature to about 71°C (Graf 1999). As the veneer assembly moves through the continuous press, the veneers are pressed intimately together and adhesive cure is completed by the addition of heat from the hot platens in zones of decreasing temperature along the length of the press (Graf 1999).

In the early 1990's Durand-Raute Industries, Ltd. (now Raute Wood Ltd.) of Canada teamed up with Thermex-Thermatron, Inc. of California to develop an LVL continuous-batch pressing system that incorporates Radio Frequency (RF) heating of the LVL veneer assembly in the press. Research conducted by Annett and Browning (1991) concluded that, compared to a double opening press line with conventional (hot platen) heating, a single opening press with RF heating could produce 38% more LVL annually. In contrast to the Dieffenbacher microwave system which heats the veneer assembly prior to its entering the press, they explained that this system applies the RF energy to the veneer assembly after it is in the press and under pressure. Most testing was conducted with the press platens heated to 149°C. However, Annett and Browning reported that they successfully conducted tests with four press loads with the platens at 21°C leading them to believe that this could be duplicated in mill production. This is discussed further in Sections 2.3.3 and 5.4.

Troughton (1999) reported on a pilot plant research trial using steam-injection for LVL production that recorded a 32% reduction in pressing time on 13 plies of 3.2 mm thick veneer (a spruce, pine, fir species mix). He further noted that steam-injection

pressing technology has been successfully used for many years for thick composite products such as particleboard and medium density fiberboard. Saturated steam is applied to the veneer assembly from both platens at a pressure of 0.57 MPa while it is under platen pressure in the press (Troughton 1999). This technology may be a very cost effective way of increasing press output when compared to the capital expense of other available technologies suggests Troughton. The low fluid permeability of veneers compared to that of particulate composite mats may however, limit the effectiveness of steam injection LVL pressing.

2.2 CHARACTERISTICS OF LVL

LVL is formed with uniaxially oriented veneers to optimize its structural properties in the longitudinal direction. In many respects, LVL is like solid-sawn lumber because of this parallel grain orientation. The main uses for LVL are for beam and headers, scaffold planking, and flange stock for wood I-joists. LVL is classified as a member of the structural composite lumber (SCL) group as defined by ASTM D5456-00. These products combine wood fiber with exterior structural adhesives to form large billets which are usually ripped to smaller dimensions for specific applications (Nelson 1997). The following is a brief summary of the three outstanding characteristics of LVL.

2.2.1 Reduced variation of mechanical strength properties

In the late 1960's and the 1970's, research with laminated rotary peeled veneer revealed that tensile strength could be significantly improved and the variability of mechanical strength properties reduced when compared to equivalent solid sawn material (Bohlen 1974, Echols 1973, Kunesh 1978, Koch 1966, Koch 1968, Moody 1972). In solid sawn material, strength reducing defects (knots, slope of grain, etc.) impact a much larger percentage of the cross section than similar strength reducing defects randomly distributed among the thin veneer in the LVL cross-section (Nelson 1997). The standard

deviation of the mechanical properties of wood laminates is, in general, proportional to the reciprocal of the square root of the number of plies in the veneer assembly cross section (Sasaki et al. 1990). The coefficient of variation for strength and stiffness properties typically ranges from 10% to 15% for LVL compared with 25% to 40% for structural grades of sawn lumber and timber. Because of this consistency, the allowable design stresses for most LVL are higher than those for solid sawn lumber (Nelson 1997, Kunesh 1978).

2.2.2 Dimensional stability and size

Because of the multi-veneer construction of LVL and it's relatively uniform and low in-service moisture content (6% - 12%) it is more dimensionally stable than solid sawn lumber (Nelson 1997, Haygreen 1996). Sawn lumber may bow, crook, twist and cup. Warpage in LVL, on the other hand, is limited to cupping across the width due to unequal moisture content on opposing plank surfaces of the LVL (Nelson 1997).

Laminated veneer lumber is made up of many relatively small lengths of veneer, which is typically manufactured in lengths to 24 m or more, thicknesses to 90 mm or more and widths to 1.2 m or more (Haygreen 1996, Vlosky 1993). This makes LVL very attractive when long lengths of straight, clear lumber are needed. It is especially well suited for use as wood I-joist flange material (Leichti 1989). The LVL may be trimmed (in batch presses) or cut (in continuous presses) to the required length to meet customer needs, thus reducing waste and manufacturing costs.

2.2.3 Log utilization

Kunesh (1978) stated that log yield may increase from 25% to 50 % when it is peeled for use in LVL as opposed to it being cut into sawn lumber. Nelson (1997) suggests a 30% increase in log utilization for LVL versus sawn lumber. This takes into ac-

count sawn lumber losses due to squaring round logs and saw kerf to cut to the lumber from the log.

Use of log for LVL manufacture can also represent a better utilization on the log in another way. As stated earlier, the veneer utilized in structural LVL is pre-sorted into grades by electro-mechanical means. By selectively applying these grades of veneer in the lay-up pattern, the producer can control the range of stiffness and strength properties in the LVL (Logan 2000, Jung 1979). The positions of the grades of veneer in the cross-section of LVL are important. Putting the higher grade veneers on the outside plies provides greater flexural strength than if the lower grade veneers were on the outside (Baldwin 1995, Koch 1966). This is especially true in the plank orientation where the greatest stresses are formed in tension and compression on the outer plies of the LVL. Thus, by pre-grading the veneer and strategically placing it in the veneer assembly, the wood fiber in the log is used to its greatest advantage. A significant amount of lower quality veneer can be utilized in the core plies to produce a high strength product.

2.3 RADIO FREQUENCY HEATING

Radio Frequency (RF), or dielectric, heating was observed as early as 1859 by von Siemens when he measured the heat produced in Leyden jars (early capacitors) which he charged and discharged with alternating current (Feldenkirchen 1994). D'Arsonval and Tesla are said to have been the first to recognize the significance of RF heating around 1890 (Mark 1986). The first significant uses of dielectric heating were in the medical field in the early 1900s. It was used to for gentle heating of deep body parts and called diathermy (Mark 1986). However, the main focus until the 1930's was on how to prevent dielectric heating in electrical insulation and electrical components (Hartshorn 1949).

Cable (1954) reports that the first industrial use of RF heating was in an experimental installation for the removal of moisture from tobacco after it is had been packed in hogsheads (large casks, up to 530 l). He notes that though this had very limited application, it was the "sparkplug" which fired up interest in RF heating for other applications

because it demonstrated that RF was able to heat through the entire volume at once and did not rely on thermal conduction from the outside. Significant industrial usage began in the new and fast growing plastics industry, followed quickly by development for use curing thermosetting adhesives for wood based board laminating and edge-bonding. RF heating was later employed for the laminating of thin veneers in curved molds (Cable 1954). It should be noted that these applications were all small in size and of low power consumption in comparison to the press which is the subject of this present study.

Now that the historical perspective has been set, the remainder of this section will focus on literature related to the general theory of RF heating, and of RF applications in the wood products industry and LVL applications in particular.

2.3.1 Theory of Radio Frequency (RF) Heating

Radio frequency heating results from the conversion of electromagnetic energy into heat within a dielectric material that is subjected to a high frequency electromagnetic field. The dipolar molecules (molecules with a definite positive or negative charge at the end) are agitated as they move to align themselves with the changing polarity of the electromagnetic field. The resultant agitation of the polar molecules and their propensity to resist or lag the aligning field leads to the generation of heat in the dielectric material (Annett 1991).

Dielectric materials are normally electric insulators or very poor conductors – such as glass, paper or wood. If the dielectric material contains molecules with polar charge distributions, thus having permanent dipole moments, these molecules are normally randomly oriented (Tipler 1982) but satisfy localized spatial stability criteria. Tipler (1982) explains that in the presence of an electromagnetic field, such as that generated between two press-platens, these dipole moments experience torque that tends to align them with the direction of the field. This arrangement is represented simplistically in Figure 2.1. The extent of alignment for a given material type depends on the strength of the electromagnetic field and the material's temperature. Tipler points out that at higher temperatures the random thermal motion works against the torque applied by the electromagnetic

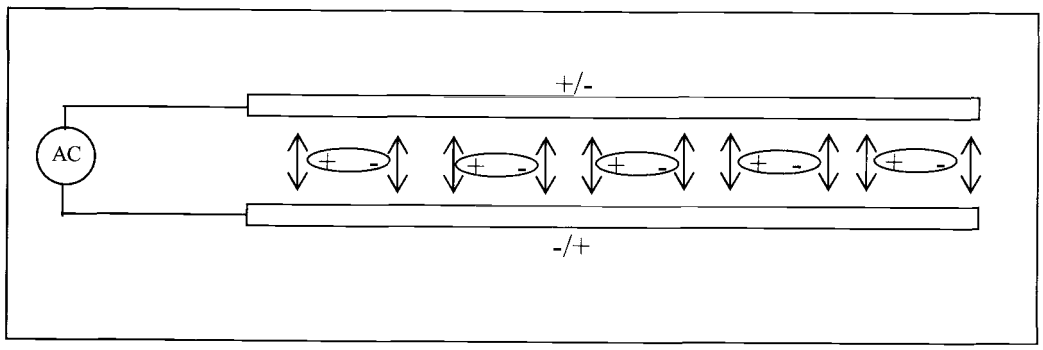

Figure 2.1 A simplified schematic illustrating the movement of dipolar molecules within an RF field. As the polarity of the charge on the plates change, the molecules move to realign themselves to the new polarity.

field. More energy is therefore dissipated from the electromagnetic field in the dielectric material. To a point, the hotter the dielectric material, the more energy it will absorb from the RF field, causing the temperature to rise faster.

Orfeuil (1987) notes that atoms within non-polar molecules, or atoms alone, are also effected by electromagnetic fields and that the negatively charged electrons within them are attracted to the positively charged plate or platen and the positively charged protons are attracted to the negatively charged plate or platen. This results in the distortion of the atoms and molecules from their normal condition. Tipler (1982) further demonstrates how field-induced torque, working to align dipolar molecules and distort non-dipolar ones, weakens the applied field. Work is expended to move molecules towards alignment and to internally distort non-polar molecules. These effects also increase the charge storing potential, or capacitance, of the plate pair because the dipole molecules return energy to the system when the electromagnetic field collapses; dipoles tend to rotate back to their equilibrium positions. Mark (1986) points out that the degree of polarization, and the energy required to achieve it, also control the loss factor or dissipation factor of a material; these terms are discussed below.

The dielectric constant of a material is expressed as the ratio between two capacitance values: that with air between the plates compared to that with the subject material interposed (Brown 1947). This can be expressed mathematically as:

$$\kappa = \frac{V_D}{V_O} \tag{2.1}$$

Where: κ = Dielectric Constant (may also be denoted as ε')

V_D = Voltage across the capacitor with the dielectric separating the plates

V_O = Voltage across the capacitor with air separating the plates

The dielectric constant ranges between unity and about 80, with water being near 80 and formaldehyde adhesives being around 4 to 6 (Mark 1986). Oven-dry wood at room temperature has dielectric constants from 2 to 5. Dielectric values of wood vary with frequency, temperature, and moisture content (U. S. Forest Products Laboratory 1972). When voltage, frequency, and all other factors remain constant, an increase in dielectric constant causes greater power to be delivered to the dielectric material (Mark 1986). However, the earlier work of Hartshorn (1949) states that the dielectric constant of a material gives no indication of the heat it will generate in an electric field. He maintains that it is the loss angle δ which is the most important indicator of the heat that will be generated in the dielectric in an RF field.

An ideal capacitor would have a high dielectric constant and, when discharged, it would return all of the electrical energy that was applied to it in charging (Langton, 1949). In reality, capacitors never realize this ideal. There is always some energy dissipated in the form of heat. Most of the energy loss occurs in the dielectric (Terman 1947). This loss of energy into the dielectric is the basis of RF or dielectric heating.

In a purely capacitive circuit, without any loss in the dielectric material, current precedes voltage by 90° of phase shift. In reality, the phase difference is always something less than 90° because there is always some loss, even if it is very minor (Terman 1947, Orfeuil 1987). Figure 2.2 portrays this graphically. At radio frequencies of roughly 10 KHz to 300 MHz (Orfeuil 1987), dielectric materials do not discharge all of their electrical energy back into the circuit when the electrical potential drops to zero across the capacitor plates before they begin charging in the opposite polarity. This lag,

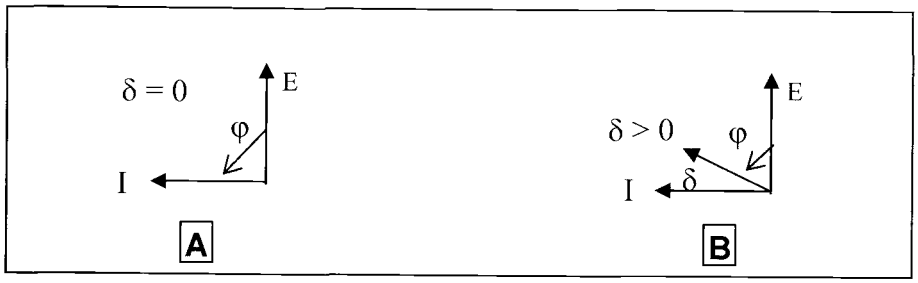

Figure 2.2 - Vector diagram of electric field strength and displacement current in the dielectric. I = current E = voltage δ = loss angle φ = current phase angle with respect to voltage. Drawing A represents the perfect dielectric in a capacitance circuit. Drawing B represents an actual dielectric in a capacitance circuit.

which is out of phase with the capacitive current, is due to the nature of the dipolar molecules discussed previously, as well as ionic conduction through the dielectric material (Brown 1963, Hartshorn 1949, Metaxas 1996). This lag represents energy that is absorbed by the dielectric material resulting in heat. The greater the loss angle δ, the greater the heating effect in an RF field. The product of tan δ and the dielectric constant is termed the loss factor, loss index or dissipation factor (Mark 1986).

Metaxas (1996) maintains that at radio frequencies resistive ionic conduction losses dominate the loss mechanism in dielectrics and should, therefore, be separated in calculations. Hartshorn (1949), however, observes that resistive heating need not be considered separately because its only effect is to increase the loss factor which is already accounted for. This can be seen in the dielectric power absorption formula (2.2).

The formula for calculating the power absorbed in a dielectric material is given by Orfeuil (1987) and in similar forms by others (Biryukov 1961, Harthorn 1949, Brown 1947) as:

$$P_{W/cm^3} = 5.56*10^{-12} f V^2 \varepsilon_r \tan \delta \qquad (2.2)$$

Where: P = Power (Watts / cm^3)

f = Frequency (Hz)

V= Electrical potential across the capacitor plates (volts)

ε_r = Relative dielectric constant (a.k.a. relative permittivity) (--)

δ = Loss angle

(Note: $5.56*10^{-12} = 2\pi * 0.08855*10^{-12}$ (*dielectric constant of free space*))

As one can see from this equation, there are several factors that can be adjusted to effect the desired rate of heating in a given dielectric material. Each factor shall be discussed briefly.

Frequency is a relatively easy variable to control in an RF heating system, Mark (1996) comments. However, he also notes that it has the following limitations. At certain frequencies, the material being heated can develop "standing waves", where reflected radio waves can reinforce the original wave in a specific area of the dielectric material and cause it to over heat while other areas remain below the target temperature. This is a more significant problem with large electrode plates (Orfeuil 1987) like the ones in the press that is the focus of this study. The use of inductive stubs can be an effective way of dealing with this problem (Mark 1986, Metaxas 1996). Another limitation on the frequency is that there are national regulations and international treaties that restrict industrial usage of radio waves to a limited number of frequencies or else additional shielding is required. A final limitation that Mark (1986) notes is that the higher the frequency required from the generator, the higher the cost per kilowatt of capability, because of the high cost of the components of the equipment that are required.

Because the electrical **voltage** across the plates of the capacitor is a squared factor it has a greater impact on the amount of energy absorbed by the dielectric material than a comparable variation in the loss tangent, the relative dielectric constant or the frequency. The upper limit of the RF voltage density that may be utilized in RF heating is determined by arcing according to Mark (1986). This may be arcing within the RF generator apparatus or arcing through the dielectric material itself if the breakdown voltage is exceeded. The most common form of arcing experienced with the subject press is on the outside edge of the laminated veneer due to excessive adhesive creating a short circuit across the platens. Most dielectric heating equipment operates with an electric field of 80 and 300 V/mm according to Orfeuil (1987). The subject press at the Albany Trus

Joist plant normally operates well below this range. Higher voltage gradients result in an unacceptable amount of arcing through the laminated veneer.

As stated earlier, the **loss factor** is the product of the **dielectric constant** and the **loss tangent**. The dielectric constant is a function of the properties of the dielectric material and is not easily changed. However, the loss tangent can be increased by adding material with strong ionic charges such as salt (Metaxas 1996) or caustic soda to the dielectric material to be heated. Biryukov (1968) reports that his attempts to increase the intensity of dielectric heating by adding various substances (salt, carbon black, metal shavings, etc.) to the adhesive were unsuccessful. He concluded that the additives only changed the conductivity of the adhesive but not the dielectric loss properties. If the material becomes too conductive as a result of these additives, it may promote undesirable arcing (Klemarewski 1995).

Resnik (1996) cites the research of Kröner and Pungs (1953), James (1997), and Pound (1959) who demonstrated that in wood, it is the moisture content which has the greatest influence on its dielectric constant. When is comes to the loss tangent, Vermaas et al. (1974) notes a peculiarity about wood. Between 0 and 8% MC, the loss tangent increases sharply. Between 8 and 20% MC, the increase is more gradual. For MCs from 20 to 30%, the loss tangent increases sharply again. Above 30% MC there is little change. The reason for this peculiarity is not clearly understood. The research of Lin (1973) reveals a relationship between MC and frequency, where the higher the frequency the greater the influence of MC on the loss tangent.

It is noted here that RF energy is absorbed as the RF wave penetrates through the dielectric material and there are formulas for calculating this loss. However, with dielectric heating RF's penetration is generally greater than 1 m and may be 10's of meters (Orfeuil 1987, Metaxas 1996) depending on the frequency and the dielectric properties of the material. The present study is limited to dielectric material less than 4 cm in thickness, and therefore this aspect is of very limited importance and this will be the limit of its discussion in this work.

2.3.2 RF heating applications for wood

RF heating has been successfully employed in a number of applications in the wood products industry. It is particularly well suited to use in wood products applications because it penetrates throughout the wood assembly instantaneously without having to rely on thermal conduction or mass transfer to carry the heat to the core. This enables the rapid cure of thermosetting adhesives within the assembly (Klemarewski 1995). In fact, the work of Biryukov (1968) demonstrated that the adhesive within the assembly actually generates heat faster than the surrounding wood.

Cable (1954) lists three general classifications of wood bonding with thermosetting adhesives where RF heating has had wide application: 1) edge bonding (esp. furniture) where boards or thin sheets are bonded at their edges to form large slabs; 2) boards (laminated beams) or veneers (face veneers, plywood and LVL) are bonded together on their flat surfaces, which is the focus of this study; and 3) joining (esp. furniture) where wood is bonded at localized joints. A fourth classification for RF application, of curing the adhesive in particle, flake and fiber boards, is given by Orfeuil (1987) and Annett (1991). Annett comments that in recent years the use of RF heating for flake and fiber boards has declined due to the advent of continuous pressing systems and new technologies such as steam injection.

2.3.3 Radio Frequency LVL Production

RF heating in LVL production was developed in the early 1990's with the collaboration of Thermex-Thermatron, Inc. (a manufacturer of RF generator equipment) and Durand-Raute Industries, Inc. (a manufacturer of LVL presses, now known as Raute-Wood, Inc.) on research into LVL RF pressing at Washington State University, Pullman, WA under the direction of Tom Maloney (Annett 1991). Maloney's research was conducted using a press equipped with 1.3 m x 1.3 m platens heated with hot oil and coupled with a 20 KW capacity RF generator. This initial research demonstrated that LVL produced

with RF heating was equivalent to LVL produced conventionally with hot platens in terms of short span shear, bending stiffness (MOE) and bending strength (MOR).

Maloney reported that the center glue line temperature, measured with a fiber optic probe, reached 100°C in 3.6 minutes utilizing RF heating at a power level of 18.84 kW/m² with the platens at 149°C. Maloney used the same RF power level with the platen temperature reduced to 121°C. It took 4.2 minutes for the center glue line temperature to reach 100°C at this platen temperature. Maloney reported that the control group, without the RF power input and with the platens at 149°C, took 24.8 minutes on average for the center glue line of to reach 100°C. It is noted that no mention is made of the press platen pressure used during these pressing cycles. It has been found that press platen pressure effects the rate of heat conduction (Strickler 1959) and therefore is an important consideration. Figure 2.3 illustrates the dramatic difference in center glue line

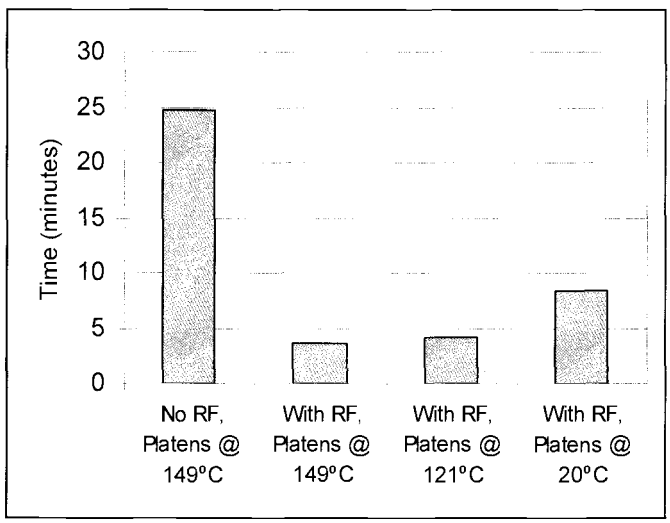

Figure 2.3 – A comparison of the time required for the center glue line temperature of a 38 mm thick LVL assembly to reach 100°C with and without RF heating at various platen temperatures. This illustrates that dramatic difference RF heating can make.

heating when RF energy is applied to the LVL assembly. Maloney also conducted a limited special test with the press platens at ambient temperature (20°C) and found that the

veneers were successfully bonded with the average center glue line reaching 100°C in 8.4 minutes.

Maloney also took measurements of the outer most glue line temperatures for the test conditions described above. The results are displayed in figure 2.4. It is of interest

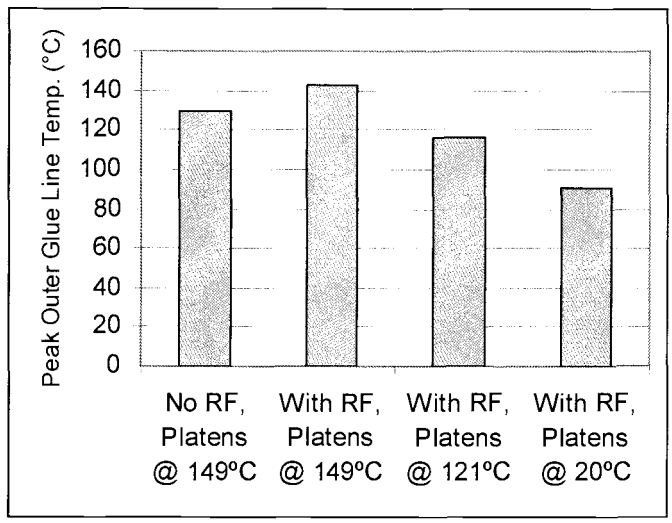

Figure 2.4 – Peak outer glue line temperatures for each of the test conditions.

to note that the peak outer glue line temperature is higher with the use of RF heating than with hot platen heating alone. This effect will be discussed later in this work in connection with this author's own research results. It is also of interest to note that in the test condition with the press platens at ambient temperature the outer glue does not achieve 100°C, the traditional temperature requirement for full cure of phenol-formaldehyde adhesives. As mentioned earlier in this work (see 2.1.3), this writer's experience in industrial LVL production with platen temperatures below 90°C was that the bond quality of the outer glue lines was unacceptable. The stiffness and bending tests on these special test boards conducted by Maloney suggests reduced values from the control group. However, the small number of samples is not sufficient to draw a conclusion.

A follow-up study was conducted by Bodenheimer (1992) specifically exploring the use of RF heating with the press platens at ambient temperature in the same press and using veneer of the same width and length as in Maloney's research. However, the veneer thickness was reduced to 2.54 mm from 3.18 mm, increasing the number of plies in the assembly from 13 to 15. Moisture content of the veneer in this study was reported at 4% - 6% and it assumed that it was similar in the Maloney study although it was not stated in Annett's report of that study. A lower RF power density of 12.9 kW/m^2 was used compared with the 18.84 kW/m^2 used by Maloney. Two adhesive formulations were employed, one with a relatively high resin solids content of 48% and the other with a resin solids content of 28%. Bodenheimer, unfortunately, does not state what press platen pressures were used to produce the LVL material.

Bodenheimer concluded his research by stating that using the adhesive with the higher resin solids content with the press platens at ambient temperature it is possible to produce LVL with RF heating that has stiffness, strength and shear values equivalent to LVL produced with RF heating with the press platens at 149°C. However, he noted that lower resin content adhesive test values for the LVL with RF heating and ambient temperature platens were lower than the control samples by a statistically significant amount. This was most notable in the edgewise static bending results, where there was also a significant difference between the LVL produced with RF heating and 149°C platens (Bodenheimer 1992 & 1993). These results suggest that resin content of the adhesive used in the subject press of the present study may have been a contributing factor to the unacceptable bond quality results when low press platen temperatures were attempted.

Klemarewski and Annett (1995) reported on an industrial LVL press with RF heating as the primary method of glue curing after a year of operation. It was a standard Durand-Raute hot oil LVL press with modifications to allow the incorporation of RF heating while retaining the capability of using hot oil to thermally heat the platens. It was noted that the heating of the LVL assembly is uniform and a diagram is provided illustrating equal temperatures through the vertical cross-section. This is inconsistent with the results obtained from the work of Maloney reported by Annett in 1991 which clearly

indicated a significantly higher temperature developing in the outer glue lines. This is also inconsistent with the results of this present study as will be seen in Chapter 5.

According to Klemarewski and Annett (1995) a special glue formulation was necessary to reduce the conductivity of the phenol-formaldehyde (PF) adhesive to prevent frequent arcing along the edges and sometimes within the veneer assembly in the press during the RF heating cycle. Standard PF adhesive contains 5.5% - 9.5% sodium hydroxide which gives it relatively high conductivity properties. They reported that a new formulation was successfully developed with a lower percentage of sodium hydroxide with a lower incidence of arcing.

They presented data for three thickness of LVL (see Table 2.1) demonstrating that the actual press production increases using RF heating. The percentage of production

Table 2.1 – Comparison of press time for conventional and RF-heated presses

LVL Thickness	Conventional Press Time	RF Press Time	RF Press Production Increase
38 mm	19.5 min.	8.3 min.	235 %
45 mm	24.0 min.	9.8 min.	245%
90 mm	70.0 min.	22.4 min.	313%

clearly increases with thickness, with the greatest percentage of press production being over 300% for the 90 mm product.

Klemarewski and Annett (1995) point out that the greatest savings in RF LVL production are not so much from increased throughput, which is offset by higher capital and operating costs, but from savings in adhesive usage. Since the overall press time is much shorter and all the glue lines are being heated simultaneously, less adhesive is required to prevent adhesive dry-out. Adhesive savings range from 16.0% for 38 mm product to 25.8% for 90 mm product.

The quality of the LVL produced in this industrial RF LVL press is equal to that of conventionally pressed of LVL according to Klemarewski and Annett (1995). They fur-

ther note that due to the shorter press times and lower platen temperatures, densification can be minimized. This could mean a savings in wood fiber utilization. Finally, they recognized that the lower platen temperatures also resulted in a reduction of damage to the face plies of the LVL assembly and surface blisters.

Though not mentioned in their report, it would be reasonable to assume that the lower platen temperatures result in a reduction of the emission of volatile organic compounds (VOC's). This writer has observed visually what appears to be a significant reduction in the emission of VOC's in the operation of the subject press of this study compared to an adjacent conventional hot platen press. Further research is required to quantify the magnitude of this reduction.

Before leaving this section, the research of Resnik et al. (1996) will be briefly discussed since it may have significance to future developments in RF LVL pressing. Water has a very high dielectric constant when compared to wood. Resnik et al. demonstrated that by controlling the placement of veneers with different moisture contents in the veneer assembly, the temperature gradient generated within the assembly may be manipulated. This manipulation may be used to compensate for temperature losses due to conduction and to enhance a uniform cure of the adhesive. Their research concluded that careful manipulation of MC distribution in the assembly may also result in a reduction of energy consumption. The practical application of these findings may be difficult in an industrial setting. Multiple supplies of each strength grade of veneer would be required along with separate conditioning rooms to maintain the desired moisture content level in the veneer. In addition to this, in some LVL production facilities, such as the subject press of this study, there are extended open assembly times which significantly effect the moisture content on the glue lines of the outer plies. This would make it difficult to precisely control moisture content in the outer plies and to account for ambient environmental conditions.

2.4 LVL PRESSING MECHANISMS

The cure of the thermosetting adhesive at the interface of the plies of veneer is most commonly accomplished in hot platen presses. In RF pressing, some of the heat transfer into the veneer assembly comes from the hot platens, but the majority of the heat is transferred by dielectric heating. This section will explore the mechanisms of heat transfer, vapor generation and movement, adhesive bond strength development kinetics, and consolidation of the LVL veneer assembly in the RF pressing process.

2.4.1 Heat Transfer

The mechanisms active in composite assemblies during hot pressing are several and have complex, interdependent relationships with each other (Zavala 1987, Strickler 1959, Thömen 2002, Wangaard 1968, Chow 1968, Kamke 1988, Bolton and Humphrey 1988, and Humphrey and Bolton 1989). Figure 2.5 illustrates the inter-relatedness of the major mechanisms of heat and moisture transfer during the hot pressing cycle. The major mechanisms of heat transfer in wood composites are: thermal conduction, phase change, convection of water vapor and electro-magnetic radiation (usually infra-red in hot pressing). A brief review of these mechanisms is presented here.

The contribution of conduction to heat transfer within the composite material depends on the nature of the material. In veneer systems, conduction is the dominant mechanism of heat transfer in conventional hot pressing (Zavala and Humphrey 1996). Zavala and Humphrey measured the temperature gradient in the vertical direction of a plywood veneer assembly during consolidation in a hot press and found that they closely resemble those produced from the classical "heat equation" for predicting one-dimensional heating of a body from two sides, as also noted in earlier research (Wangaard 1968, MacLean 1942, Carruthers 1959).

Because wood is porous and hygroscopic material, significant heat transfer occurs through its voids. During the initial stages of hot pressing particulate, significant vapor

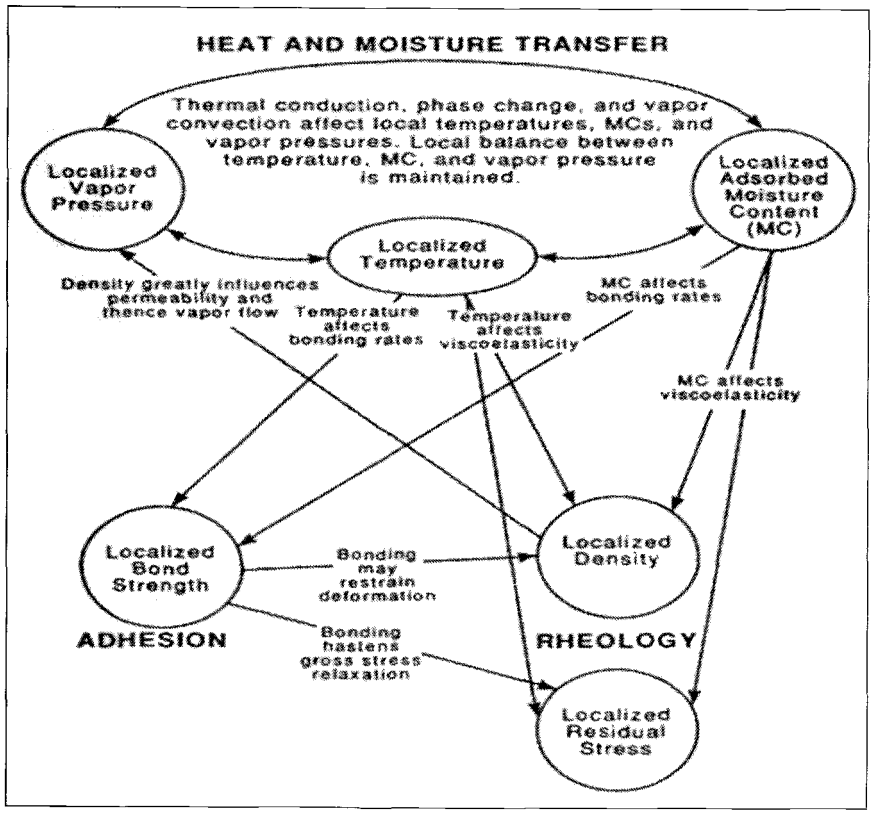

Figure 2.5 – A schematic representation of the interdependencies among mechanisms operative within dry-formed wood-based composites during hot pressing. (Humphrey 1994).

pressure gradients are generated as temperature of the outside of the wood fiber mattress rises liberating bound water from the wood fibers while the temperature at the core of the mattress is little changed. This pressure gradient causes the movement of the heated vapor towards the lower pressure zone of the core (Humphrey 1989). Because fiber, particle, or flake composites are much more permeable than veneer assemblies, convection of water vapor is the dominant mechanism for these composites (Thömen 2000). As shall be demonstrated later in this study, in RF pressing it is unlikely that vapor convection plays a significant role because the veneer assembly is more uniformly heated (by RF radiation) and the veneer has relatively low permeability in the vertical dimension.

Radiation transfers heat by imparting energy directly to the molecules of the composite assembly without conduction or vapor transfer. In conventional hot pressing, ra-

diation energy transfer mainly occurs on the top of the composite mattress between the time it enters the press and the upper hot platen makes contact. This time is usually less than one minute creating a small amount heat transfer into the surface of the mattress by radiant heating.

Within the veneer assembly there is a very small amount of radiant heat transfer occurring. Experiments with packed beds of dry glass beads, where there is no moisture-driven convective heat transfer, suggest that heat transfer by radiation is likely to be insignificant at temperatures as low at 200°C (Chen and Churchill 1963). Therefore, it will not be considered further.

2.4.2 Vapor Pressure Generation and Vapor Movement

The relationship in wood between temperature, equilibrium moisture content (EMC), and the within void relative humidity has been explored by Kauman (1956). He developed a reference table with the relative humidity specified for given EMC and temperature. A similar, though more refined, reference table was developed by Engelhardt (1979). Engelhardt's table (see Appendix B) is utilized later in this study as part of the equation used for the prediction of within void vapor pressures in the LVL laminate.

Research conducted by Zavala and Humphrey (1996) resulted in important information about heat and vapor generation, and vapor movement, within veneer assemblies. Vapor pressure and temperature measurements were taken in the vertical (at the horizontal center), horizontal (at the vertical center) and longitudinal (at the vertical center) axes of a veneer assembly during hot pressing. The veneer assemblies consisted of five plies of coastal Douglas-fir (*Pseudotsuga menziessii*) at 6.3% moisture content with the second and fourth plies at cross-grain to the adjacent plies. A liquid PF adhesive with 43.5% total dry solids was applied between the veneers.

The research demonstrated that significant and changing vapor pressure gradients are generated in the vertical dimension of the veneer assembly. In the early stages of the pressing cycle the hotter areas near the platens rose in temperature and vapor pressure rapidly while the core temperature and vapor pressure rose more slowly. However, later

in the pressing cycle the vapor pressure of the core areas surpassed the outer areas achieving more than double the pressure even though the core temperature was significantly lower than the outer plies. Zavala and Humphrey (1996) theorized that the water vapor of the outer areas moved to the core as a result of the steep early pressure gradient. It was trapped there by the low permeability of the veneer in the tangential direction and by the increasing impermeability of the polymerizing adhesive lines as they cured with the rising temperature from the outside towards the core.

Zavala and Humphrey's research also revealed that vapor pressures in the core required about 70 seconds to decay to half of their values at press opening in this five ply veneer assembly. This is consistent with the theory that water vapor is trapped at the core as described above. It was pointed out that this delay in vapor pressure dissipation has serious implications for bond strength necessary to resist rupture of the adhesive line at press opening and for a significant time afterwards.

The research of Klemarewski and Annett (1995) and Annett and Bowering (1991) suggests that the vapor pressure gradients that may be present would be much less severe and would be distributed differently in the veneer assembly for RF pressing than they would for conventional hot pressing. This is due to the more uniform heat generation in the veneer assembly by RF radiation. Vapor pressure measurements were not made in their experiments to verify this. There is a need for further research in this area to better understand the dynamics of vapor pressure generation and movement in the RF pressing process.

Zavala and Humphrey (1996) found that vapor pressure gradients are also generated in the horizontal plane of the panels although they do not attain the magnitudes associated with similar sized flake or fiber boards. They noted that the vapor pressures were nearly uniform across the entire plane, except at the very edges as they fall away to the partial pressure of atmospheric vapor. Their research reveals that vapor flows a little more easily longitudinally than tangentially. They note the implication for the LVL assembly is that it makes it more difficult for vapor to dissipate through the edges. Longitudinally, vapor can only escape at the ends of the veneer sheets where they overlap if they are not scarfed (beveled).

2.4.3 Adhesive Bond Strength Development Kinetics

The adhesive used in the subject press of this study is a thermosetting phenol-formaldehyde (PF). When the completion of the chemical reaction between the phenol and the formaldehyde occurs, the adhesive is cured (Tsoumis 1991). It should be noted that a chemical reaction between the adhesive and the wood fibers also occurs. Chow (1968) reports that the reaction between the carbohydrate in wood cellulose and the phenolic resin occurs first and then the resin-resin bonding occurs. Therefore, it is the resin-resin reaction that is the cure rate controlling step. The rate of cure can be manipulated by the addition of catalysts, other additives, and the temperature of the adhesive (Tsoumis 1991).

It has been found that bond strength begins developing very early in the reaction process and increases over time as the polymerization of the adhesive advances until it achieves full cure (Humphrey and Zavala 1989). Based on this fact, Zavala and Humphrey employed an instrument previously developed by Humphrey to analyze the time and temperature dependent bond strength development characteristic of a given adhesive. This instrument is described in detail in Chapter 4 in this work. A brief summary of the method will be given here since research presented later in this work is based on this method.

Humphrey and Zavala explain that small adhesive bonds (up to 25 x 25 mm) are formed using very thin adherends (0.8 mm) in the machine under highly controlled conditions of temperature, pressing load, and time. Immediately after each bond is partially cured to the predetermined level, it is tested to failure in shear mode. A data acquisition device captures the peak load (adjusted for the area of the bonded surface) at shear failure. When this testing procedure is done repeatedly for a range of pressing times, while the platen temperature is held constant, an isothermal bond strength development versus time plot may be constructed. The linear regression of this plot is the bond strength development rate for this adhesive at this temperature. Other isothermal bond strength development rates are determined in the same manner for a range of temperatures. Once a family of isothermal bond strength development rates has been determined, they are plot-

ted against the forming temperatures. The formula for the fitted line is the characteristic bond strength development pattern for that particular adhesive formula. This formula may be used for numerical predictions of bond strength development in composite assemblies (Humphrey 1996).

2.4.4 Consolidation of the LVL Assembly

Consolidation of the LVL assembly is not a focus of this present study but it is a significant aspect of the mechanisms of the pressing process. Therefore, a brief discussion of it is appropriate here.

As illustrated in Figure 2.5, the visco-elastic property of wood is effected by localized changes in temperature and moisture content during the pressing process (Zavala and Humphrey 1990). Zavala and Humphrey reported that beyond the initial elastic deformation under platen pressure, veneer assembly densification during the hot pressing progressed as the heating fronts moved through the assembly. The densification is noted as having a positive effect on heat transfer in the assembly, which in turn, increases densification as residual stresses in the veneer relax under the influence of higher temperature. The degree of stress relaxation will also effect the amount of spring back there is when the platen pressure is removed. There is a need for further research to numerically describe this complex relation to predict densification of the veneer assembly.

Though not attempting to produce a numerical formula for densification, Wellons, et al. (1982) explored the effects of various platen pressure schedules on the resulting densification of five ply panels of 3.2 mm various species of veneer. They found that densification increased with higher platen temperatures, with increased press pressure, and longer times at the same pressure. It was also determined that the more effective way of reducing densification was by lowering the platen pressure early in the pressing cycle, while maintaining it long enough to force intimate contact between the relatively rough veneer surfaces at the adhesive lines. A stepped pressure approach worked best, from 1.4 MPa to 0.7 MPa over the duration of the press cycle. With a scanning electron microscope they were able to determine that the fibers near the adhesive line were the

first to show signs of densification. This seems intuitive since that is an area where there is high moisture content. At higher pressures they also found evidence of densification in the early wood growth areas away from the adhesive lines. This demonstrates that weaker cell wall structure of the early wood begins to collapse before the stronger and denser late wood.

2.5 MODELING OF PRESSING MECHANISMS

Limited models for predicting temperature change in composite panel assemblies based on thermal conduction of solid wood at a given moisture content have been developed (MacLean 1942, Maku 1954, and Carruthers 1959). However, comprehensive numerical modeling of the dry-formed wood-based composite pressing process was pioneered by the work of Bolton and Humphrey (1988) with the use of FORTRAN programming (Humphrey and Bolton 1989). The basic principles of this model form the basis for the deterministic model of this present work. Therefore, a brief review will be given here. Further details are found in Chapter 5 of this work.

The model of Humphrey and Bolton (1989) utilizes a modified finite difference approach with special provisions for boundary conditions and phase change of water. The panel to be modeled is divided into a three dimensional matrix of small regions. The net flow of heat and water vapor between adjacent regions is calculated during a short time interval using steady-state formulas. The calculations are based on known physical characteristics of the regions at the beginning of the time interval. This information is used to recalculate the thermodynamic equilibrium conditions for each region. This calculation takes into account the division of energy in the region used to change the mass temperature and that involved in the production of water vapor. These calculations are repeated over and over again for the duration of the pressing cycle being modeled.

This model depends on a crucial assumption stated by Humphrey and Bolton: that the steady state theory adequately describes the behavior of the system during each time increment. In general, this is more likely to be correct when very short the time intervals are used. However, if the time intervals are too short, computation times become unac-

ceptably long. As with the time intervals, the volume of the mattress is divided into very small regions.

The model developed by Humphrey and Bolton (1989) is complex. This three dimensional model predicts the movement of heat and mass between each region throughout the panel and the resulting temperatures and vapor pressures generated within those regions. This model was modified and expanded by Thömen and Humphrey (2000) to numerically model the continuous press process of fiberboard in three dimensions. It takes into account the changing boundary conditions as the fiber mat moves through the press.

CHAPTER 3
GOALS AND OBJECTIVES OF THE RESEARCH

The review of the relevant literature in Chapter 2 demonstrates that hot pressing of LVL involves complex interactions of many mechanisms and involves a large number of variables. The RF component in the pressing process introduces a fundamentally different way of heating the resin to effect its cure. There have been a number of studies of the veneer laminating process in conventional hot presses, and on the use of RF heating in other types of wood laminating applications. The review of the literature suggests that the impact of RF heating on LVL pressing has not been extensively studied and its effects on the complex mechanisms involved in the process are not well understood.

The goal of this study is to gain greater understanding of the interaction of the complex array of raw material and press variables present in the RF LVL pressing process. This study seeks to evaluate how this means of heating effects the operative mechanisms in the veneer assembly during pressing.

The following objectives have been set forth in order to achieve this goal:

1. To quantify the following processes:
    - The transfer of heat to the veneer assembly: In the process under study, a portion of the necessary heat comes from heated platens, but the vast majority of the heating energy comes from the effect of the RF energy applied to the press load. Both means of energy transfer will be studied to understand the total combined effect. Temperature measurements will be recorded at two vertical positions in the press load by means of fiber optic sensors to discover relative variations in the rate of heating of these different positions.
    - Bond strength development in the press load: The review of the relevant literature in Chapter 2 makes it clear that adhesion kinetics is central to the LVL composite pressing process. Therefore, one of the objectives of the study is to explore the adhesive strength development characteristics of the particular PF resin used in the RF LVL pressing process under investigation. Using the

ABES instrument and associated methods reviewed in Chapter 2, miniature bonds will be formed and tested in the lap shear mode to establish bond strength development rates at various isothermal temperatures. This information will then be used elsewhere in the study as a means of predicting bond strength development in the industrial pressing environment.

- The development of vapor pressure within the press load: Vapor pressure is a function of temperature, moisture content of the veneer and the resistance to the escape of the pressure generated. In order to measure actual vapor pressures very small stainless steel tubing tubes will be inserted into the press load at various positions in the vertical section. Very small Teflon® tubing will be employed to connect the stainless steel tubing to pressure transducers to measure changes in vapor pressure throughout during the pressing cycle.

2. The development of a numerical modeling tool to predict temperature, bond strength development, and vapor pressure at any given point in the press load during the pressing cycle. The model will account for the following:
   - The heat applied to the load from the hot platens. Conduction is the major agent of heat transfer to be accounted for.
   - The RF energy absorbed by the press load. Factors to be considered are frequency, applied wattage, the electrical properties of the press load, the thickness of the press load, and the efficiency of the energy transfer between the RF generator and the press load.
   - The physical properties of the press load. This includes the density, veneer moisture content, and amount of adhesive applied to the veneer.

Achieving the objectives of this study will result in a better understanding of the behavior of RF LVL pressing process. This understanding will help to maximize the efficiency of RF energy input, minimize pressing time, and maximize the strength properties of the product. Also, this study will serve as a basis for future research into possible changes in the press operating parameters, the possible modification to equipment and possible experimentation with changes to the adhesive formulation.

CHAPTER 4
MATERIALS AND METHODS

4.0 INTRODUCTION

The materials and methods used in both the adhesive kinetic study and during data collection on actual LVL pressing at the subject plant are presented. The adhesive was the same type and formula for the adhesive kinetics study and the LVL pressing.

4.1 MATERIALS

The materials used in this study are described below. They include the adhesive used both at the subject plant in the RF pressing process and in the adhesive kinetics study, the veneer used at the subject plant, and the adherends used in the adhesive kinetics study.

4.1.1 Adhesive for LVL production and bond testing

Pre-mixed, ready to use, liquid PF adhesive (GP® 272A79, produced by Georgia Pacific Resins, Inc.) was used for the adhesive kinetics study and the manufacture of LVL in the subject press. This adhesive contains 36% PF resin solids, 10% fillers and extenders, and 1% 0.5N sodium hydroxide. Viscosity range upon delivery at the mill is 1600 ± 400 cP @ 25°C, and the conductivity is 19.5 ± 2 mS (milli-Siemens).

The adhesive formula is specifically manufactured for use in the subject plant. The adhesive must uniformly coat the veneer sheets moving at speeds up to 150 m/minute with a relatively low adhesive spread rate. It must withstand open assembly times up to 45 minutes without appreciably drying out. The adhesive must have relatively low electrical conductivity to prevent arcs (short circuits across the platens) from occurring in the press during the RF cycle.

4.1.2 Veneer for LVL Production

The veneer species used in the press during data collection was Douglas-fir (*Pseudotsuga menziessii*) and was nominally 1.22 m wide and 2.44 m long. This species is very commonly utilized for LVL production in the Pacific Northwest because of its high strength and stiffness.

Ten plies of 3.2 mm thick veneer were used for the bulk of the veneer assembly: a single veneer of 2.5 mm thickness lay beneath and two above. The thinner surface veneers were included in order to produce the correct finished billet thickness. The veneer was commercially dried to an average of 4.5% moisture content at other facilities of the company, and was visually graded as C/D plywood veneer according to the PS 1-95 grading standard (US Product Standard 1995). It was also electromechanically graded using the Metriguard® grading system described in Section 2.1.1 of this work.

4.1.3 Adherends Used in Adhesive Evaluation

Adherends were specially prepared to provide a platform upon which to form miniature test bonds for adhesive kinetic studies with the Automated Bonding Evaluation System (ABES) (see Section 4.2.1). The adherends need to have low variability in micro-structure in order to minimize variability in measured bond strengths. Further, the tensile strength of the strips must be sufficient to transfer shear stresses into the bonds sufficient to break fully cured test bonds. Adherend strength is determined both by the wood material employed (predominantly, its density) along with its thickness.

Prior adhesive studies with the ABES have successfully used rotary peeled Western Red Maple (*acer rubrum*). This diffuse porous hardwood species generally has clear, straight grain and good strength and stiffness (U. S. Forest Products Laboratory 1987). It is also readily available. For these reasons, this veneer was chosen for use with the ABES.

4.2 METHODS

The methods of research are presented below for the adhesive kinetics study, using the ABES, and the data collection from the subject LVL RF press.

4.2.1 Adhesive Kinetics Study with the ABES

Adhesion kinetics of the PF adhesive used in the RF LVL pressing process study was investigated using the ABES technique. The device enables the adhesive bonding of very small test samples to be explored under precisely controlled conditions of pressure, temperature and time. In this way the bonding characteristics of a particular adhesive and how it is likely to respond to the changing temperature conditions that occur at bonding sites in the industrial press may be quantified.

4.2.1.1 The Automated Bonding Evaluation System

The ABES consists of three major components:

1. Main test unit
2. Control and interface unit
3. Computer control and data acquisition software

Each of these major components will be described in turn and a typical testing sequence will be presented.

The Main Test Unit

The **press platens** ("A" in Figure 4.1) are electrically heated. Thermocouple junctions in the platens sense their temperature and provide signals to PID controllers which direct power to embedded electric cartridge heaters.. The platen anvils (stainless steel to provide ease of cleaning and to resist corrosion and oxidation) are mounted on

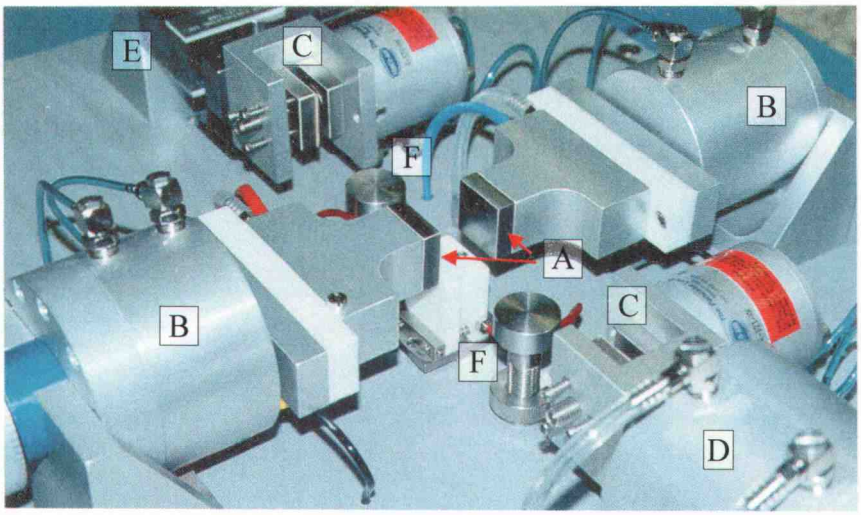

Figure 4-1 The ABES main test unit: A – Heated platens; B – Double acting pneumatic press cylinders; C – Sample grips; D - Double acting pneumatic load cylinder; E – Load cell; F – Adjustable sample supports.

aluminum bodies which contain the cartridge heaters. The aluminum bodies allow for rapid heat transfer to the stainless steel anvils. The platens have a network of air holes which are used for air cooling when necessary. Air cooling is automatically activated by the temperature control system providing enhanced control of the pressing temperature. Temperatures between ambient and 250°C maybe achieved within ± 1°C. A pair of double acting pneumatic cylinders ("B" in Figure 4.1) provides the pressing pressure to the small press platens. Pressing forces between 10 N and 1.5KN maybe achieved. One of the cylinders has an adjustable stroke so that when the sample is pressed it is properly aligned with the sample grips.

Sample Grips are air-actuated clamps ("C" in Figure 4.1) which tightly grip the ends of the test samples (adherends) and enable tensile load to be transferred to the bond between the two strips and thereby effect shear loading of the bond. The clamps are lined with a course sandpaper surface to prevent sample slippage. The sand paper surface can be replaced as needed to assure a positive grip on the samples. One side of each

of the grips has a floating anvil for auto-alignment, providing a secure grip on the sample.

Another pneumatic, double acting cylinder ("D" in Figure 4.1) is attached to one grip clamp providing the tensile load to the sample. The maximum pulling force ≅ 1.5 kN and the loading rate is set at 0.4 kN/sec. Such a rate has been established as a standard for the ABES method when evaluating wood bonding thermosetting adhesives. It was selected following tests, conducted by the inventor, ranging from near impact to prolonged creep testing. The selected load rate lies in a range where loading rate effects are minimized.

Attached to the other grip clamp ("E" in Figure 4.1) is a **shear bridge load transducer** which enables the load being applied to the sample to be rapidly sensed by the analog-to-digital sampling system. The transducer has a capacity of 2.5 kN and an accuracy of 0.25% of full scale. It is excited by a DC voltage and produces an analog output signal.

The two **activation switches** (not shown in Figure 4.1) must be depressed simultaneously to initiate the software controlled testing cycle. This is a safety feature to prevent the operator from inadvertently activating the apparatus before hands are clear of the press platens and other moving parts.

The two adjustable **sample supports** ("F" in Figure 4.1) enable precise vertical alignment of the test sample strips to be achieved. Such precision is essential since it effects the bond area.

Computer activated **bond cooling heads** are mounted beneath the test bond on each side. When activated, the heads rise between the retracted pressing heads and the bond and direct cooling air onto the partially cured bonds. This device may be used to explore the temperature dependence of the strength of the partially cured bonds. It has not been used in this study; all bonds were tested (pulled) three seconds after the platens were retracted. Investigation of the thermoplastic characteristics the adhesive used in the industrial RF pressing process may be warranted in future studies.

The Control and Interface Unit

This unit (Figure 4.2) controls the operating parameters of the main testing unit, including the following:

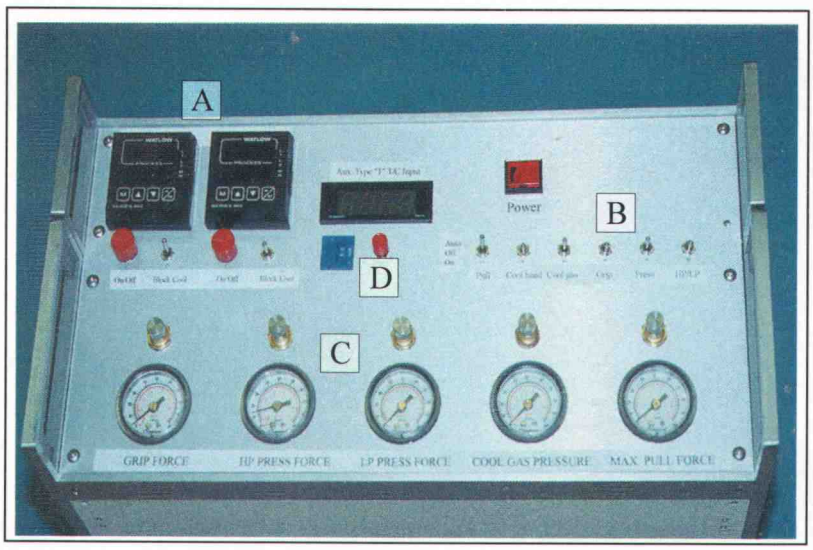

Figure 4.2 The ABES Control Cabinet: A-Platen temperature controls, B-Toggle switch controls, C-Pressure gauges and pressure regulators, D-Auxiliary temperature input and display.

1. **Temperature Control:** The temperature control section ("A" in Figure 4.2) contains digital read outs of each platen plus the set point controls for setting each platen to the desired temperature. It is an adaptive P. I. D. controller with auxiliary air cooling. The controller maintains the platen temperature at ± 1°C over the 25° to 150°C temperature range.
2. **Toggle Switches:** A bank of six toggle switches ("B" in Figure 4.2) control which parts of the mechanical test apparatus will be activated either manually or under computer control.

3. **Gauges and Pressure Regulators:** Pressure gauges and regulators ("C" in Figure 4.2) control the air pressure to the various air actuated cylinders of the apparatus. By adjusting these regulators the desired bond pressing pressure, gripping pressures and test load force can be controlled. Provision is also made for the activation of the miniature bond cooling head to rapidly cool bonds prior to their being pulled. This function is not used in the present study and therefore will not be described further.

The Computer Control Software

The ABES is controlled by computer with software that is configured by the operator to determine the test sequence, timing, data collection, and graphical display of sample testing.

A Typical Testing Sequence of the ABES

Below are listed the order of operations used to form and test a single bond:

1. The ABES is turned on and air pressure is supplied to the system.
2. The computer used with the ABES is turned on.
3. The desired platen temperatures are set. (Usually both platens are set to the same temperature.)
4. The pressures for the various air-actuated cylinders are set.
5. While the platens are heating up, the sequence and duration of the test events can be set by editing the BOND.PRG file.
6. The BOND.BAT file, which starts the bond testing program, is run.
7. The appropriate test parameters and machine settings are selected from within the bond testing program.
8. Once the platen temperatures have stabilized at the desired temperature setting, (typically 10 – 15 minutes) one selects the "COLLECT" (data) option.
9. If the default pressing time is acceptable, one can select "START" to begin the testing sequence. (If a different pressing time is desired, one can select "CHANGE PRESS TIME" and set the desired pressing time.)

10. Selecting "START" initializes the ABES. However, the test sequence will not begin until the activation buttons on the mechanical test apparatus are pressed.
11. Now that the machine is initialized, a test sample, which has been prepared as described in Section 4.2.1.2, is set in place and the activation buttons are pressed. This starts the testing sequence beginning with press closure on the bond.
12. When the testing sequence is complete, the test sample pieces can be removed from the apparatus while the test data is being processed and transferred to the data file.
13. A graphical display of the data for the current test sample is presented to the operator showing load over time beginning from when the pull head is activated. A cumulative graphical display of maximum load over time from all test samples taken in the current testing session can be displayed if the operator so desires.

4.2.1.2 Adherend Preparation

This section describes how the adherends were cut to size and how the adhesive was applied.

Adherends Cut to Size

The veneer used in the ABES testing for this study has been described in Section 4.1.3 above. The manner in which these samples were prepared for testing shall be described here.

Large sheets of rotary peeled veneer (0.7 mm x 1.2 m x 2.4 m) were stored in an ASTM standard climate room maintained at 21°C and 65%RH. According to the Wood Handbook (U. S. Forest Products Laboratory 1987), the equilibrium moisture content of wood in this atmosphere should be 12%. Very thinly peeled veneer is used so that the heat from the platens of the ABES test apparatus may penetrate rapidly to the adhesive. This provides near-isothermal curing conditions for much of the duration of each bond forming period. Portions of the veneer, approximately 13 cm by 20 cm, were cut from these sheets in order to facilitate ease of handling in the precision cutting process.

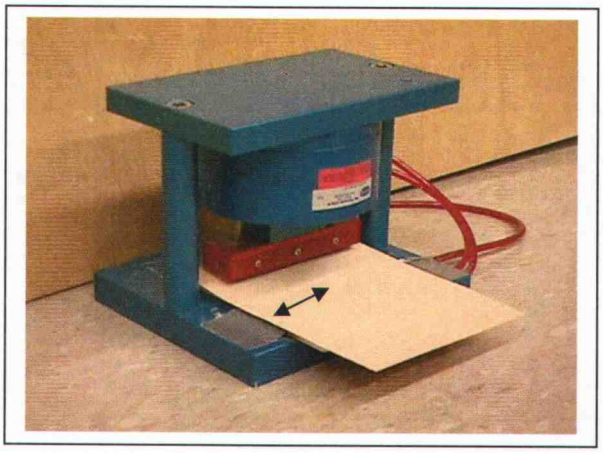

Figure 4.3 Pneumatic veneer test sample cutter. The arrow indicates the longitudinal direction of the grain.

Precision cutting of the veneer to the finished size was accomplished with an air powered die cutter especially designed for this purpose (see Figure 4.3). The die cuts the veneer to 20 mm wide by 118 mm in length. Tolerances for the samples were ±0.1mm for length, ±0.15 mm for width, and ±0.015 mm for thickness. The accuracy of sample length is important since it controls the bond overlap length for test bonds. Care was taken to insure that the grain ran almost parallel to the length of the sample when it was cut. This insured the highest tensile strength of the sample and avoided the possible effect of fiber orientation on bond formation and failure mechanisms. The razor sharp blades of the die cutter make clean, straight cuts through the veneer, further insuring the samples' strength and uniform dimensions. Approximately 100 sample adherends veneer were cut from the veneer in preparation for the isothermal bond testing conducted on the ABES. Having been stored in the ASTM standard room, samples were stored in an open tray in the test lab, which resulted in mean equilibrium moisture content of 7.4%.

Adhesive Application

The adhesive (See Section 4.1.1) was obtained directly from a bulk resin storage tank at the subject plant in Albany, Oregon. The adhesive had been delivered to the fa-

cility two days before this sample was obtained. Approximately 470 ml of the adhesive was stored in a refrigerator maintained at about 4°C in a sealed container. Prior to each adhesive testing session, 10 to 20 ml of the adhesive was placed in a small beaker and allowed to warm to room temperature prior to being applied to the veneer test samples for testing. This was done for two main reasons: 1) to reduce the viscosity to allow for ease and consistency of application to veneer samples; and 2) so that the beginning temperature of the bond would be consistent. The remaining adhesive was returned to the refrigerator for future use and to inhibit advancement of the polymers in the adhesive.

The adhesive was carefully applied to the end of one of the veneer test samples using a flat wooden spatula (in this case, one of the veneer test samples) to evenly spread the adhesive. Care was taken to apply approximately the same thickness of resin on each veneer test sample, although no precision system of measurement of application rate was employed. Such a system is under development and may be employed in future testing.

Ascertaining the approximate spread rate on the bond samples

An effort to determine the approximate adhesive spread rate was made. The density of a veneer test sample was determined to be 0.783g/cm^3. Adhesive was applied, in the manner described above, to one end of the sample. A 10mm x 20mm area of the adhesive coated sample was removed with scissors and weighed as quickly as possible after the application of the adhesive on a precision scale. The weight of the veneer, as calculated from its density, was subtracted from the total weight of the adhesive and the veneer. Thus, the adhesive weight was determined for the 10mm x 20mm area. This procedure was repeated three times. The results are presented in Table 4.1.

Working with such small samples makes it difficult to get accurate results and the results that were obtained demonstrated significant variability. The lack of an accurate means of applying the adhesive to the test samples necessitated an investigation of the effect of adhesive spread variability on the measured bond strength values (See Appendix A) Once the veneer samples had been prepared as described above they were ready to be bonded and tested in shear. Details of this are described in section 4.2.1.4.

Table 4.1 Adhesive spread test results. Average spread rate = 184 g/m²

Sample	#1	#2	#3
Total weight of veneer & adhesive (g)	0.144	0.1506	0.1456
Minus the calculated weight of veneer (g)	0.11	0.11	0.11
Weight of adhesive (g)	0.034	0.0406	0.0356
Resulting spread rate (g/m²)	170	203	178

4.2.1.3 Data Collection

Using the ABES device described above, adhesive bonds were tested in shear mode, having been pressed for various lengths of time at various pressures as outlined in Section 4.2.1.4 below. At the completion of the adhesive bond test cycle of each sample, the computer processes the collected data and presents a graphical display of the load ap-

Figure 4.4 The ABES display screen of typical bond strength test results. Time is seconds is displayed on the X axis and Load in Newtons is displayed on the Y axis.

plied to the bond over time. A sample display is presented in Figure 4.4. One can see from this sample display how the load increases over time until suddenly the bond breaks and the load immediately drops to zero. If the sample should happen to slip in the grips during the testing cycle it would show as a plateau in the loading curve. Such test samples were excluded from the test results. The display also gives the time and date when the sample was tested along with the maximum load to failure and the duration of the loading cycle. Maximum deflection of the sample can also be measured and is displayed on the screen. This feature was not used in this study and therefore, will not be discussed further here.

The maximum load values were recorded for each test sample and entered on a spreadsheet. Once the data of several test samples was recorded, the data was used to create graphs for analysis of bond strength developed over time at various platen temperature settings.

4.2.1.4 Experimental Plan

The goal of this portion of the study was to explore the adhesion kinetic characteristics of the PF resin used at the Albany LVL facility. Bond strength development rates were determined by testing the bond strength of small test samples in shear mode after curing them for various time intervals using the same platen pressure and platen temperature. Plots were made of the strength of each bond for each time interval (see Figure 4.5). The bond strength development rate for a given temperature was derived from the slope of the linearly regressed line fitted to the plot of these points (see Section 2.4.3).

The selection of platen temperatures used with the ABES was designed to use temperatures within the normal range the resin is subjected to in the pressing process. Preliminary testing revealed that the rate of bond strength development below 70°C was too low to be a significant factor. Temperatures above 130°C are unlikely to be achieved or used in normal press operation. Preliminary testing and data from previous studies demonstrated that as the resin temperature increases the bond strength development rate rises

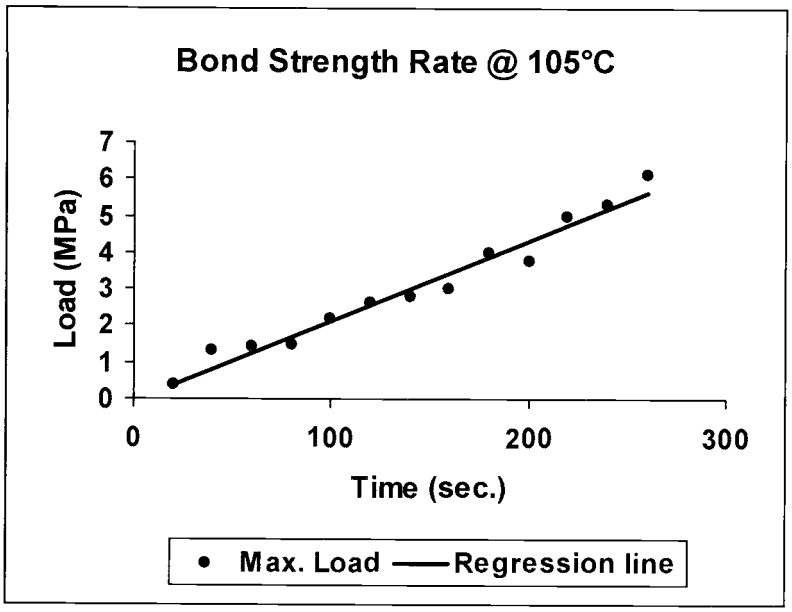

Figure 4.5 Sample of a bond strength development rate plot for 20 second time intervals at 105°C

rapidly. Therefore, smaller temperature increments were used in the upper half of the range of platen temperatures.

The time intervals used were varied according to the platen temperature because the higher temperatures produced faster bond strength development rates. Also, no significant bond strength is developed at the lower temperatures for a longer period of time. Therefore, the start times also varied. Table 4.2 shows the temperatures and times that were selected for use in this study.

All test samples were given a three second time interval to cool down after the platens were removed and then the bond was tested to failure in shear. No attempt was made to ascertain the actual temperature of the bond at the time of testing.

Table 4.2 Schedule of shear test starting times and subsequent test intervals for each isothermal platen temperature setting.

PLATEN TEMPERATURE	STARTING TEST TIME	TEST TIME INTERVAL
70°C	90 seconds	30 seconds
95°C	60 seconds	30 seconds
105°C	40 seconds	20 seconds
110°C	40 seconds	20 seconds
115°C	20 seconds	20 seconds
120°C	20 seconds	10 seconds
125°C	20 seconds	10 seconds
130°C	10 seconds	10 seconds

4.2.2 Mill Data Collection

The equipment utilized at the subject plant for the production of LVL is described. Sensor design for the collection of data from the subject press and their use is detailed. The experimental plan is presented.

4.2.2.1 Mill Equipment

The operation of the LVL press assembly bears directly on many aspects of the formation of adhesive bonds within the product. The following is a description of the equipment employed on the LVL press line at the subject facility where the LVL press data was collected. The description will be confined to the equipment used in veneer assembly and pressing. A discussion of the veneer and its processing prior to arrival at the subject facility is contained in Section 4.1.4. Processing of the finished product is not relevant to the present study and will not be discussed here. The description of the equipment will follow the order in which the material passes through the plant.

The Veneer Feeder System

The press line begins with a series of veneer feeders (see Figure 4.6). Stacks (units) of veneer (nominally 1.2 m x 2.4 m) are placed on the infeed of the feeders. Various grades and thicknesses of veneer are placed on the feeders according to the grade of the finished product to be produced. Some of the veneers are turned over. This is done for two reasons: 1) So that the exposed faces will have the "tight side" (the side without lathe checks) to the outside; and, 2) because there is a curvature to rotary peeled veneer, it is necessary to alternate the orientation of this curvature to prevent cupping (curvature across the width of the press load) of the finished product.

Once the veneer has been set onto the infeed, it is transported a short distance to the infeed hoist that lifts the veneer unit up. Each feeder uses an air suction system to lift individual sheets from the veneer unit, and to transport them to the lay-up conveyor system.

Figure 4.6 One of the seven automated veneer feeders. Powerful fans provide the suction that lifts the sheets from the stack. Belts take the veneer over to the lay-up line conveyer and knock off arms place it on the conveyor.

The first five feeders make up the main veneer feeders to the lay-up conveyor system. A programmable logic controller (PLC) determines the drop sequence from these feeders. Programming the drop sequence makes it possible to place the various grades and thicknesses of veneer at the desired vertical positions in the veneer assembly. Veneer from these first five feeders passes through a moisture detection system where the average moisture content of the veneer is checked. If the average moisture content of the sheet is above a pre-set limit, a reject system is automatically activated and the "wet" sheet is removed from the conveyor system and a sheet of veneer replaces it from the sixth veneer feeder. The veneer on this feeder is the highest grade and thickness used in the lay-up. That way, the replacement sheet will be of the same grade and thickness or better than the sheet it is replacing.

After the veneer passes through the moisture meter, the feeder operator visually inspects it to ensure it meets the visual standards set by the Manufacturing Standard of the subject plant. Sub-standard veneer is rejected and the feeder operator substitutes a sheet from the replacement sheet feeder.

The Adhesive Curtain Coater

Veneer continues moving down the lay-up conveyor system where it passes through an adhesive curtain coater. (The adhesive used in the curtain coater is discussed in detail in Section 4.1.2.) The adhesive head (an enclosed oblong metal box, see Figure 4.7.) is filled with adhesive from the day tank system. There are three means of adjusting the rate of the adhesive spread. One is by changing the flow volume. A second means of adjusting the rate of the adhesive spread is by changing the size of the opening in the bottom of the head that allows a curtain of adhesive to flow out of the adhesive head. A manual adjustment mechanism allows for the entire opening to be adjusted all at once changing the volume of adhesive flowing through the opening. A third means of adjusting the spread rate is to increase or decrease the speed at which the veneer passes through the adhesive curtain. This is accomplished by the use of a variable speed motor that drives the conveyor belts that carry the veneer through the curtain coater.

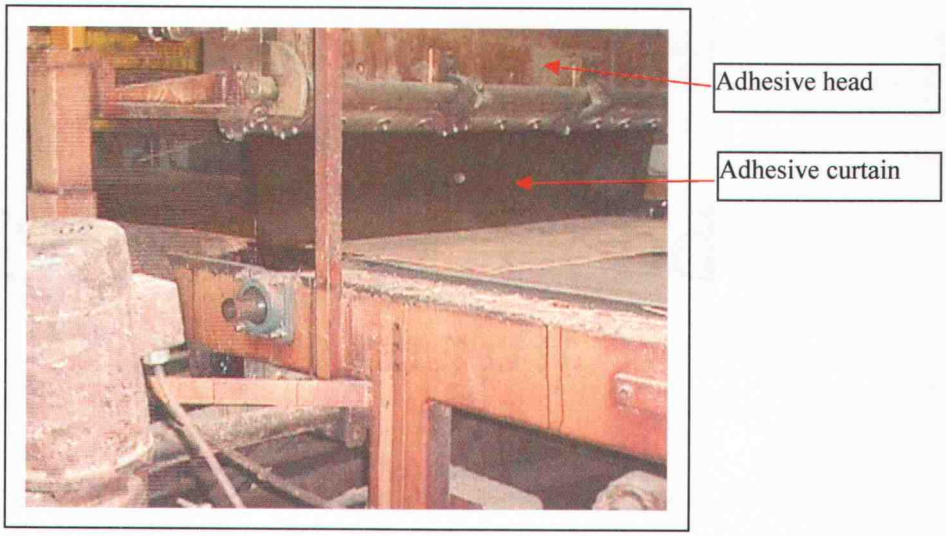

Figure 4.7 A curtain coater applies a controlled amount of adhesive to the veneer as it passes through the adhesive curtain.

An approximate veneer belt speed is selected to achieve the desired spread rate once the flow rate and the adhesive head bottom opening have been set. Stainless steel metal plates 1.5 mm thick and 15 cm square are used to measure the actual spread rate of the adhesive. The plates are weighed prior to being placed on a sheet of veneer that is to be passed through the adhesive curtain. The weight is recorded on the plates to be used later for calculating the weight of the adhesive deposited on the plates. Typically, three plates are on placed across the sheet about 50 cm from the leading end. One plate is placed in the middle of the sheet and the other two are placed about 15 cm from each edge. After the plates have been secured to the veneer, the veneer is passed through the adhesive curtain coater.

The metal plates are removed from the veneer sheet. The plates are weighed again and the original weight is subtracted to determine the weight of adhesive on each plate. Using the area of the plate and the weight of the adhesive on that area, the adhesive spread rate is determined. The spread rate determined for the three plates is then averaged to determine the average adhesive spread rate being applied to the veneer. The belt speed can be adjusted to change the spread rate to match the targeted value. Another

spread test will be conducted to confirm that the change in belt speed has produced the desired adhesive spread rate. The maximum difference of spread rate between the three plates is calculated. If the difference is too great, then adjustments are made and the spread rate will be re-checked. This procedure is repeated until acceptable results are achieved.

The Veneer Lay-Up System

After the veneer is coated with adhesive it is conveyed to the lay-up stop by means of a telescoping conveyor system. (NOTE: The top sheet is placed onto the conveyors after the curtain coater system so that it is not coated with adhesive.) When the sheets arrive at the lay-up stop (see figure 4.8), a tablet conveyor extends to support the sheets until they are stopped by the backstop. Then the tablet conveyor retracts allowing the sheets to fall into place on the veneer below that is lying on the lay-up table belt. The lay-up stop moves forward a set distance (approx. 15 – 20 cm) with each successive sheet until

Figure 4.8 The veneer travels on the telescopic conveyors to the lay-up stop where it is positioned in the LVL veneer assembly on the lay-up belt.

the full number of plies (i.e. 13 plies for 380 mm thick product) for that section has been laid down. The top sheet that has no adhesive coating on it is the last ply of veneer laid in place. Lay-up personnel apply a narrow band of adhesive with a roller to the trailing end of the top sheet to effect bonding from one top sheet to another. The lay-up stop then moves back to begin another section, overlapping each ply of the previous section by about 35 cm. This process continues section by section until a sufficient length of the veneer assembly has been laid in place to allow charging of the press.

The lay-up and pressing system utilizes a continuous lay-up concept. This means that the veneer assembly being laid up is connected to the assembled product in the press. The veneer is laid up on a conveyor belt and as it moves forward into the press during press charging, it transfers onto a special press belt. This is a loose veneer assembly with no pre-pressing (see Figure 4.9). While a 24 m portion is being pressed, additional veneer is assembled onto the end of the 10 m long veneer assembly that is outside of the press waiting to be pressed. So, while one 24 m section is being pressed an additional 24 m is being added to the end of the veneer assembly. When the 24 m section in the press

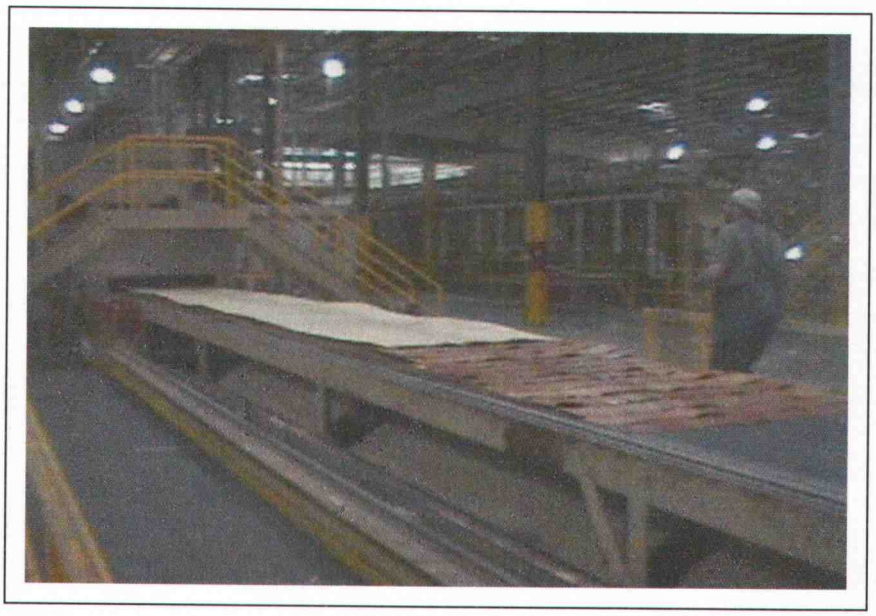

Figure 4.9 The veneer assembly has just moved forward into the press. While the section in the press is curing, more veneer is added to this section outside of the press.

has completed its pressing cycle, the press opens and the whole assembly moves forward 24 m beginning another pressing and lay-up cycle. In this manner, the veneer assembly exits the press as one continuous, consolidated panel. Billets in lengths of up to 24 m are cut from it.

The LVL Press

The LVL press employed is a single opening unit with hot oil heated platens. The press was manufactured by Durand-Raute of Canada in 1994. An RF generator provides the major portion of the heat to cure the adhesive in the veneer assembly (see Section 6.2.1). The press is 24 m long and 1.5 m wide. Hydraulically powered rams enable it to apply pressures in excess of 2.0 MPa to the veneer assembly between the platens. The operation of the press is controlled with a programmable logic controller (PLC) with manual overrides. When the press is running in automatic mode, the operator presses the button to close the press that starts the pressing cycle. During this cycle, platen heat, pressure and RF energy are applied according to the set-point settings described below. When the set point cycle is completed and sufficient veneer has been assembled for the next 24 m of pressing, the press opens and the belts move the veneer assembly forward 24 m and stops. The press cycle is repeated again when the operator presses the button that closes the press. It is important that the press cycle start in a timely manner to avoid drying out the adhesive when the veneer assembly is not under pressure between the hot platens.

The PLC uses a series of set points to adjust the platen pressure and length of time the RF energy is applied to the press load during the course of the pressing cycle. Up to 20 set points may be used. Each set point designates the duration of time, in seconds and the platen pressure. The set points function in the following manner. If a set point contains 1.38 MPa and 120 seconds with the current actual pressure at 0, the platen pressure will rise from 0 to 1.38 MPa, linearly, over the 120-second interval. If the next set point is 1.38 MPa and 300 seconds, it will hold the platen pressure at 1.38 MPa for 300 seconds. If the next set point is 1.03 MPa and 100 seconds, the platen pressure will fall,

linearly, from 1.38 MPa to 1.38 MPa over the 100-second time interval. An example of a possible 600 second press cycle set point series is shown in Table 4.3 for illustrative purposes. The shaded set-points indicate the portion of the cycle during which the RF

Table 4.3 – Possible set point series for a 600-second press cycle.

Set point	Pressure (MPa)	Time	Cumulative Time
1	1.72	30	30
2	1.72	30	60
3	1.24	120	180
4	1.03	120	300
5	0.90	120	420
6	0.83	120	540
7	0.76	60	600
8	0	0	600

energy is applied to the load. Additional set points can be designated to keep the RF generator in automatic operation. The RF generator may also be run manually to apply RF energy during other press cycle set points if desired.

The hot oil circulating through the platens is heated by means of a natural gas fired system with a heating capacity of 1,000 MJ. A thermostat system maintains the platen temperature at the desired setting ± 2°C.

The RF Generator

The RF generator used in the subject plant was manufactured by Thermex-Thermatron and has a maximum rated output of 500 kW. In simplest terms, the RF generator is a high-powered oscillator that converts 4,160 volts of 60 Hz electrical power into radio frequency energy oscillating between 3.5 and 8.5 MHz at up to 500 kW. The radio frequency energy is conducted to the electrically isolated lower press platen by means of eight coaxial conductors. The distance from each of the eight connections on the platen

back to the generator is the same so that the RF energy waveform is synchronized along the 24 m length of the press.

The amount of RF energy transferred into the press load is determined by a number of complex and interactive variables. Chapter 2 contains a discussion of these variables. The focus here is on how the RF generator is operated. In day to day operation, the press operator controls the amount of RF energy applied to the press load with four principle settings: the plate voltage, the plate amperage, the grid amperage, and the length of time the RF generator is on during the pressing cycle.

The plate voltage is set by means of the step up transformer settings. The settings can range from 8,000 volts to 15,000 volts at 60 Hz. This setting has a direct impact on the resulting RF voltage level. The plate voltage is usually set and left at a level that works well with all the various press applications and is rarely changed.

The plate amperage setting determines the degree of coupling between the RF oscillator load circuit and the press load. Changing the plate amperage setting on the operator console causes the RF generator to retune the frequency setting of the RF oscillator circuit in relation to the frequency of the load circuit by use of a variable capacitor to increase or decrease the degree of coupling.

The grid amperage setting is another means of controlling the amount of RF energy applied to the press load. The grid is like a valve that controls the energy flow between the cathode and anode of the triode tube in the RF oscillator. Changes to the frequency of the grid circuit changes the duration of the flow of energy into the load circuit during each cycle of the RF waveform. Increasing or decreasing the energy flow between the cathode and the anode results in a corresponding increase or decrease in the amperage flow in the grid circuit. Therefore, adjusting the grid circuit frequency controls the grid amperage. Changing the grid amperage setting causes the RF generator to automatically adjust the frequency of the grid circuit using a variable capacitor to achieve the amperage setting entered by the press operator.

The settings of the plate voltage, the plate amperage and the grid amperage along with the dielectric properties of the veneer assembly in the press determine the RF voltage cross the veneer assembly. These settings are limited by the electrical load capacity

of the RF generator and the dielectric break down voltage of the veneer assembly. The break down voltage is the voltage level the dielectric material can withstand before it allows electrical current to pass through it. If the dielectric break down voltage is exceeded, an electrical arc results, burning through the veneer assembly. The RF generator must be shut off immediately once an arc has started to prevent damage to the press and/or the RF generator. The RF generator has a built in arc detection system.

The difference in electrical potential (voltage (E)) between the press platens across the veneer assembly is a major factor in determining the amount of heat generated in the veneer assembly. This is because RF voltage is a squared factor in the equation for calculating the heat absorbed by a dielectric material ($P = E^2 * 2 * \pi * f * C$) (see Section 2.3.1). RF power absorption by the veneer assembly determines the rate at which the temperature of the adhesive in the veneer assembly will rise. This, in turn, determines the bond strength development rate. Therefore, the highest levels of RF voltage are used within the limitations of the RF generator and breakdown voltage of the veneer assembly as noted above.

To summarize, the feeder system places the veneer onto the lay-up conveyor belts according to a pre-determined sequence controlled by the PLC. The veneer passes through an in-line moisture detector and is visually inspected. Next, the veneer is evenly coated with adhesive as it passes through the curtain coater. Then the veneer travels on a telescopic conveyor system to the lay-up stop. At the lay-up stop the veneer is laid in place on a lay-up belt system. The lay-up belt system conveys the press assembly forward 24 m at a time for pressing in the RF press. Once the pressing cycle is completed, the consolidated veneer assembly exits the press as a continuous panel of LVL product and is cut to the desired length.

4.2.2.2 Experimental Plan

The experimental plan encompasses the variables measured, the number of pressing cycles for which measurements were made, and how all the measurements were coordi-

nated. Prof. P. E. Humphrey and the associates at the subject plant assisted in coordinating the placement of sensor probes and recording measurements.

Variables Measured

The main purpose of the measurements taken in the veneer assemblies during the pressing cycles was to validate the appropriateness of the deterministic model developed in this study (see Chapter 5) for predicting temperature and vapor pressure development in the veneer assembly during RF LVL pressing. There were several other areas of curiosity to be explored at as well. Therefore, the variables of interest measured during the RF LVL veneer assembly pressing cycles for this study and discussed here include:

- Internal temperatures of the veneer assembly
- Internal vapor pressures of the veneer assembly
- Thickness of the veneer assembly
- RF voltage between the platens
- RF frequency
- Amperage flowing through the plate of the RF power tubes

Internal temperatures of the veneer assembly

Internal temperature was measured because it is directly related to bond strength and vapor pressure development within the veneer assembly. Also, the distribution of temperature in the veneer assembly in an LVL RF press is predicted to be non-uniform by the deterministic model of this study; contrary to the assertions of Klemarewski and Annett (1995).

Available equipment for temperature measurements in the RF field limited temperature measurements to one location per pressing cycle. The high cost of press production downtime limited the number of pressing cycles for experimentation to five. Therefore,

it was determined to take temperature measurements in only two vertical locations and to repeat measurements at those locations at least twice to have confidence that the measured temperature was truly representative of the region. The center region (7^{th} veneer ply from the top) was chosen as one of the locations because this is typically the critical region for adhesive cure. The vast majority of under-cured adhesive delaminations occur in this region. The second region was chosen to be near the outer plies (2^{nd} ply from the top) of the veneer assembly because the deterministic model predicted this to be the region of highest temperature development. This is also the region where the subject plant experiences a high percentage of ruptures in the consolidated veneer assembly due to excessive heating in this area.

Internal vapor pressures of the veneer assembly

Vapor pressures were explored because they are a source of stresses on adhesive bonds when the press is opened. Perhaps there are opportunities to minimize the impact of the development if they were better understood. Also, the deterministic model predicted a different pattern of vapor pressure gradient developed in the veneer assembly than that reported by Zavala and Humphrey (1996). Therefore, it is important to investigate this difference to validate the deterministic model and to gain an understanding of the true nature of the differences between conventional hot platen LVL pressing and RF LVL pressing.

Two vapor transducers were used so that two regions could be measured during each pressing cycle. For the reasons mentioned above and those mentioned in the rationale for the locations of the temperature measurements, the same locations were chosen for the vapor pressure measurements. Also, it was desirable to have the temperature and the vapor pressure measurements from the same regions to validate the relationship between partial pressure of water vapor and temperature. The groove cut in the veneer for the insertion of the fiber optic probe may allow some vapor pressure to escape to the outside edge. Therefore, the location of the temperature probe and the vapor pressure tube open-

ing were placed in the same veneer ply and at the same distance from the outer edge but they were separated by 30 cm to 40 cm along the length of the same veneer sheet.

Thickness of the veneer assembly

Thickness densification is widely known to be a function of heat, moisture content and external pressure (Wellons et al. 1982, Wellons 1983). This is due to the hygro-thermo-viscoelastic properties of wood. Thickness measurements were taken to observe the densification of veneers in the RF pressing process.

RF voltage between the platens

The heating effect in an RF field is a function of the square of the voltage of the field (see Equation 2.2) Therefore, it was thought it would be of interest to measure the RF voltage level across the platens during the pressing cycle and to compare it to the rate of temperature rise in the veneer assembly.

RF frequency

Similar to the effect of RF voltage on the transfer of power into the veneer assembly, the frequency of the RF field also impacts the rate of energy transfer. Capturing this variable was easy and so it was captured to see if there was a discernable relationship between the frequency of the RF field and the rate of temperature rise in the veneer assembly.

Amperage flowing through the plate of the RF power tubes

The plate amperage varies during the pressing cycle while the plate voltage is held constant. The total RF power (minus efficiency losses) applied to the veneer assembly at

any particular moment of the pressing cycle is the product of plate amperage and plate voltage. Plate amperage is therefore an important variable in determining the energy applied to the veneer assembly. It is an essential variable in the deterministic model for determining how much energy is being applied to each region. Knowing the actual plate amperage so that it can be incorporated into the deterministic model is the only way a valid comparison can be made between the deterministic model and the actual press measurements.

The Number of Measurements Made

The data collecting software was set to record the values for each of the variables listed above at one second intervals. This was decided on based on preliminary experiments showing that the processes being recorded are not changing rapidly enough to warrant a faster sampling rate. The focus of this study was on the overall trends and relative changes between variables during the pressing cycle. It was determined that a faster sampling rate was not necessary for the purposes of this study.

The actual number of press cycles that measurements were taken on was limited due to the production constraints of the subject plant. The interruptions to the industrial production process are very costly and can also have an impact on the quality of the product. The purpose of the deterministic model was to provide a picture of the general patterns of temperature and vapor pressure development in the LVL veneer assembly and to demonstrate the general effects each of the variables has on those patterns. Therefore, it was determined that measurements on as few as four pressing cycles would provide enough information to validate the ability of the deterministic model to provide meaningful information.

4.2.2.3 Sensors and Methods

The sensors and their method of use for capturing the veneer assembly internal temperatures, vapor pressures, and densification are described here. Also the sensors and methods of measuring the RF generator operation and the ambient plant conditions are briefly described.

Veneer Assembly Internal Temperature

Taking temperature measurements inside a high powered industrial RF LVL press is challenging. In this RF energized environment, the thermocouple wire becomes a conductor of RF energy which can destroy thermocouple meters. Even if the thermocouple meter is not connected to the thermocouple wire, the wire alone may cause arcing and destroy the probe as well as triggering the automated arc detection system which shuts down the RF generator. Also, some types of thermocouple wire may be heated directly by the RF field and give false readings.

A considerable amount of effort was made to use thermocouple probes because of their ease of use with a datalogger, they are inexpensive, and multiple probes can be connected to the data logger at once. It was theorized that an RF choke system could be used to block the RF energy on the probe wires. After several attempts using different RF choke designs, limited success was achieved. Ultimately, the use of thermocouple probes had to be abandoned as unworkable.

A FISO® FOT-L fiber optic probe and a FISO® FTI-10 single channel signal conditioner were used to measure the temperature within the LVL veneer assembly during the RF pressing cycle. The probe has a temperature range of -40°C to 250°C with a response time $\leq$ 1.5 seconds and an accuracy of $\pm$ 1°C with a resolution of 0.1°C. The calibration of the probes is certified by the manufacturer. The probes are very expensive ($250+ each) and are easily damaged. The signal conditioner has a sample rate of 10 Hz and a $0-5$ V output. The output of the signal conditioner was connected to a Campbell 21X datalogger.

The RF LVL press is fully shielded to prevent the leakage of RF energy during operation. Therefore, to gain access to the LVL veneer assembly in the press, the RF generator must be shut off and locked out for safety reasons. Because of this fact, and to save time connecting probes once the press was charged with the veneer assembly, a 2.5 mm deep and wide groove was cut with a small circular saw into the veneer ply where the desired temperature measurement was to be taken. The groove had to be large enough to allow the insertion of the 1.7 mm diameter fiber optic probe once the veneer assembly was in the press and under pressure. It also had to allow the probe to be removed, undamaged, after the veneer assembly finished its pressing cycle. The cutting of the groove was done while the veneer assembly was outside of the press on the lay-up table. The cut was made from the outside edge of the veneer toward the center. The length of the groove was about 30 cm. Zavala and Humphrey (1996) demonstrated that there were no significant horizontal temperature gradients in a veneer assembly in a hot press during the pressing cycle. Therefore, we were confident that at a distance of 30 cm in from the edge our temperature measurements would not be effected by temperature losses at the outer edge of the veneer assembly.

Once the press was charged with the veneer assembly and full platen pressure had been applied, but before the RF power was applied, the fiber optic probe was inserted fully into the pre-cut 30 cm groove. Access to the assembly was gained by an existing door on the side of the press. Once the fiber optic probe was inserted and the connections for the vapor pressure sensors (described below) were accomplished, the access door was closed. The RF generator was then unlocked and the RF power applied to the press load. Temperature readings were recorded at one second intervals.

Vapor Pressure

The work of Humphrey (1982) and Zavala and Humphrey (1996) demonstrated a method for capturing internal gas pressure (predominantly the partial pressure of water vapor (Bolton and Kavvouras 1989)) measurements in composite assemblies during the

pressing cycle by using stainless steel hypodermic tubes connected to vapor pressure transducers. A similar method was employed in this study.

Stainless steel tubing was chosen with an inside diameter if 0.4 mm and outside diameter of 0.8 mm. This small diameter minimizes the impact of dead-volume in the measuring system on pressure measurements. The tubing was cut to lengths of about 35 cm. Outside of the press, on the lay-up table, a small gouge was cut into the veneer ply where a pressure measurement was to be made about 30 cm from the outside edge. An improvised small drill was used to make a small hole inside the gouge parallel to the surface of the veneer and about 3 mm in length. One end of the stainless steel tubing was inserted into this hole. This prevented adhesive from entering the tube and clogging it. The pressure recorded was the pressure within the veneer and was representative of the pressure between the adjacent adhesive lines. A small piece of masking tape was used to hold the tube in place but far enough from the end so that there was no chance that it would block the end of the tube. The other end of the tube extended out beyond the edge of the veneer assembly by about 5 cm. Experimentation demonstrated that the pressure of the pressing process and the adhesive on the surface of the veneer ply formed a tight seal around the tubing. Therefore, a groove like the one used in the Zavala and Humphrey (1996) study was deemed unnecessary.

Small Teflon® tubing, with an inside diameter slightly less than the outside diameter of the stainless steel tubing, was slipped over the exposed end of the stainless steel tubing for a distance of about 3 cm. Testing had determined that this formed a leak proof connection. The Teflon® tubing was about 40 cm in length. This tubing was coiled up along the edge of the veneer assembly. After the veneer assembly moved into the press, the Teflon® tubing was uncoiled and connected to short length of stainless steel tubing extending from the end of another short length of Teflon® tubing that was connected to the pressure transducer (See Figure 4.10). To facilitate timely connections, one person was assigned to work specifically on attaching the Teflon® tubes to the extension from the pressure transducers that were outside of the RF shielding of the press. None of the tubing was filled with silicone oil as in the study done by Zavala and Humphrey (1996). Experimentation indicated it to be unnecessary for this study. The total distance through

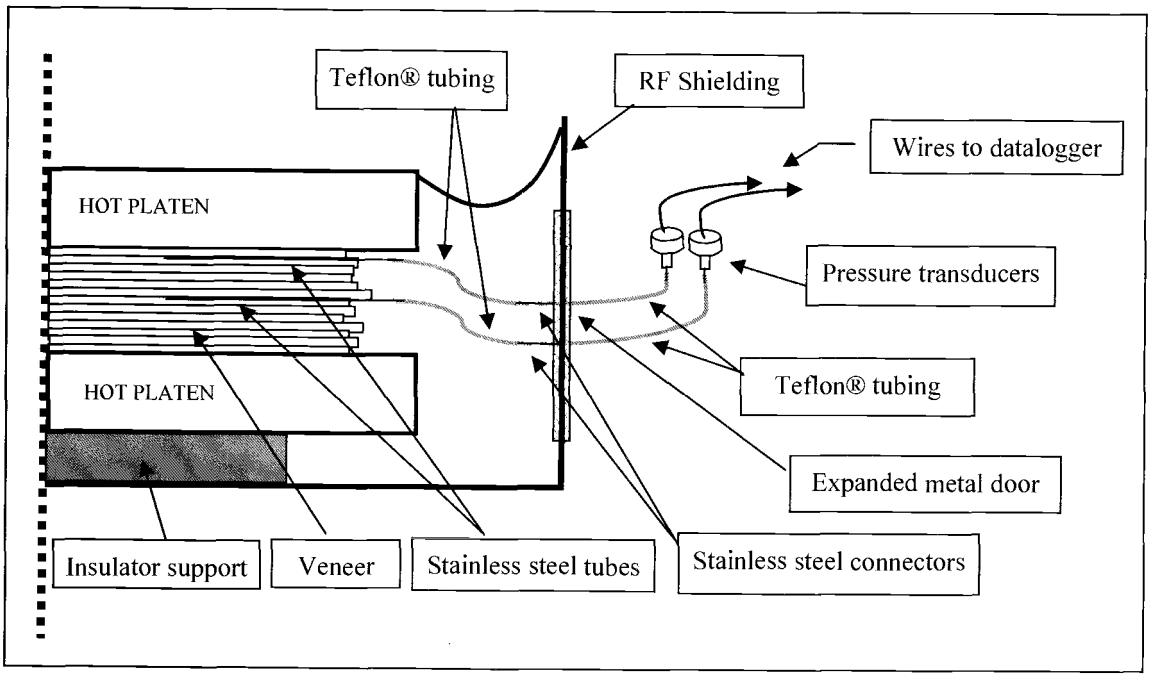

Figure 4.10 Schematic diagram of the set up of the vapor pressure sensors.

the tubing assembly from the open end in the veneer to the pressure transducer was about 1 m. Two stainless steel tubes, at the second and seventh plies of veneer, were inserted into the veneer assembly when measurements were made.

The pressure transducers were Omega PX176-015A5V piezo-resistive pressure transducers with an operable range of 0 to 350 kPa. They were selected for their high temperature stability and linearity. The pressure transducers were calibrated using a standardized dead weight tester. An especially designed adapter was fitted to the transducers to connect the Teflon® tubing to them. The pressure transducers were connected to the Campbell 21X datalogger.

Once the connections to the vapor pressure transducers and the fiber optic temperature probe had been inserted (as described above), the access door on the press was closed. With the access door closed, the RF generator was unlocked and the RF power was applied to the press load. Readings from the pressure transducers were recorded at one second intervals.

Veneer Assembly Densification

A linear variable differential transformer (LVDT) was mounted between the movable upper platen of the press and the press frame. Absolute platen separation was determined by closing the press when there was not a veneer assembly inside. Since the subject press is of the continuous-batch type, it was not possible to verify the absolute platen separation prior to each test load. However, the relative changes from the start to the end of the pressing cycle were of greatest interest, rather than the absolute thickness of the veneer assembly. The conditioned signal output from the LVDT was fed to the Campbell 21X datalogger. Readings from the LVDT were recorded at one second intervals along with those for temperature and vapor pressure.

RF generator operating parameters

The RF generator's programmable logic controller (PLC) recorded the unit's operation parameters from existing sensors in the system. This was a convenient and timely method of capturing information since the program and sensors were already in place at the subject plant. Data recorded included: amperage flow in the grid circuit; total amperage flow through the plate (anode) of the RF power tubes; RF voltage potential between the press platens; and, the frequency of the load circuit (press platens and veneer assembly). Readings were recorded at one second intervals. Occasionally, the PLC did not capture the data for every one second interval due to the limitations of the PLC. In those cases, it was necessary to interpolate the missing readings to coordinate the data with the Campbell 21X datalogger. The internal clock of the Campbell 21X datalogger was synchronized with the internal clock of the PLC so that the data could be directly correlated.

Ambient Plant Conditions

The ambient air temperature and humidity were recorded by the RF press operator (as well as on a circular chart recorder) from existing sensors at the subject plant at about 6 m in front of the press and 1 m directly above the veneer assembly on the lay-up table. These sensors are connected to a circular chart recorder with a real time digital display. Since these readings did not change much during the pressing operation they were only recorded once at the beginning of each pressing cycle.

CHAPTER 5
A SIMULATION MODEL OF THE RF PRESSING PROCESS

5.1 THE SYSTEM TO BE MODELED

A deterministic model has been developed to simulate the conditions within an LVL veneer assembly while being consolidated in a radio frequency heated batch press such as the one at the subject plant. The model may aid in the understanding of the dynamics of the pressing process and also be used as a tool to converge on optimal raw material and pressing parameters.

The mechanisms included in the model will be summarized along with reasons that others were excluded. Basic assumptions are listed and justified. An explanation of how the model is structured is followed by a typical set of model predictions in graphical format. The model will be validated in Chapter 6 by comparing predicted behavior with measurements made in a corresponding industrial press (RF LVL batch press of Trus Joist Corp. in Albany, Oregon.).

5.1.1 Mechanisms Included

Four mechanisms operative within material during RF pressing are included in the deterministic model and discussed in this Section. They are:

1. Thermal conduction
2. RF heat generation
3. Phase change of moisture
4. Bond strength development of the adhesive

5.1.1.1 Thermal Conduction

As noted in Chapter 2, the main mechanism of heat transfer within the veneer assembly is that of thermal conduction. Heat enters the veneer assembly from the hot oil heated steel press platens due to intimate contact between the two. (The assumption of intimate contact is dealt with in Section 5.1.3 to follow). Thermal conduction makes a significant contribution to phase change in the porous material and to effecting the heating necessary to cure the thermosetting adhesive used to permanently bind the veneer together in the LVL laminate.

Fourier's first law is used to describe energy conduction through the regions of the laminate. Fourier's first law can be written as:

$$Q_t = (\Delta T \bullet K_t \bullet t \bullet A) / L \qquad (5.1)$$

Where:

Q_t = energy transferred (Joules)

ΔT = temperature differential (°C)

K_t = coefficient of thermal conductivity (in J (s m °C)$^{-1}$)

t = time (seconds)

A = area (m^2)

L = length of flow path (m)

Thermal conductivity, K_t, of wood is effected by a number of factors including density, moisture and extractive content, grain direction relative to flow path, structural irregularities (i.e. knots & checks), fibril angle, and temperature (Wood Handbook, 1999). The major factors of density and moisture content are included for calculating K_t in the following formula while the other less significant factors are excluded:

$$K_t = D (B + CM) + A \qquad (5.2)$$

Where:

K_t = coefficient of thermal conductivity (J (s m °C)$^{-1}$)

D = density based on oven dry weight and volume at given moisture content M (%)

A = 0.01864 (constant, no units)

B = 0.1941 (constant, no units)

C = 0.004064 (constant, no units)

The values for the constants are as indicated when the specific gravity is >0.3 and at temperatures close to 24°C with moisture content values <25%:

Temperature is not accounted for in equation (5.2). Temperature has a relatively minor effect on thermal conductivity of wood (2% to 3% per 10°C). The actual conductivity of wood may vary by as much as 20% from calculated values because of the several factors listed above (Wood Handbook 1999). Even though the effect is small, in an effort to make the model more accurate, a temperature adjustment factor was added to the model using the following formula derived from information in the Wood Handbook:

$$\text{Adjusted } K_t = K_t * ((((T-24) / 10) * 0.025) + 1) \quad (5.3)$$

Where:

K_t = K_t as calculated in equation (5.2) (J (s m °C)$^{-1}$)

T = current temperature of the veneer assembly (°C)

5.1.1.2 RF Heat Generation

Radio frequency radiation is known to be the main source of heating energy for curing the thermosetting adhesive in the veneer assembly in the RF press. The theory of RF heat generation was discussed in Chapter 2. What is presented here is how the contribution of the RF energy to the heating of the veneer assembly was calculated in the deterministic model under discussion.

The formula for calculating the contribution of RF energy to each region is as follows:

$$E = (I * V * F * A * L * t) / U \quad (5.4)$$

Where:

E	=	the energy added to the region (Joules)
I	=	plate current of the RF oscillator (amperes)
V	=	volts of the RF oscillator (volts)
F	=	estimated efficiency factor (--)
A	=	area of region (m^2)
L	=	length of the region (m)
t	=	time interval (seconds)
U	=	volume of the entire veneer assembly in the press (m^3)

An efficiency factor is included in equation (5.4) because not all of the energy applied by the RF generator is transferred into the veneer assembly in the press. The discussion in Chapter 2 indicated that a number of variables influence the efficiency of transference and many of these change in value during the RF pressing cycle. It is not feasible to satisfactorily accommodate all of these effects in the model. Future enhancements may be warranted if such additions are found to be necessary after the initial model has been established. Remembering that the purpose of the present model is not to predict precise values, but to identify trends and the interaction of the various factors, a simpler approach was employed as described below.

Estimation of an RF efficiency factor

An "efficiency factor" was estimated in the following manner to determine how much of the energy applied by the RF generator is actually transferred into the veneer assembly in the press. This procedure was conducted after the main model had been established. The deterministic model was run using all the known material and press parameters to simulate a typical press cycle. Since the beginning and ending centerline average temperatures have been measured, the average temperature rise during a typical press cycle is known. Therefore, assuming all other calculations in the model are rea-

sonably correct, the efficiency factor can be determined by trial and error. That is, by adjusting the efficiency factor until the model produces a centerline temperature that is close to the measured average when the RF cycle is complete. The manufacturer of the RF generator states that the efficiency factor for general RF wood heating is typically around 75%. However, this trial and error approach resulted in an estimated efficiency factor of 56%.

This difference of 19% in RF efficiency is significant. Therefore, an attempt to confirm that 56% is a reasonable efficiency factor was made. Readings from the volt and amperage meters on the RF generator during typical press cycles were used to determine the total amount of energy applied by the RF generator during a typical pressing cycle. The RF energy applied to the veneer assembly was determined by the following formula from Ohm's Law:

$$P = V * A \tag{5.5}$$

Where:

P	=	power (Joules)
V	=	plate volts
A	=	Plate amperage

The total mass of the veneer assembly in the press during the pressing cycle was estimated and the beginning and ending temperatures were measured. The amount of energy from the hot, oil heated, platens conducted into the veneer assembly was calculated using the present deterministic model which calculates the energy conducted into the veneer assembly from the platens during the pressing cycle. This energy was added to the calculated amount of energy from the RF generator.

The following formula was used to calculate the expected temperature rise if RF energy transfer is 100% efficient:

$$T_R = (E_{RF} + E_P) / (M * Cp) \quad (5.6)$$

Where:

T_R = temperature rise if RF is 100% efficient (°C)

E_{RF} = energy input from the RF generator (Joules)

E_P = energy input from the hot platens (Joules)

M = mass of the entire veneer assembly (kg)

Cp = estimated heat capacity of the veneer assembly (J / °C)

When the appropriate values are substituted for the variables in equation (5.6) above, the result is as follows:

$$T_R = (154{,}287{,}900 \text{ J} + 14{,}330{,}327 \text{ J}) / (671.95\text{kg} * 1684 \text{ J(s kg °C)}^{-1}) = 149°\text{C}$$

Substituting the actual measured average temperature of 88°C for the 149°C in the computation above and then solving for E_{RF} results in E_{RF} = 85247287 J. Dividing this result by the 100% E_{Rf} value gives an estimated RF efficiency factor of 0.55. The difference between the calculated RF efficiency (.55) and the RF efficiency factor arrived at by trial and error (0.56) is 0.01. Realizing that the calculated RF efficiency factor is effected by the initial RF efficiency factor chosen and knowing that the temperature rise in this equation is the average of two press cycles, a 0.01 difference is, it is suggested, acceptable. Therefore, 0.56 has been used as the RF efficiency factor for the deterministic model. Clearly, this is not an entirely acceptable solution because the value may be effected by press and raw material variables. The value employed is, however, specific to the setup typically used at the mill.

It is interesting to note here that the calculations above reveal that over 90% of the heating in veneer assembly comes from the RF heating. Less than 10% of the heating is contributed by the hot platens at the current operating temperature in the subject plant.

5.1.1.3 Vapor Pressure Development

As moisture contained in the veneer and the adhesive of the veneer assembly is heated, vapor pressure in the pore spaces of the wood increases. Because of the impermeability of the steel press platens and the relative impermeability of the veneer in the tangential direction (Zavala 1987), the vapor pressure within the veneer assembly can not readily dissipate until the press is opened. If vapor pressures are sufficient to break the bonding of the thermosetting adhesive when the press is opened, delaminations will occur between the plies of veneer. This will cause a costly loss of product. Therefore, vapor pressure is an important variable to be predicted. The model may provide a means of finding how to adjust the pressing process to manipulate the relative magnitude of vapor pressures and bond strength attained when the press is opened. This may lead to greater production efficiencies.

The partial pressure of water vapor may be expressed as:

$$\varphi = p_v / p_{sat} \tag{5.7}$$

Where:

φ = % relative humidity

p_v = partial pressure of water vapor

p_{sat} = saturated water vapor pressure

The equilibrium relationship between moisture content, temperature and within-void relative humidity of wood is determined from a table based on the work of Engelhardt (1979) in Appendix B. Interpolation between tabular values has been employed in order to gain the resolution necessary for stability and convergence to be achieved within the model. Using this table one can approximate the RH in the voids of mathematically discrete regions of the modeled veneer assembly for a given temperature and moisture content.

The saturated vapor pressure is influenced by temperature and may be calculated according to an empirical equation (Humphrey and Bolton 1989):

$$p_{sat} = 10\text{^}(10.475 - (2141.0/(T + 273.15))) \quad (5.8)$$

Where:

T = temperature (°C)

p_{sat} = saturation vapor pressure (pascals)

Vapor pressure may now be calculated for various temperatures and levels of relative humidity utilizing equation (5.7) above and by multiplying the result by % RH calculated to be present in the voids of the veneer assembly.

5.1.1.4 Bond Strength Development

The study of the rate of bond strength development between the plies of veneer in the veneer assembly is of high importance. The faster bond strength is developed, the earlier the press can be opened. Shortening press cycle times is an important key to production efficiency. Therefore, this mechanism is included in the deterministic model.

Exploring the rate of bond strength development was discussed in Section 4.2.1 where it was shown that characteristic bond rates of an adhesive can be determined for various temperature levels. Taken together, the rates for the various temperature levels were used to produce a fitted curve that can be used to predict a bond strength development rate for any given temperature present in the typical pressing cycle. The formula, presented in Section 6.1, for this fitted line is incorporated into the deterministic model utilizing the modeling regions' temperature and time interval to determine the increase in bond strength for that region. The formula is as follows:

$$B_e = B_b + (0.30111 * EXP(0.044) * ((T_1+T_2)/2) * t) / 1000 \quad (5.9)$$

Where:

B_e = ending bond strength (kPa)

B_b = beginning bond strength (kPa)

T_1 = beginning temperature (°C)

T_2 = ending temperature (°C)

t = time (seconds)

5.1.2 Mechanisms Excluded From the Model

Research by others (Strickler 1959, Zavala and Humphrey 1996, Chen and Churchill 1963, Wellons, et al 1982) has demonstrated that there are some additional mechanisms in the pressing process that are present that have not been included in this present deterministic model. They will be briefly discussed here and reasons given for their exclusion.

5.1.2.1 Vapor Migration

Vapor migration is an important mechanism of energy transfer by in particulate composites as pointed out by Strickler (1959). However, in the LVL veneer assembly, the relatively low permeability of veneer in the radial direction greatly reduces the effect of this mechanism (Zavala & Humphrey 1990).

The concept for conventional hot platen pressing is that moisture in outer layers of the veneer assembly is converted to steam by the heat of the platen generating a vapor pressure differential within the veneer assembly. The steam moves from the highly pressurized outer plies to the cooler, less pressurized inner ply region. This wave of steam carries some heat and water with it. This heat, in turn, raises the temperature of this region to the point where the moisture in this cooler region is turned to steam. Thus, more steam pressure is created and continues the push to the lower pressure, cooler inner regions carrying heat energy to the inner regions. As the adhesive between the veneers cures it becomes less and less permeable. Thus, the moisture becomes entrapped in the

inner regions where the greatest vapor pressures are developed as the temperature rises in this region (Zavala & Humphrey, 1990).

When the RF pressing process is compared to conventional hot platen pressing there are some obvious differences. First, the bulk of the heating of the veneer assembly is accomplished by the infusion of RF energy (by means of dielectric heating or resistive ionic heating) within the laminate. This form of heating raises the temperature of the veneer assembly in a fairly uniform manner between the platens. Second, the platens themselves are usually heated to a substantially lower temperature than are conventional hot oil platens, which can be over 175°C. Platens in the RF pressing process are typically below 135°C. A third consideration is the shorter press cycle time. The veneer assembly is typically in the RF press the less than half of the time than it is in a conventional hot platen press.

Considering these three factors, it becomes evident that the great vapor pressure differentials that develop in conventional hot platen pressing are unlikely to be generated in the typical RF pressing process. Also, as mentioned above, the movement of water vapor becomes more and more restricted as the adhesive between the veneer cures becoming less and less permeable. Further, vapor loss horizontally through the veneer (in the tangential direction) appears to be much less than in particulate panels where permeability is much higher. Zavala and Humphrey (1996) demonstrated that vapor pressure gradients do not fall off significantly at the edges of plywood. One would expect it to fall off even less in an LVL assembly with all of the veneers lying with the longitudinal direction of the veneer grain running parallel with the length of the press.

Vapor migration does play a role in RF pressing but, compared to the other mechanisms, it was thought to be minor and was not incorporated it into the present deterministic model. However, there were significant discrepancies between the predicted and measured pressures, as reported in Chapter 6, suggesting there may be significant vapor migration. Therefore, it should be given high priority in future improvements to the model.

5.1.2.2 Radiant Heat Transfer

Certainly, there is radiant heat present in the RF pressing process coming from the heated platens. Radiant heat transfer mainly occurs as the veneer assembly is being loaded into the press prior to the platen closing on it. However, as noted earlier (Section 2.4.1) radiant heating is likely insignificant compared to the other heating mechanisms active in the veneer assembly in conventional hot platen pressing. In the RF pressing process, with the reduced platen temperatures, the contribution of radiant heat transfer is expected to be even less. Therefore, no radiant heating factor is included in the present deterministic model being presented in this work for radiant heat transfer.

5.1.2.3 Densification

Some densification takes place in all wood pressing processes due to the pressure of the platens and the softening of the wood as a result of elevated temperatures in the presence of sorbed moisture. In LVL hot platen pressing, typical densification is in the range of 3% to 10% (Wellons et al 1982). It would be of interest to have a better understanding of the inter-relatedness between densification, temperature, pressure, moisture content and vapor pressure. However, the focus of this study is on press efficiencies from temperature and bond strength development to overcome the developing vapor pressure within the laminate. Therefore, it was decided not to include this mechanism in the deterministic model. Again, this would be an opportunity for future development of the model. It should also be pointed out that such densification is likely to have some effect on heat transfer and phase change mechanisms in the pressing system (thermal conductivity and void volume are effected). This is another reason that it may be useful to include rheological mechanisms in future forms of the model. The acquisition of materials properties data does, however, present significant challenges.

5.1.3 Basic Assumptions of the Model

Assumptions are required to be made in order to make any model workable. Some assumptions are made to reduce the complexity of the model, while others are made because there is no known way to quantify them. The following is a brief discussion of the assumptions related to the present deterministic model.

5.1.3.1 Boundary Condition Assumptions

- The boundary condition between the press platens and the surface of the veneer assembly is assumed to have perfect thermal contact. That is, the SURFACE HEAT TRANSFER COEFFICIENT is considered = 1. In reality, it is known that the thermal contact is not perfect, but because of the pressure of the platens against the veneer assembly and its relatively smooth surface, intimate contact is very good. In future model enhancements such a parameter may be warranted. This would require additional laboratory investigation.
- The portion of the veneer assembly being modeled is located in the middle area of the veneer assembly. The modeled portion lies about 15 cm from the veneer assembly's outer edge, perpendicular to the grain of the veneers. The distances to the edges parallel to the grain are over 12 m for the ends of the press. Therefore, TEMPERATURE LOSSES AT THE HORIZONTAL EDGES will not be considered. Newtonian and convective cooling certainly occurs but its magnitude is not considered large enough to warrant inclusion at this stage.
- A related assumption to the one above, based on the location of the portion of the veneer assembly being modeled, deals with VAPOR PRESSURE LOSSES THROUGH THE BOUNDARY REGIONS. As discussed above, there is limited vapor movement in the radial and tangential directions through the veneer assembly. Research with vapor pressures in plywood

demonstrates (Zavala 1987) that there is very little decrease in vapor pressure towards the edges of the veneer assembly when measured perpendicular to the grain. This is especially true of distances greater than 14 cm. The decrease would be assumed to be even smaller in an LVL veneer assembly where the grain of all veneer plies lay in the same orientation.

The metal platens are impermeable to water vapor movement and a seal is formed between the platens and the surface of the veneer assembly. Therefore, no provision is made in this model to account for loss of vapor pressure through the boundary regions.

5.1.3.2 Other Assumptions

- The two press platens are assumed to be at the same temperature.
- The RF energy is assumed to be evenly applied throughout the veneer assembly, producing SYMMETRICAL HEAT TRANSFER within the horizontal mid-plane. The veneer assembly is also assumed to be symmetrical around the horizontal mid-plane, causing the physical processes taking place on either side of this horizontal plane to be the same. Therefore, the model will only calculate the heat transfer from one platen to the middle of the veneer assembly. An asymmetrical model could be developed in future refinements without too much difficulty
- The model assumes that there is no significant TEMPERATURE DRAW DOWN OF THE PLATENS during the press cycle. This assumption is based on the fact that the hot oil heating system is rated at a heating capacity of 1.054×10^9 joules/hour. Also, the mass of the iron platens and hot oil reserve are large enough, compared to the mass of the veneer assembly, to ensure that temperature draw down is small. To confirm this, a thermocouple temperature probe was placed between the press platen and the veneer assembly prior to press closing and temperature was monitored during the first 30 seconds of

the pressing cycle. (Because the thermocouple probe can not be used while the RF power is on, the temperature could not be measured during the remainder of the pressing cycle.) No discernable temperature drop was measured.

- The EFFICIENCY OF THE RF GENERATOR in transferring energy to the veneer assembly is assumed to be constant throughout the pressing cycle. It is not practical to account for all the variables that influence the changes that occur in RF energy transfer efficiency during the pressing cycle. Therefore, an average efficiency was estimated (see Section 5.1.1 above) and used as a constant in the present deterministic model. This parameter may, however, be easily adjusted for sensitivity studies. Later refinements to the model could include a provision for a changing efficiency factor as the characteristics of the veneer assembly change during the press cycle.
- For purposes of the deterministic model, it is assumed that the RF ENERGY IS UNIFORMLY DISTRIBUTED within the veneer assembly. It is known that there can be a number of localized factors within the veneer assembly that effect the absorption of RF energy. These factors include, but are not limited to, local moisture content, irregularities in the number and sizes of knots, veneer density, mineral content, RF frequency and position in the press. It is not practical to endeavor to account for all these factors in the deterministic model.
- The model assumes that the VENEER ASSEMBLY IS HOMOGENOUS. Specifically, adhesive lines are not taken into account in this model. It is beyond the scope of this study to determine the effect of the adhesive lines on the temperature development is the various regions of the laminate. This is especially true because of the nature of RF heating which penetrates through the entire veneer assembly during the pressing cycle. Perhaps this can be taken up in a later study.
- It is assumed that THE MID-POINT BETWEEN THE BOUNDARIES OF EACH MATHEMATICAL MODELING REGION REPRESENTS THE

AVERAGE FOR THE WHOLE REGION in regards to temperature, vapor pressure and bond strength. The regions are sufficiently small that the gradients are not large from one boundary to the next. Averaging within regions is implicit to the finite differencing deterministic method employed.

- It is assumed that the VENEER ASSEMBLY DENSITY REMAINS CONSTANT throughout the pressing cycle. Densification was discussed in Section 5.1.2 above. Again, attempting to quantify the changing density of the veneer assembly during the pressing cycle would add considerable complexity to the model. Furthermore, mill measurements presented in Section 6.2.3 demonstrate that the veneer assembly does not compress significantly after the first 20 seconds of the pressing cycle. The particular RF pressing process being studied includes control of densification by the adjustment of platen pressure during the pressing cycle. An average density based on the finished density of the veneer assembly was used in the present model.
- It is assumed that ALL CONDITIONS WITHIN EACH MATHEMATICAL MODELING (finite difference) REGION REMAIN CONSTANT FOR THE DURATION OF EACH SMALL TIME INTERVAL. At the end of each time interval the conditions are updated to newly calculated values as a result of the net energy change in each region during that time period. These new values are used in the calculations for the next time interval. By making the time intervals relatively short (about 1 second) the changes to each characteristics are kept small. Therefore, the error introduced by assuming they remain constant is minimized. Values for spatial sub-division and time step duration may be selected to enable desired accuracy, convergence and stability to be achieved.

5.2 THE SIMULATION MODEL DEFINED

5.2.0 Introduction

As stated previously, the goal of the present deterministic model is to obtain a better understanding of the temperature, vapor pressure and bond strength developments in the vertical dimension of the veneer assembly during the RF pressing cycle. Deterministic models developed for particleboard, OSB and even plywood, to a lesser degree, require a three dimensional approach to capture the full dynamic of these pressing processes (Humphrey and Bolton 1989). However, the dynamics within the RF LVL pressing process are less complicated because of the nature of the veneer assembly and the way in which heat is generated within the laminate.

It was calculated earlier in this study that over 90% of the heat developed in the veneer assembly is a result of the application of RF energy (see Section 5.1.1.2). This energy is essentially applied throughout the whole mass of the veneer assembly. Therefore, temperature and vapor pressure gradients are greatly reduced from that typically found in the above-mentioned pressing processes. Significantly lower platen temperatures also reduce the temperature and vapor pressure gradients within the veneer assembly.

A further factor is the orientation of the veneers in the veneer assembly. The grain of the veneer is all lying longitudinally along the length of the press. Permeability to water vapor movement perpendicular to the press platens (radial wood orientation) is impeded by the relatively low gas permeability of wood in the radial direction (about 10-15 m^2). The vertical permeability of flakeboard is 10-12 to 10-14 m^2 for material of 650 kg m^{-3} density, and still higher for dry formed fiber products (Bolton and Humphrey 1994). Permeability in the tangential direction is even lower than the radial direction in veneer. Zavala and Humphrey (1996) state, "In LVL, vapor escape (and by inference, vapor movement) is limited by the relatively low permeability of the veneers in their tangential direction; only at the ends of the long billets, can vapor escape longitudinally. ... The overlapping veneer joints used in some parallel-laminated products (*i.e. LVL*) may

also help vapor to escape." The vapor flow is significantly limited by these radial and tangential properties of the veneer in the veneer assembly.

One other consideration is that the RF pressing process being modeled is a batch-type pressing process as opposed to continuous pressing processes. The veneer assembly remains stationary between the long platens until the pressing cycle is completed. Therefore, adjacent regions on either side of the modeled region along the length of the press are experiencing the same mechanisms at the same time and there is very little if any differential gradient between them.

Considering all of this, a one-dimensional model, modeling the vertical dimension only, is appropriate. Further, since the energy transfer in the veneer assembly is assumed to be symmetrical, only the portion of the veneer assembly from the hot platen to the mid-point of a typical thickness is modeled. A mirror image of the model should fairly represent the other half of the vertical dimension of the veneer assembly.

5.2.1 The Finite Differencing Method

The basis of the model is similar to the finite differencing approach used by others to numerically model the pressing process (Humphrey and Bolton 1989, Thömen and Humphrey 2002). The veneer assembly is divided into small adjacent regions along the vertical axis of the assembly with special provision made for the platen to veneer assembly interface region and the region bordering the central plane of symmetry. The net flow of energy between regions during short time intervals is calculated using the physical characteristics of the veneer assembly within the region and its temperature, vapor pressure and bond strength developed at the beginning of the time interval. The net energy change to the region is then used to recalculate the region's temperature, vapor pressure and developed bond strength of the adhesive that may be present within the region. These new values then become the basis of the physical characteristics used for calculating the net energy change during the next time interval. This process is repeated for as many time intervals as may be contained in the total pressing cycle.

The model uses steady-state theory calculations for short time intervals to model unsteady events over the length of the pressing cycle. This method is based on a crucial assumption: that steady-state theory adequately describes the behavior of the system during each short time increment. Intuitively, the shorter the time increment, the more likely it is that this assumption will be correct (Humphrey and Bolton 1989). However, the shorter the time increment the more calculation iterations are required. This leads to longer computation times and a more cumbersome model to work with.

A sensitivity study was conducted to determine the effect of changing the time interval from 0.1 to 7.0 seconds (see Figure 5.1). Based on these studies, model time inter-

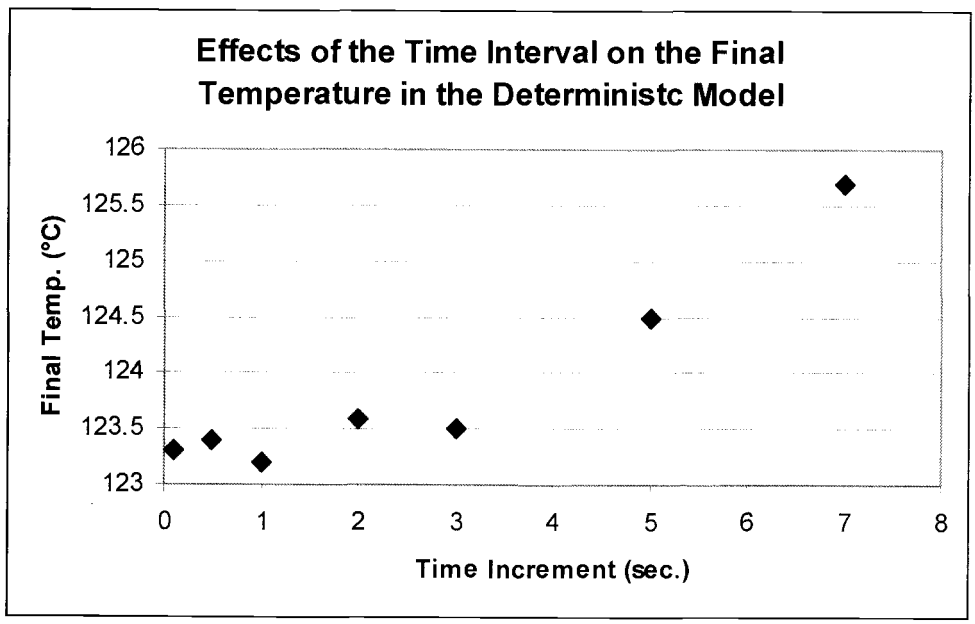

Figure 5.1 Results of a sensitivity study comparing the effects of various time interval settings in the deterministic model and the predicted final temperature for a simulated 400 second RF pressing cycle.

vals between 0.1 and 3.0 seconds produced an ending temperature within a few tenths of one degree from each other. However, it was observed that as the time interval was in-

creased beyond that range the ending temperature began to rise significantly. Based on these studies, a 1 second time interval was selected for use in the model with confidence that the predicted model results will not be skewed by the time interval selected. A one second time interval proved to be very manageable for use in the model.

The finite differencing approach also divides the veneer assembly into units or regions with a short distance between their centers (see Figure 5.2 in Section 5.2.3). This allows the energy flow between adjacent regions to be calculated during the short time intervals. In this manner, the movement of energy in the veneer assembly can be predicted over the pressing cycle and vapor pressure development and bond strength development in each region can be determined for each region during the pressing cycle. Using small regions gives greater resolution to the results and greater accuracy. But, there is a point of diminishing returns and the calculations can get very cumbersome to work with, if the veneer assembly is too finely divided. Therefore, the region distance center-to-center chosen for this model is 1.5 mm.

5.2.2 Incorporation of Mechanisms Into the Deterministic Model

5.2.2.0 Introduction

The following is a discussion of how the mechanisms of energy transfer, temperature change, vapor pressure development, and bond strength development have been incorporated into the deterministic model in an EXCEL® spreadsheet. A discussion of the fixed variables used in the spreadsheet model necessarily precedes the discussion of how the mechanisms are incorporated into the model.

An EXCEL® spreadsheet format was used to perform the calculations for this deterministic model. This format was chosen for several reasons.

- First, it is a convenient format to work with. It allows the results of various formulas to be easily combined while still allowing them to be worked with separately. Also, labels can be added for clarity and extensive explanations or comments can be attached to specific spreadsheet cells.

- Second, it is easily modified. Simply copying rows, columns or individual cells, can extend the model and the relative cell references are automatically extended.
- Third, it offers immediate results after changes are made. And those changes can be easily removed with the use of the "undo" feature.
- Fourth, results of all the intermediate calculations are displayed so the progress throughout the press cycle can be easily traced.
- Fifth, the charting and graphing features make it convenient to visually display trends and process changes modeled by the simulation.
- Sixth, results are produced very rapidly (<1 minute) even with 10,000 or more iterations.

5.2.2.1 Fixed Variables

Fixed variables refer to variables that do not change during the press cycle simulation or they are used to establish the beginning values of the press cycle being simulated. However, one may change these values to conduct sensitivity studies. For instance, one could incrementally change the moisture content of the veneer assembly to determine its general effect on vapor pressure development.

Fixed variables are each discussed in turn below:

- PLATEN TEMPERATURE: The platen temperature is used to calculate the heat energy applied to the veneer assembly through the outer boundary region (see Section 5.2.2.2). The temperature can be an actual measured temperature or a proposed temperature.
- TIME INTERVAL: This is the duration of time for each interval in the modeled pressing cycle. All intervals within the model are the same length.
- REGION AREA: This is the area of the model region. In this present model it is assumed that the region is located in the middle of the veneer assembly. It is used to calculate the volume and mass of the regions. The area is the same for all regions

- DISTANCE FROM REGION CENTER TO REGION CENTER: This distance is used to calculate the volume and mass of the regions. It is also the length used in calculations of energy transfer from adjacent regions. This distance is the same for all regions except the boundary region (see discussion of the boundary regions in Section 5.2.2.2).
- VENEER ASSEMBLY DENSITY: Initial densification occurs early in the press cycle and does not change significantly during the remainder of the press cycle due to adjustments in platen pressure. Therefore, it seems reasonable to use a fixed variable with no provision for adjustments during the press cycle. This value, including moisture content is used in the calculation of the mass of each region. The oven dry density is used in the calculation of the thermal conductivity of each region.
- VENEER ASSEMBLY MOISTURE CONTENT (MC): The initial moisture content of the veneer assembly is used throughout the press cycle in this present model. The MC value is calculated from the average oven dry MC of the veneer used in the veneer assembly plus the moisture in the adhesive applied to the veneer.
- RF PLATE VOLTS: This is the voltage applied to the plates of the RF power triodes in the RF generator. This value is used to calculate the RF energy applied to the veneer assembly during the RF portion of the press cycle.
- RF EFFICIENCY FACTOR: It is known that significant portion of the RF energy produced by the RF generator is not converted to heat in the veneer assembly. The percentage of RF energy that is converted to heat in the veneer assembly is known as the efficiency factor. Unfortunately, because the lack of adequate instrumentation, the efficiency factor could not be directly measured during this present study. Therefore, it was estimated as discussed earlier in Section 5.1.1. This factor is used to calculate the amount of energy applied to the veneer assembly by RF energy.

- TOTAL PRESS VOLUME: The volume of a region of the deterministic model is divided by the total press volume. That ratio is used to determine the portion of the total RF energy applied that is being applied to that region.

5.2.2.2 The Model Explained

This section provides a detailed description of how each mechanism is incorporated into the deterministic model. However, a general overview the structure of the deterministic model will be given first as an aid to understanding the general relationship between each aspect. The model is based on the finite differencing method discussed previously in Section 5.2.1.

Model Overview

The model begins with the selection of appropriate fixed variables discussed above. These are usually based on the best estimates of actual RF press and product parameters. Thermal conductivity at the initial temperature of the veneer assembly is calculated. This value, with a minor adjustment for the current temperature of the region, is used throughout the model. Calculations are then performed, in sequence, in each region and for each successive time interval, to determine the heat capacity, the net energy change, and the resulting temperature change along with the accumulated vapor pressure and bond strength development. The results of the previous time interval become the values used in the calculations for the current time interval, which in turn, become the values for the succeeding time interval. The number of regions and number of time intervals can be adjusted as is appropriate for the veneer assembly being modeled.

Energy Transfer

Energy is transferred into the veneer assembly from two sources, conduction from the hot platens and absorption from the RF energy field. For each region of the deterministic model the net energy change at the end of each time interval is calculated. It must account for the energy gained and/or lost through conduction to or from adjacent regions. It must also account for the energy absorbed from the RF energy field applied to the veneer assembly during that time interval. The basic formulae for calculating the energy flow were presented in Section 5.1.1. How these formulae are used in the present model is presented here.

Table 5.1 – Veneer assembly regions & time intervals

	Regions		
Time interval 1	1-1	2-1	3-1
Time interval 2	1-2	2-2	3-2
Time interval 3	1-3	2-3	3-3

For purposes of illustration, consider the calculation of energy change for region 2 during the second time interval (the shaded cell) in Table 5.1 from heat conduction. The following formula is used to calculate the energy ($\Delta E2$) gained or lost, from or to, region 1 in Joules:

$$\Delta E2 = ((T1 - T2) * K_t * S * A) / D1 \qquad (5.10)$$

Where:

T1 = Temperature of region 1 at the end of the first time interval (1-1) (°C)

T2 = Temperature of region 2 at the end of the first time interval (2-1) (°C)

K_t = Conductivity of the veneer assembly of region 2 at temperature T2 from formula 5.2 & 5.3. (J (s m °C)$^{-1}$)

S = Length of the time interval (seconds)

A = Area of the region (m^2)

D = Distance from center of region 1 to center of region 2 (m)

The same calculation is performed for the energy (ΔE3) gained or lost, from or to, region 3 during the first time interval. Thus, ΔE2 - ΔE3 = ΔEc change by conduction.

Next, the ΔERF is calculated for any absorption of RF energy during the second time interval for region 2. This is done using formula 5.4 from above as follows:

$$\Delta E_{RF} = (I * V * F * A * L * t) / U \qquad (5.11)$$

Where:

I = RF generator plate current (amperes)

F = Efficiency factor for RF energy absorption as a percentage of total RF power

A = Area of the region (m^2)

L = Distance between the vertical boundaries of the region (m)

t = Time interval (seconds)

U = Total volume of the veneer assembly in the press (m^3)

Net ΔE in region 2 equals $\Delta E_c + \Delta E_{RF}$.

Temperature Calculation

To calculate the change in temperature resulting from the net ΔE to the region, the heat capacity must be calculated. Heat capacity is calculated using the following formula from Haselein (1998):

$$Cp = (1131 + 4.19T + 4190u) / (1 + u) \qquad (5.12)$$

Where:

Cp = Heat capacity ($J\ (kg\ °C)^{-1}$)

T = Temperature (°C) of region 2 at the end of the last time interval

u = Moisture content ratio in decimal form from the fixed variables for the veneer assembly.

Now that the amount of energy required to change the temperature of a kg of the material contained in region 2 is known, the temperature in region 2 at the end of the second time interval is calculated as follows:

$$T = Tp + (\Delta E / (A * L * D * Cp) \quad (5.13)$$

Where:

T = Temperature of region 2 (°C) at the end of time interval 2

Tp = Temperature of region 2 (°C) at the beginning of time interval 2

ΔE = Net energy change to region 2 (Joules)

A = Area of region 2 (m^2)

L = Distance between the vertical boundaries of the region (m)

D = Density of the material in region 2 ($kg\ m^{-3}$)

Cp = Heat capacity of the material in region 2 ($J\ (kg\ °C)^{-1}$)

Vapor Pressure Calculation

Having determined the temperature in region 2 at the end the second time interval, the new vapor pressure level can be calculated using the following method. The VLOOKUP function of the EXCEL® spreadsheet program is employed in this calculation. VLOOKUP is an EXCEL® spreadsheet function that allows a value (in this case % RH) to be selected from a table of values based on X (in this case temperature) and Y (in this case the oven dry MC of the laminate). It follows the format: (lookup_value, table_array, column_index_number). Using the fixed variable for moisture content of the veneer assembly as the lookup_value, the correct moisture content row from the table_array is selected. The current temperature of the region is used as the column_index_number to select the correct column. A copy of this table is found in Appendix B. The value in the cell at the intersection of the selected row and the selected column is the % RH value used to calculate the vapor pressure using the following formula from an empirical equation (Bolton and Humphrey 1989):

$$VP = ((RH*100) * (10^{(10.745-(2121/(T+273.1)))})/1000 \quad (5.14)$$

Where:

VP = Vapor pressure (kPa) at the end of time interval 2

RH = % relative humidity at current temperature and moisture content (from Table B.1)

T = Temperature of region 2 at the end of time interval 2 (°C)

Bond Strength Development

Knowing the average temperature during time interval 2, the amount of additional bond strength developed in the adhesive that may be present in this region during this time interval may be calculated. This calculation is based on the bond strength development equation for this particular adhesive derived from the research presented in Chapter 6 (equation 6.1). The formula for this calculation is as follows:

$$BS = BS_p + ((0.3011*EXP(0.044)*((T_1+T_2)/2)) *t)/1000 \quad (5.15)$$

Where:

BS = Bond strength of adhesive in this region after time interval 2 (MPa)

BS_p = Bond strength accumulated in this region prior time intervals (MPa)

T_1= Temperature at the beginning of time interval 2 (°C)

T_2= Temperature at the end of time interval 2 (°C)

5.2.3 Geometrical Arrangement of the Model Regions

The following is a brief description of the relationship between the various regions of the modeled veneer assembly. The regions can be divided into three types: 1) platen and veneer interface region (#1); 2) middle regions (#2 – #12); and 3) line of symmetry border region (#13). (See Figure 5.2) Each of the discrete regions in the present deterministic model is identical in size and shape.

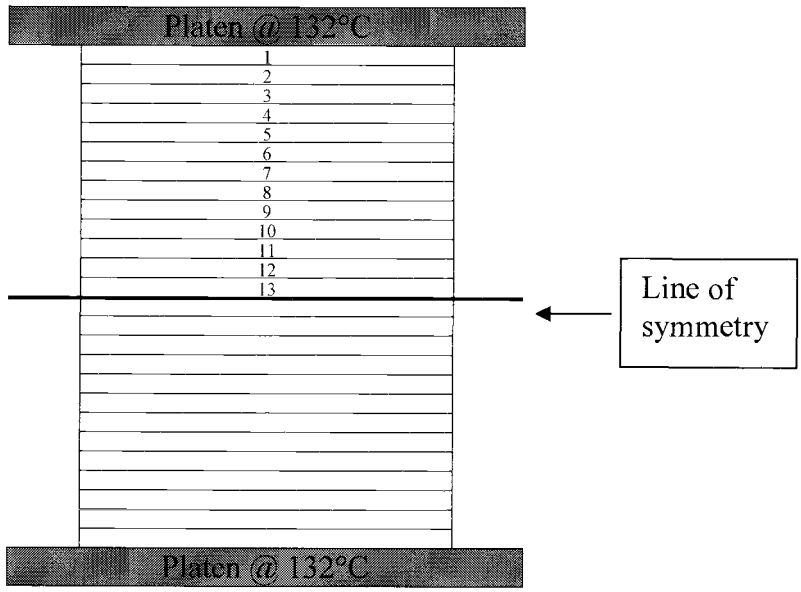

Figure 5.2 – The 40 mm veneer assembly divided into 1.5 mm regions.

All regions, except for boundary regions 1 and 13, lie between two identical regions, one above, and the other below. For purposes of heat conduction calculations, no boundary or impediment is considered to exist between the adjacent regions. The veneer assembly is considered to be a homogenous mass, arbitrarily divided into discrete regions. As stated earlier, glue-line boundaries are not accounted for in this model. The center point of each region is assumed to represent the average for the whole region in terms of temperature, vapor pressure and bond strength development.

Platen and Veneer Assembly Interface region

Region 1 is the boundary region of the veneer assembly that makes contact with the hot platen. As stated earlier, the surface heat transfer coefficient is assumed to be unity. In that respect it is the same as all the other regions. This region differs from the other regions in terms of the distance used to calculate the energy movement to and from

this region in relationship to the platen. In the other regions, the distance is measured from the center of one region to the center of the adjacent regions (See Figure 5.3).

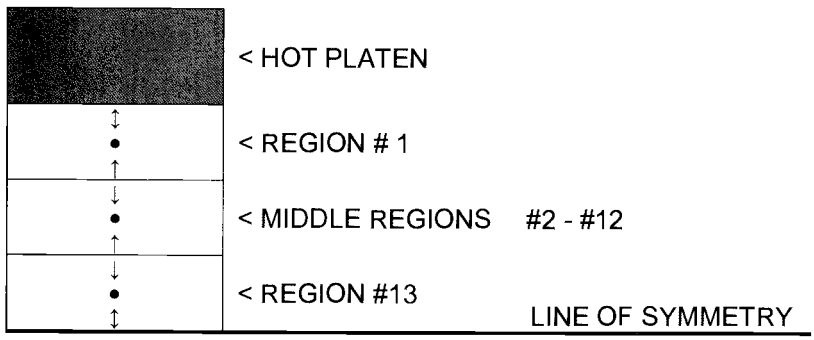

Figure 5.3 – Relationship between middle regions and boundary regions for the calculation of distance between the region centers. The "•" represents the center of the region

Since it is assumed that the hot platen is all the same temperature and that there is no temperature draw down, then the distance the energy travels is from the contact of the hot platen with region 1 to the center of region 1. This is half the distance (0.75mm) used in the calculations for the other regions (1.5mm). However, the volume of region 1 is the same as all the other regions.

Middle Regions

The distance between the middle regions (#2 - #12) is measured from region center to region center for purposes of calculating energy migration from region to region. The formulas used in each of these regions are the same except for the relative cell references.

Boundary Region at the Line of Symmetry

Region #13 is the region that lies next to the line of symmetry. As discussed in Section 5.1.3, it is assumed that energy is applied symmetrically to the veneer assembly. Therefore, only one half of the assembly is modeled, assuming that the other half of the assembly would be a mirror image. Thus, the boundary region adjacent to region #13 would not present any differential in temperature or vapor pressure. So, there would be no migration of energy into or out of this region. The model takes this into account and treats this boundary as neutral.

5.3 A TYPICAL MODEL RUN

A typical run of the deterministic model is presented in this section for a 40 mm thick LVL veneer assembly. The fixed variables used for this typical run are presented below:

- **PLATEN TEMPERATURE**: 132°C
- **TIME INTERVAL**: 1 second
- **REGION AREA**: 1 m^2
- **DISTANCE FROM REGION CENTER TO CENTER**: 1.5 mm
- **VENEER ASSEMBLY DENSITIY**: 567 kg m^{-3} at 8.76% MC & 521 kg m^{-3} Oven Dry
- **VENEER ASSEMBY MOISTURE CONTENT**: 8.76% Oven-dry Moisture Content
- **RF PLATE VOLTS**: 11,700 volts
- **RF EFFICIENCY FACTOR**: 0.56
- **TOTAL PRESS VOLUME**: 1.176772 m^3

A graphical presentation of the temperature data results of this typical model run showing the predicted temperature development in each of the thirteen vertical regions of one half of the veneer assembly is presented in Figure 5.4. A detailed discussion of the model results for temperature is presented in Section 6.3 of this work

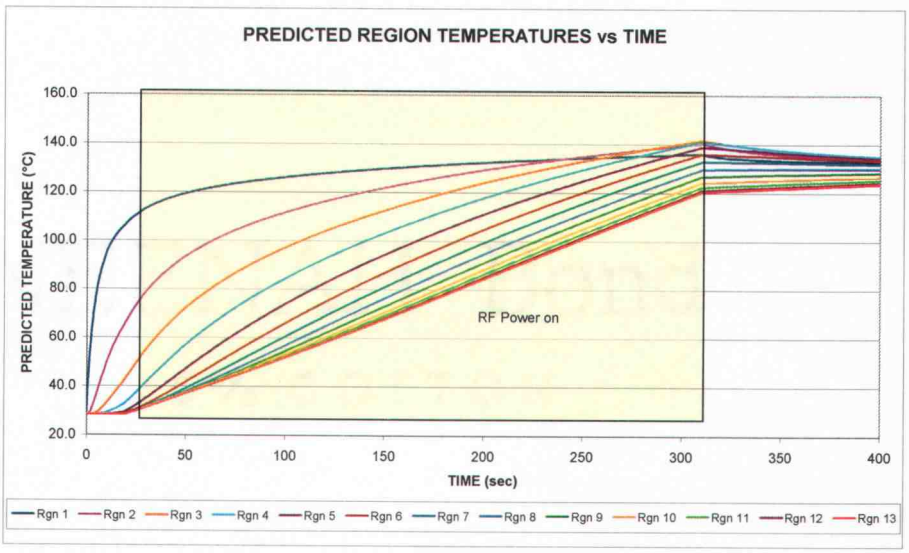

Figure 5.4 Typical deterministic model results for predicted temperature development in the veneer assembly in an RF pressing cycle. The shaded area represents the time that the RF energy was applied.

A graphical presentation of the vapor pressure data results of this typical model run showing the predicted vapor pressure development in each of the thirteen vertical regions of one half of the veneer assembly is presented in Figure 5.5. A detailed discussion of the model results for vapor pressure is presented in Section 6.3.

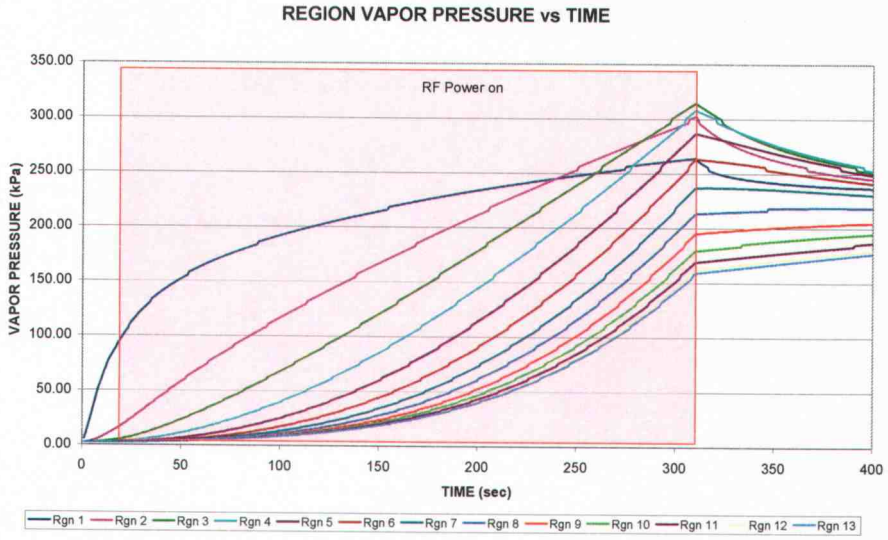

Figure 5.5 Typical deterministic model results for predicted vapor pressure development in the veneer assembly in an RF pressing cycle. The shaded area represents the time that the RF energy was applied.

Figure 5.6 is a graphic presentation of the predicted bond strength development in this typical model run showing the predicted cumulative bond strength in each of the thirteen vertical regions of one half of the veneer assembly. A detailed discussion of the model results for bond strength is presented in Section 6.3.

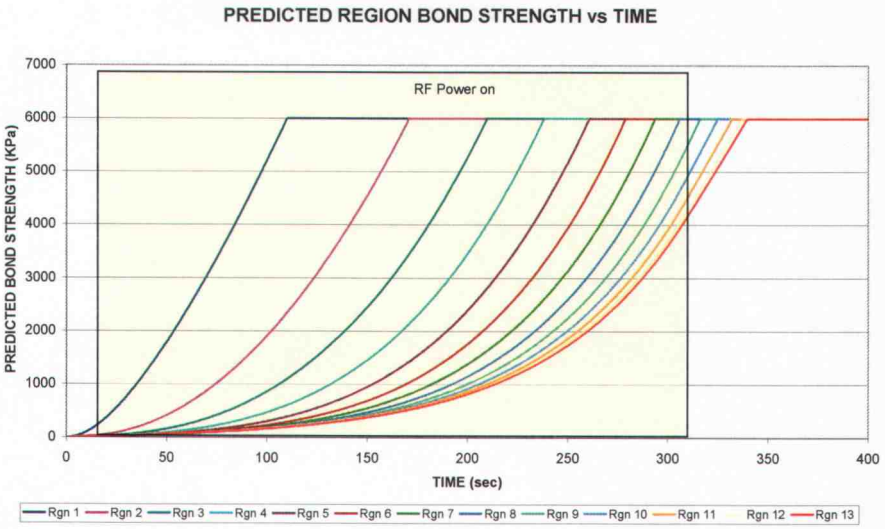

Figure 5.6 - Typical deterministic model predictions for bond strength development in the veneer assembly during an RF pressing cycle. The shaded area represents the time that the RF energy was applied.

CHAPTER 6
RESULTS AND DISCUSSION

Results of the adhesive kinetic bond strength development studies and the data collected from the subject RF LVL press are presented and analyzed. Comparison of the RF LVL press data is made to values of temperature and vapor pressure predicted by the deterministic model when set to the same operating parameters and material properties. The chapter concludes with a discussion of possible sensitivity studies that may be made using the deterministic model.

6.1 ADHESION KINETICS STUDIES

The data from the adhesive bond strength development studies using the ABES are presented in Figure 6.1. The time intervals between data points were decreased with the

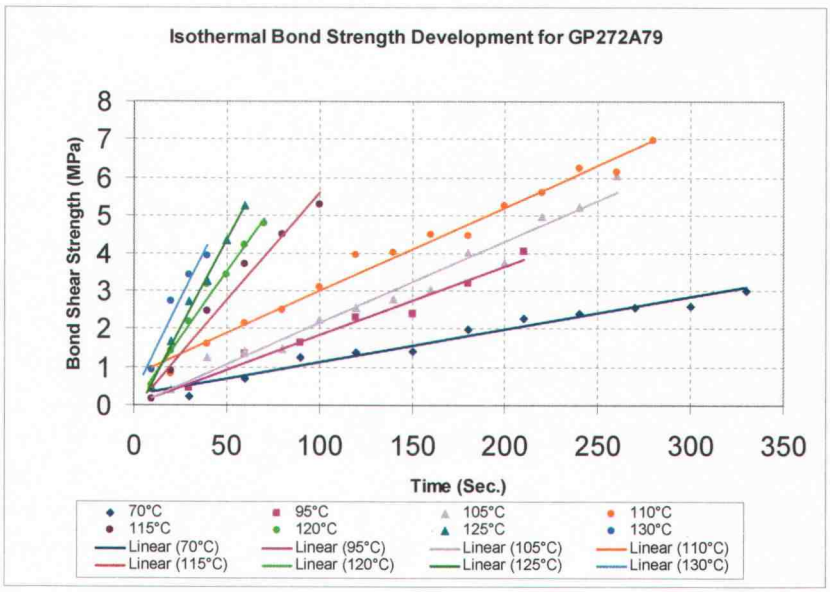

Figure 6.1 Isothermal bond strength development data plotted with linear regression lines for Georgia Pacific Resin, Inc. formula GP272A79.

increased isothermal strength development rate associated with increased temperature. The number of data points for each isothermal temperature ranged from 4 to 14. This is due to the varying time intervals and the differing lengths of time required for the bond strength development to reach the upper limit of the linear bond rate development for each isothermal temperature.

The data plots demonstrate that the bond strength development rate for each isothermal condition is quite linear. The fitted linear regression lines resulted in R^2 values ranging from 0.916 to 0.993. The few outliers present are likely due to a combination of minor variations in adhesive application and minor variations in the bonding surfaces of the adherends. The slope for each isothermal series regression line is presented in Table 6.1. The slopes are given in terms of kPa of bond shear strength development per second. As expected, the rate of bond strength development increases with temperature.

It is of interest to note the sudden increase in the bond strength development rate between 110°C and 115°C. This suggests that there may be a critical temperature threshold that significantly influences the rate of bond strength development in the adhesive. It is beyond the scope of this study to investigate this phenomenon further, but it may be of interest for future research.

Table 6.1 Comparison of adhesive bond strength development rates for Georgia Pacific Resin, Inc. formula GP272A79 derived from the linear regressions of the isothermal data presented in Figure 6.1.

Forming Temperature (°C)	**Bond Strength Development rate (kPa/sec.)**
70	8.6
95	18.2
105	21.7
110	22.1
115	57.4
120	75.0
125	93.2
130	97.4

The Bond Strength Development rate (kPa/sec.) data from Table 6.1 is plotted in Figure 6.2. This plot represents the characteristic bond strength development rate over

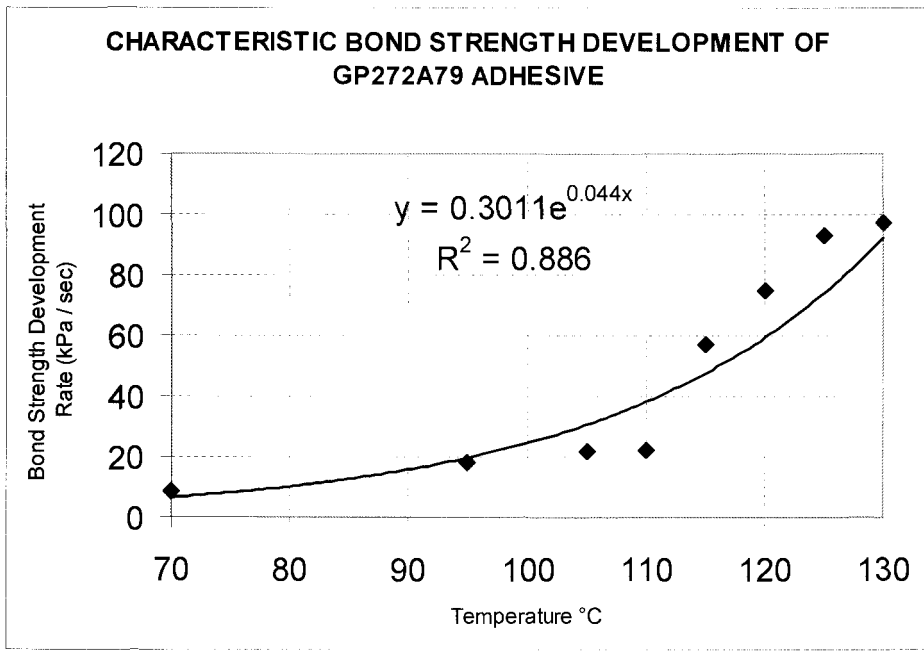

Figure 6.2 Isothermal bond development rates fitted with an exponential equation for the Georgia Pacific, Inc. GP272A79 adhesive formula.

the temperature range of 70°C to 130°C for the GP272A79 adhesive formulation. An exponential equation (6.1) was fitted to this plot using an MS EXCEL® program. Other

$$y = 0.3011e^{0.044x} \tag{6.1}$$

Where:

y = bond shear strength (kPa)

x = temperature (°C)

types of equations (linear regression, polynomial, logarithmic, and power) were explored. The exponential equation produced a reasonably good fit for the data over the

whole range. This equation may be used to estimate bond strength development for this adhesive formulation for a given time interval and temperature. Accumulated bond strength may be predicted by summing the bond strength developed over multiple time intervals at different temperatures. This equation is incorporated into the deterministic model presented in Chapter 5.

6.2 DATA FROM THE SUBJECT PRESS

The data acquired from the RF LVL press at the Weyerhaeuser Trus Joist plant in Albany, Oregon are presented here. The data acquired includes temperature and vapor pressure measurements at two vertical locations in the LVL veneer assembly, thickness changes of the veneer assembly, and the pressing parameters of the RF generator and the press. Temperature data is presented first followed by vapor pressure data.

6.2.1 Temperature Measurements

Temperature measurements were attempted on five press loads. However, the temperature probe could not be inserted into the first press load because of a blockage in the groove in the veneer for the probe (see Section 4.2.2.2). In press load runs 2 and 3, the probe was located in the 7^{th} ply of veneer from the top. This was approximately the center of the veneer assembly. The data for these measurements are presented in Figure 6.3. The platen temperature was measured at a sustained 128°C.

Unlike conventional hot platen pressing, there is almost no time delay in temperature rise at the core of the veneer assembly once RF energy is applied. The temperature increases at what appears to be a fairly linear rate over the pressing cycle. When the RF energy is shut off the temperature rises just a few more degrees and levels off. This indicates that the application of RF energy was solely responsible for the temperature rise in the core and that there is not a significant temperature differential close by. This suggests near uniform heating throughout the core region of the veneer assembly.

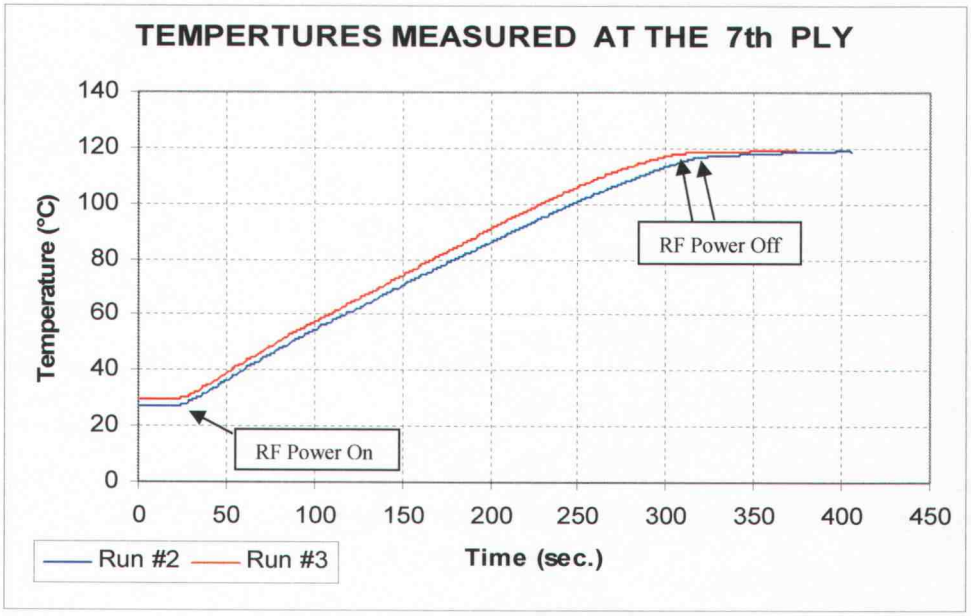

Figure 6.3 Temperature rise measured near the center of the veneer assembly at the 7th ply during the second and third pressing cycles.

When one examines the rate of temperature increase at the center of the veneer assembly during ten second intervals of the RF cycle, it becomes clear that the heating rate diminishes over time (see Figure 6.4). After a peak at 3.7°C/10 sec. early in the cycle, it plateaus at approximately 3.3°C/10 sec. for about 30 seconds and then holds steady at between 2.6°C and 3.0°C/10 sec. for about 120 seconds and then starts dropping off gradually for about 60 seconds. In the last 40 seconds the temperature rise drops off at a faster rate.

The cause of the decrease in the rate of temperature may be rationalized as follows. As the RF heating cycle progresses the RF voltage increases. Research indicates that the dielectric constant increases moderately with temperature (James 1977). According to formula 2.2, the increasing RF voltage and dielectric constant should cause an

$$P_{W/cm^3} = 5.56 * 10^{-12} f \ V^2 \varepsilon_r \tan \qquad (2.2)$$

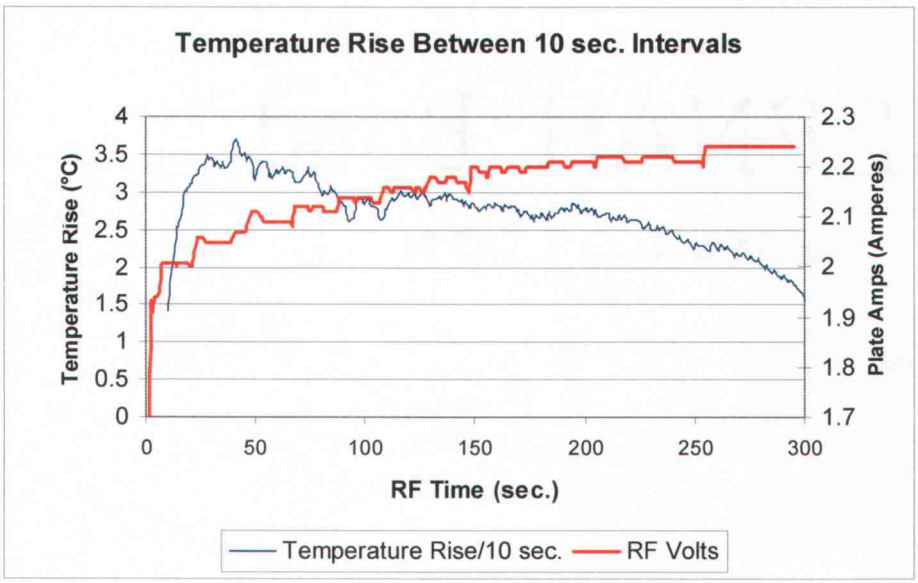

Figure 6.4 Degrees of temperature rise per 10 seconds during the RF cycle with the RF volts overlaid. Note the decrease in the rate of heating over the duration of the RF cycle.

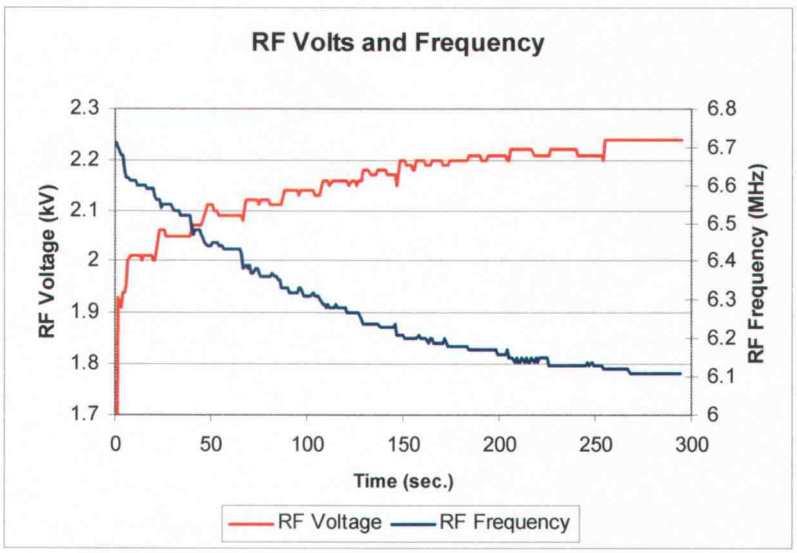

Figure 6.5 RF voltage increases while the RF frequency decreases during the RF heating cycle, reflecting changing dielectric properties of the veneer assembly. (Run #2 data)

increase in the energy transferred into the veneer assembly. The other variables in Equation 2.2 are the RF frequency and the loss tangent. One can see in Fig. 6.5 that the RF frequency decreased over the duration of the RF heating cycle. The decreasing frequency indicates that the capacitance of the veneer assembly progressively decreases. However, this decrease is not enough to offset the increase in RF volts, which is a squared function in Equation 2.2. One must conclude that a rapidly decreasing loss factor is mainly responsible for the decrease in the rate of temperature rise in the veneer assembly. Also, the loss factor must decrease more rapidly near the end of the cycle since this is where the greatest drop in the heating rate is evident. The loss factor of the adhesive prior to polymerization is known to be much greater than it is after polymerization (10 to 32 compared to 0.12 to 0.60 (Orfeuil 1987)). This reduction in loss factor is consistent with the decreasing RF frequency since the loss factor contributes to the capacitance of the LVL assembly. One may, therefore, conclude that the rapid slow down in the rate of temperature rise near the end of the RF heating cycle in an indication that most of the adhesive has reached the final stages of full polymerization.

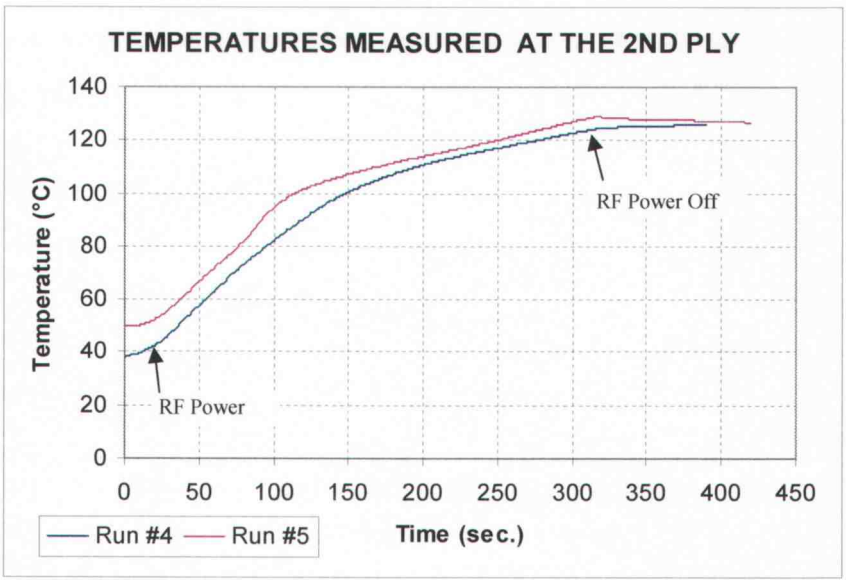

Figure 6.6 – Measured temperature rise at the second ply from the hot platen in the LVL veneer assembly which demonstrates considerable influence by the hot platen.

The focus of the discussion now turns to the temperature rise in the outer plies of the veneer assembly during RF heating. Figure 6.6 displays the measured temperature rise in the second ply from the hot platen of the LVL veneer assembly. These measurements differ markedly from the temperature measurements of the seventh ply of the assembly as shown in Figure 6.7 comparing the average temperature rise of the second and seventh plies.

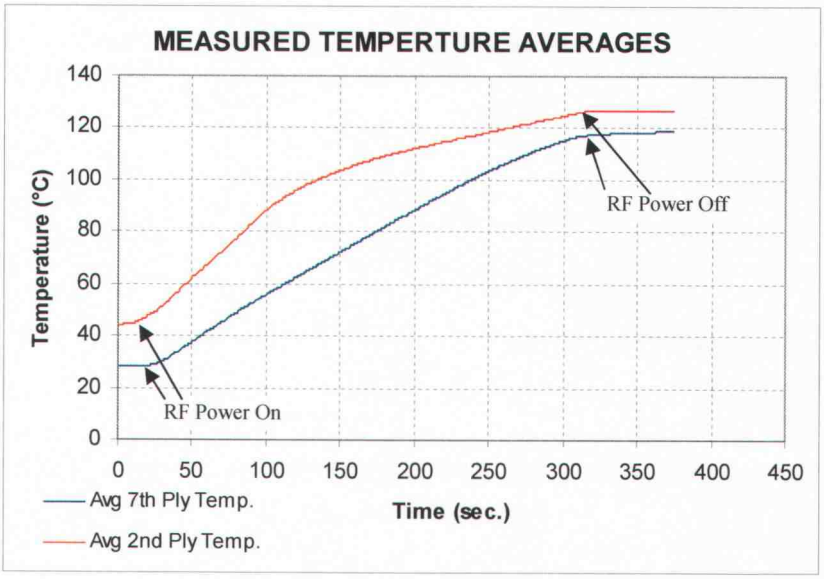

Figure 6.7 – A comparison of the average temperature rise at the second and seventh plies of the LVL veneer assembly.

One difference to note concerns the beginning temperature. The first 20 seconds of the graph is prior to the application of RF energy, yet the average temperature of the second ply is 16 °C higher than that of the seventh ply. Unfortunately, because of the methods required to execute the temperature measurements, the graph does not show the temperature rise from the moment the hot platen contacts the veneer assembly. The platen was in contact with the veneer assembly for about one minute prior to what is displayed on the graph. That minute of contact explains the higher beginning temperature.

Though there is some temperature rise prior to the application of RF energy, once the RF power is turned on the rate of temperature rise increases sharply. The slope of the temperature rise slows noticeably at around 100 °C and then continues at an almost linear rate after about 110 °C, but much more slowly than it did below 100 °C. This is a more dramatic and sustained shift in heating rate than that of the seventh ply, but still consistent with the idea that the heating rate is related to the completion of the polymerization of the adhesive.

A further observation that can be made from this graph is that the temperature reaches a peak of 128.6°C on run #5 shortly after the RF power is turned off, and then drops by 1.7°C over the next 105 seconds. It is possible that the platen temperature was in the low part of its heating cycle. The heat could be dissipating into the platen in that case. The other alternative is that the heat was migrating towards the center of the veneer assembly where the average temperature was measured at 116.7 °C. However, if that were the case then data for Run #4 should show the same pattern. On that run the temperature continued rising from 124.2°C to 126°C. Either the core temperature was higher or the platen was at the high part of its heating cycle and heat was continuing to migrate in from the platen or it could be a combination of these two. Either way, there does not seem to be a consistent pattern. Further research needs to be conducted to determine what causes the temperature to rise or fall in this region after the RF power has been turned off.

There is a difference between the temperature of the core region of the veneer assembly and that of the outer region. This evidence contradicts the assertion of Klemarewski and Annett (1995) that heating in the LVL veneer assembly in an RF press is uniform; it corroborates the work of Resnik et al (1997). The result also explains why the vast majority of the under-cure delaminations occur at the core region of the veneer assembly and most of the heat ruptures occur in the outer plies of the veneer assembly.

6.2.2 Vapor Pressure Measurements

Vapor pressure measurements were taken at the second and seventh plies of the LVL veneer assembly, along with the temperature measurements discussed above. As discussed in Chapter 5, vapor pressure is a function of temperature and moisture content of the LVL veneer assembly including the contribution of the water in the liquid adhesive, assuming that the accumulated vapor pressure can not escape. The vapor pressure measurements in Figures 6.8 and 6.9 present wide variations from one veneer assembly to another at the center region and in the outer region.

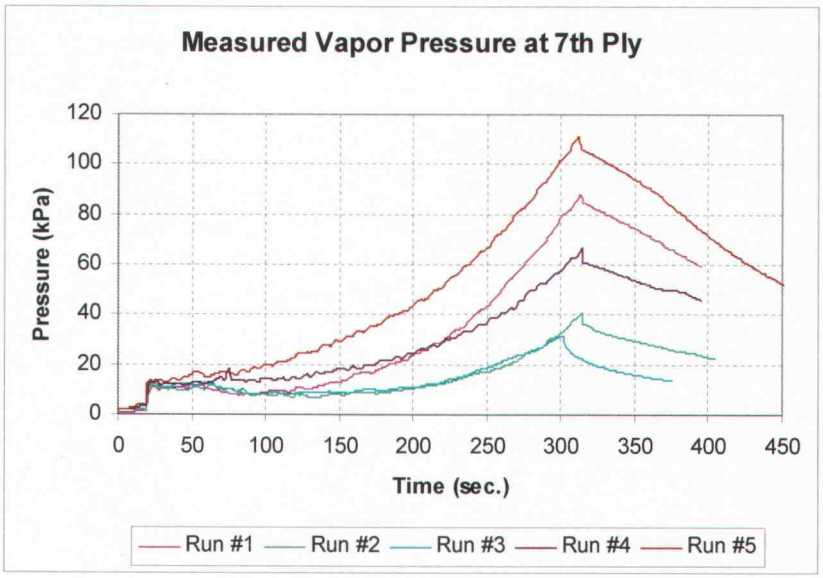

Figure 6.8 Vapor pressure measurements at the 7^{th} ply (center of the veneer assembly).

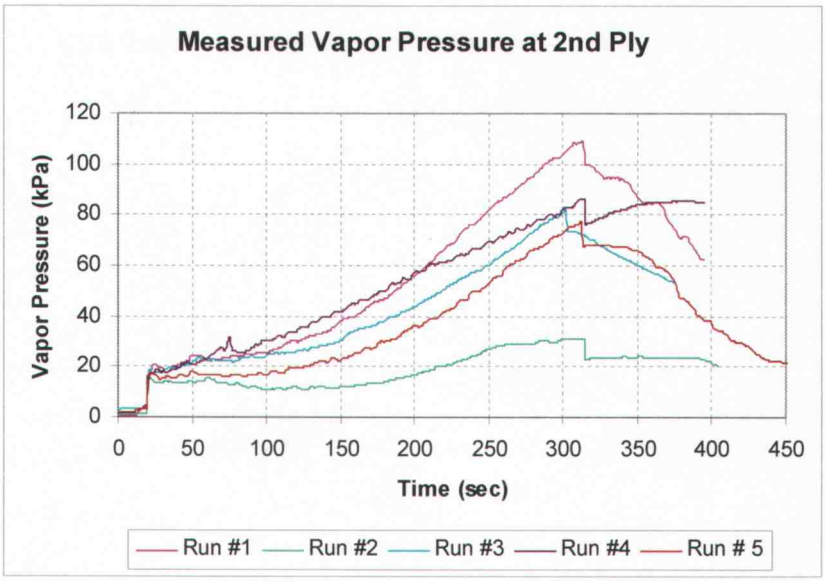

Figure 6-9 – Vapor pressure measurements at the 2nd ply (outer region of the veneer assembly.

The variations between veneer assemblies may be explained by one or more of the following factors:

1. Wide variations in the local veneer moisture content are probable. The record of veneer moisture content taken by plant staff reveals a possible range of veneer moisture content in localized areas of the veneer from less than 1% to over 15%.
2. A poor seal at the connections between the Teflon® and stainless steel tubing may be responsible for some of the low measurements. Tests in the laboratory did not suggest that leakage was likely, but it is possible. Run #2 in Figure 6.9 is suspected of having a leak, since it is significantly lower that all of the other runs. These measurements will be excluded from the comparison of averages of the two regions of the veneer assembly.
3. It is possible, though unlikely, that some vapor escaped along the small gap formed by the tubing between the veneer sheets. The tubing was very small

and the adhesive should have easily formed a seal around it once the veneer assembly was under pressure.

The variation in local veneer moisture content is the most plausible explanation for the variations in the vapor pressure measurements.

There are several observations that should be noted about these vapor pressure measurements. The sensors picked up RF interference when the RF generator was on, and this caused a jump in the pressure reading at the beginning of the RF heating cycle and a drop at its end. Even though this throws off the absolute pressure measurements, all of the runs were equally effected, so the relative comparisons are still meaningful. In future testing, an effort should be made to eliminate the RF interference.

Another observation is that the vapor pressure starts decaying after the RF power is shut off, even though the temperature remains relatively stable. This indicates that the veneer assembly is permeable to some degree. During run #5 the probes were left connected until after the press was opened. No discernable sudden drop was detected at either location in the veneer assembly when the press was opened. This suggests that there is little vertical vapor migration in the consolidated veneer assembly. Because of the tangential resistance to vapor migration, it is assumed that the majority of the vapor pressure is escaping by moving longitudinally in the veneer until it is able to escape from the end of the veneer assembly at the lap joint. Observations of steam escaping from the lap joints after the veneer assembly exited the press add credibility to this assertion.

Run #4 in Figure 6.9 is unusual in that the vapor pressure continues to rise after the RF power has been turned off. This suggests that the probe was located in a highly impermeable region of the veneer assembly and as the temperature continued to rise slightly so did the vapor pressure in this region. High density, slope of grain, or pitch may explain the impermeability of this region.

The average vapor pressure measurements taken at the seventh ply are compared to the average of those taken at the second ply in Figure 6.10. The measurements for the second run of the second ply region were excluded from the average in this figure because it was believed that there was leak in the tubing connections as noted in the above discussion.

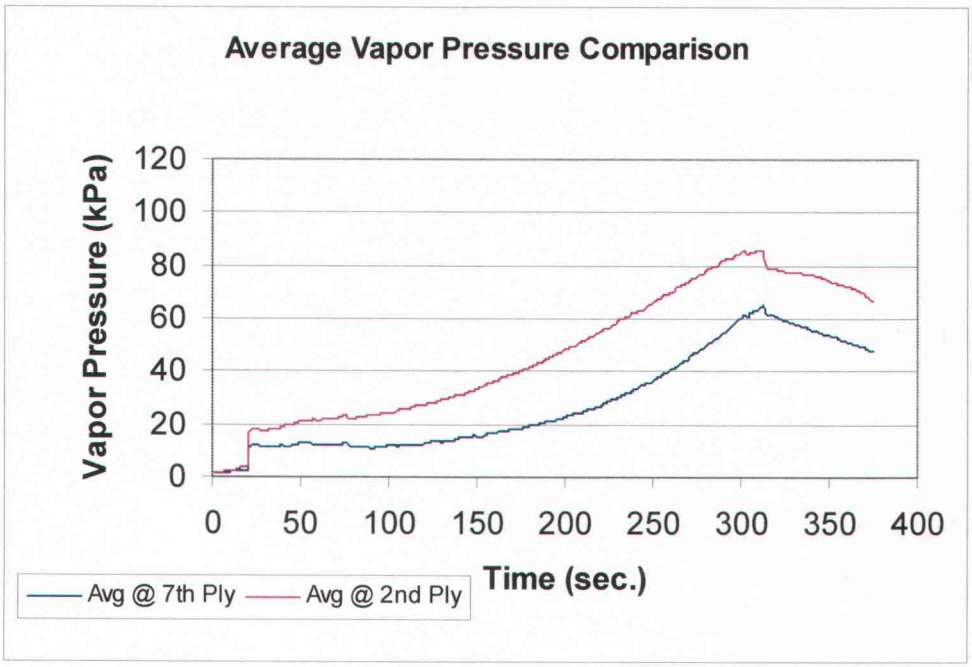

Figure 6.10 – Comparison of the average vapor pressure measurements at the second and seventh plies of the veneer assembly.

Even with the great variations between the runs, it is evident that in the RF LVL press greater vapor pressure is developed in the outer plies than in the inner plies of the veneer assembly. This contrasts with the development of higher vapor pressures at the core of the veneer assembly in conventional hot platen pressing as presented in the research of Zavala and Humphrey (1996). They theorized that the vapor pressure gradient created by the application of heat to the outer plies of the veneer assembly drove the moisture to the core where it was trapped as the adhesive lines polymerized and became impermeable. It is evident from the temperature and vapor pressure measurements presented in this study that there is little if any vapor migration to the core of the veneer assembly when it is consolidated in the RF LVL press.

This data also suggests that an optimum platen temperature may be found that would help reduce the occurrence of vapor pressure delaminations in the outer plies without reducing press through-put efficiencies. Future research is warranted.

The fact that the greatest vapor pressures are developed in the outer plies where bond strength is the most developed, rather that in the core where bond strength is the least developed would suggest that the RF LVL press can be opened with lower core bond strength development than in conventional hot platen presses without the vapor pressure causing a delamination.

6.2.3 Veneer Assembly Thickness

Thickness measurements were attempted during the RF pressing cycles as described in section 4.2.2 of this work. The averaged data from the 5 pressing cycles are presented in Figure 6.11. Due to improper grounding, the RF energy interfered with the LVDT sensor and introduced a great deal of noise into the signal. When the RF power was turned on, a 1.2 mm drop in the thickness measurement was induced. Conversely, when the RF power was shut off, a 2.9 mm jump occurred. The data is still meaningful if one allows for this offset due to RF interference. It should also be noted that between the times when the LVDT was zeroed out when the press was empty and when this data was collected something happened to cause the LVDT assembly to be moved off of zero by about 10 mm. Even though the actual measurements are in error the relative measurements are useful. The relative measurements are the ones that are of greatest interest in this study.

At the beginning of the pressing cycle plotted in Figure 6.11, the weight of the upper press platen assembly is resting on the LVL veneer assembly. The estimated load on the veneer assembly is 0.14 kg/cm^2. The average thickness measurement at that point in time is 52.6 mm. After the hydraulic pressure was applied it reached its peak of 15.1 kg/cm^2 within 20 seconds. The average thickness was reduced by 3.7 mm, or 7%, to 48.9 mm. During the pressing cycle the data demonstrates that there is small amount of additional compression of the veneer assembly until about 150 seconds has elapsed. This is attributable to the stepped pressure program of the pressing process. The thickness remains relatively stable from there until the end of the pressing cycle. Once the RF power is shut off and the RF interference is eliminated from the LVDT measurements, the

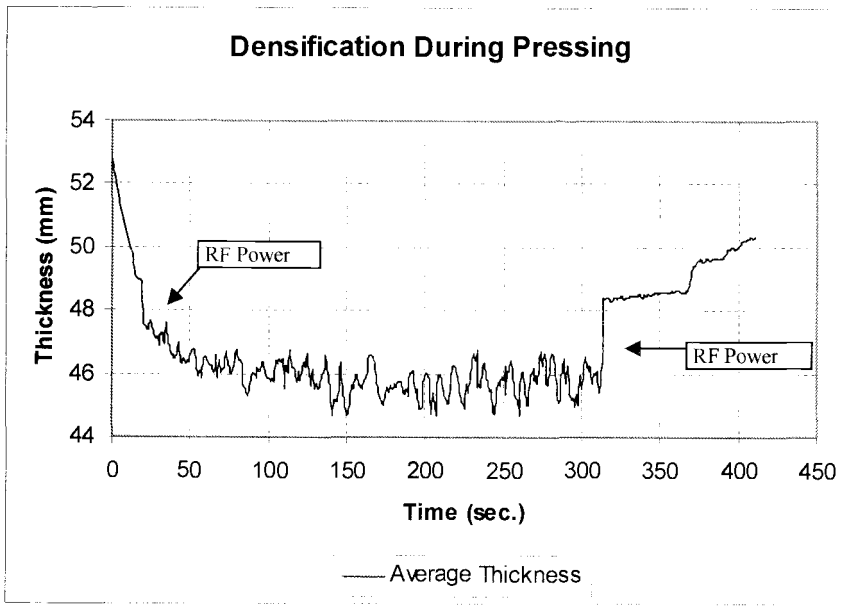

Figure 6.11 – The averaged data from the 5 RF pressing cycles are presented here.

thickness average is 48.3 mm which is an 8.2% reduction from the starting thickness. Pressure on the veneer assembly at this point is about 8.0Kg/cm^2. When the pressing cycle ends at 370 seconds, the hydraulic pressure is released and a jump in thickness of the veneer assembly of about 1 mm occurs. The final thickness is 49.7 mm which represents a 5.5% densification from the starting thickness of the veneer assembly.

Wood is widely known to be hygro-visco-elastic and that densification is a function of time, temperature, moisture content and pressure. The time in the RF pressing cycle is about one third that of conventional hot platen pressing and the platen temperature is significantly lower. Therefore, one would tend to expect that densification in the RF LVL press would be less than that of conventional hot pressing. However, the 5.5% densification measured here is comparable with the results reported by Wellons et al (1982) in similar stepped pressure hot pressing of Douglas-fir plywood panels. This similarity in densification may be explained by the fact that the whole veneer assembly is heated at once by the RF energy and therefore the whole assembly softens rapidly and is compressed by the platen pressure. Whereas, in conventional hot platen pressing the tem-

perature rise moves slowly to the core of the veneer assembly. This would suggest that in conventional hot pressing the outer portion of the veneer assembly would experience greater densification that the core region. However, in RF pressing, one would expect a more uniform densification of the assembly. Further research needs to be conducted to verify this hypothesis.

6.3 THE DETERMINISTIC MODEL EVALUATED

The deterministic model presented in Chapter 5 is evaluated here in terms of the predicted temperature and vapor pressure values compared to the actual measurements from the subject press when the variables of the model are set to the conditions of the subject press. The bond strength predictions of the model were not evaluated in this manner as there is no practical way to do so at the subject LVL production plant.

The following values were used in the deterministic model for this evaluation. They were derived from data collected at the subject RF LVL pressing plant when the pressing data was collected.

- RF generator plate volts = 11.7 kV
- RF efficiency factor = 0.56
- Press platen temperature = 128°C
- Veneer assembly density (OD) = 0.521 g/cm^3
- Veneer assembly moisture content = 8.76%
  (includes contribution of water in the adhesive)
- Initial veneer assembly temperature = 28.5°C

6.3.1 Temperature Development

A typical set of predicted temperature values are presented in Figure 6.12. Region 1 is located 0.75 mm from the interface of the hot platen and the veneer assembly. Regions 2 through 13 represent locations at 1.5 mm intervals with region 13 at the center of the as-

sembly illustrated in Figure 5.2 in Chapter 5. Differences in rate of temperature rise across the vertical dimension of the theoretical veneer assembly are evident

The model results illustrate the dramatic influence of the hot platens on the temperatures of the outer regions of the veneer assembly. Predicted temperature rise in the outer five regions rises rapidly before any RF energy is applied. This is due to the ex-

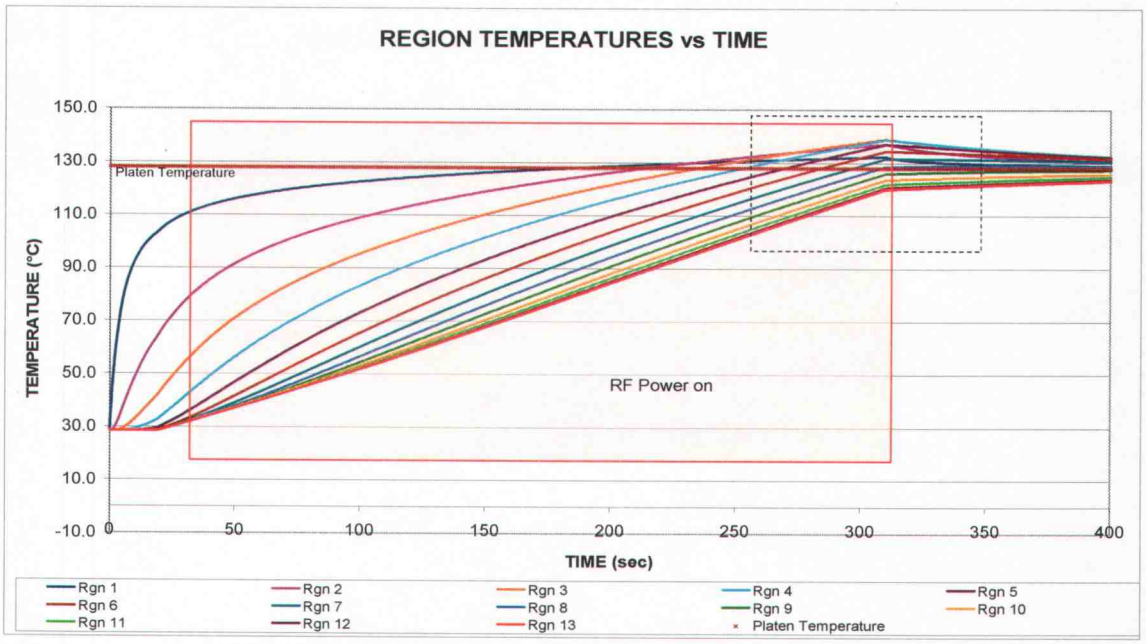

Figure 6.12 – Temperature results from the deterministic model with the fixed variables set to the pressing parameters the day the pressing measurements were made at the subject plant. The dashed boxed region is enlarged in Figure 6.14 for clarity.

treme temperature gradient between the hot platen and the much cooler veneer assembly. After the initial rapid rise in temperature, the rate of predicted temperature rise moderates as the temperature differential between the veneer assembly and the hot platen is becomes smaller. After about 175 seconds into the pressing cycle, the model predicts that the majority of the energy added to these outer regions comes from RF energy and the temperature rise nearly parallels that of the central regions.

The model predicts an interesting phenomenon during the later portion of the RF heating cycle. This region is enlarged for clarity in Figure 6.13. Predicted temperature differential in the outer plies actually reverses beginning at about 185 seconds into the pressing cycle. At that point the model predicts that the heat begins migrating from the outer regions into the hot platens as well as towards the central regions. The model predicts that the greatest heat develops about 2.5 to 3.5 mm (regions 3 & 4) in from the hot platen. This is consistent with the subject plant's experience in which the vast majority of heat related ruptures occur in this region.

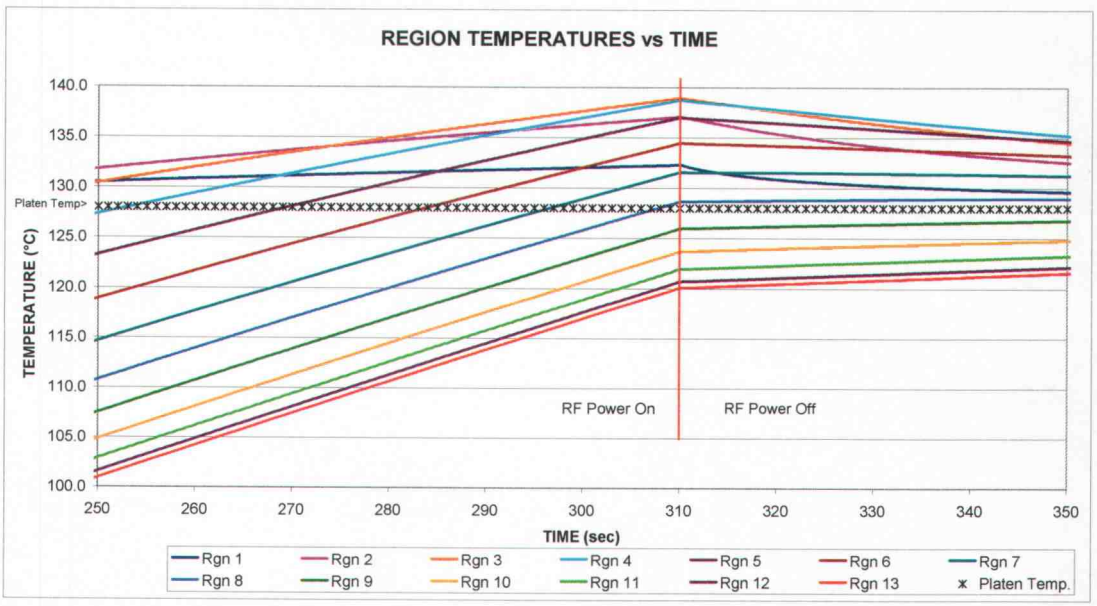

Figure 6.13 – Enlarged area of Figure 6.12 showing the predicted temperatures of the outer regions exceeding the platen temperature of 128°C. Once the RF power is turned off the heat in outer regions migrates into the platen and to center regions of the veneer assembly.

Almost no influence from the hot platens is predicted for the five regions at the core of the veneer assembly. The heating of these central regions is almost entirely the result of the applied RF energy. Once the RF power is applied, the predicted temperature begins to rise immediately and continues rising at a near steady rate until the RF power is

turned off. Once the RF power is turned off, the model predicts that the temperature of the central regions continues to rise slowly as heat from the hotter outer regions migrates toward the central regions. The model predicts that the central region develops the lowest temperature in the veneer assembly during the RF pressing cycle. This is again consistent with experience gained at the subject plant; under cure delaminations occur in this region the vast majority of the time.

The measured temperatures from Section 6.2 above are compared to the predicted temperatures of the deterministic model in Figures 6.14 and 6.15. The data from the two pressing cycles for each of the two locations in the veneer assembly were averaged together and plotted on the graph along with the regions of the model that best approximated these measurement locations. Data for the core of the veneer assembly is plotted in Figure 6.14. The 2nd ply location and region 4 are plotted in Figure 6.15.

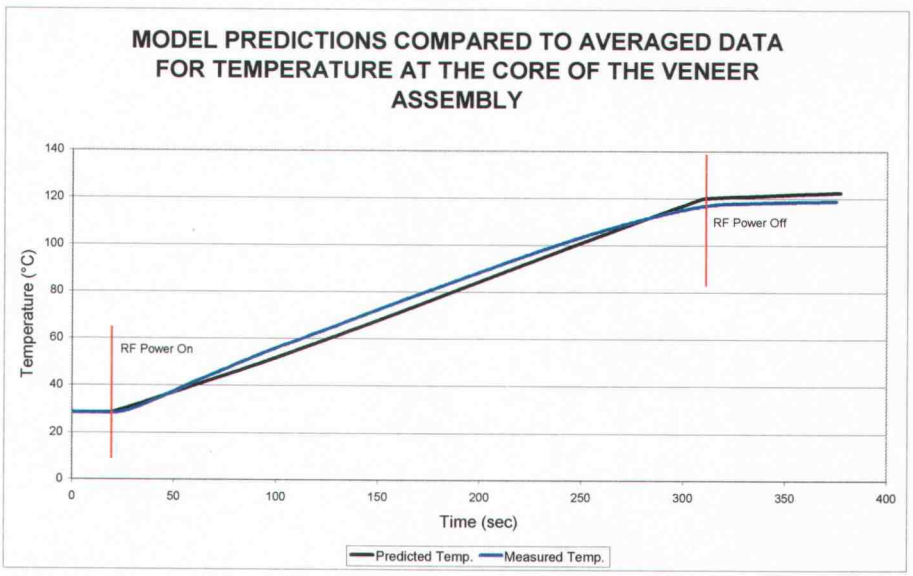

Figure 6.14 – Predicted model temperature data compared to the averaged actual temperature measurements at the 7th ply (center) of the veneer assembly.

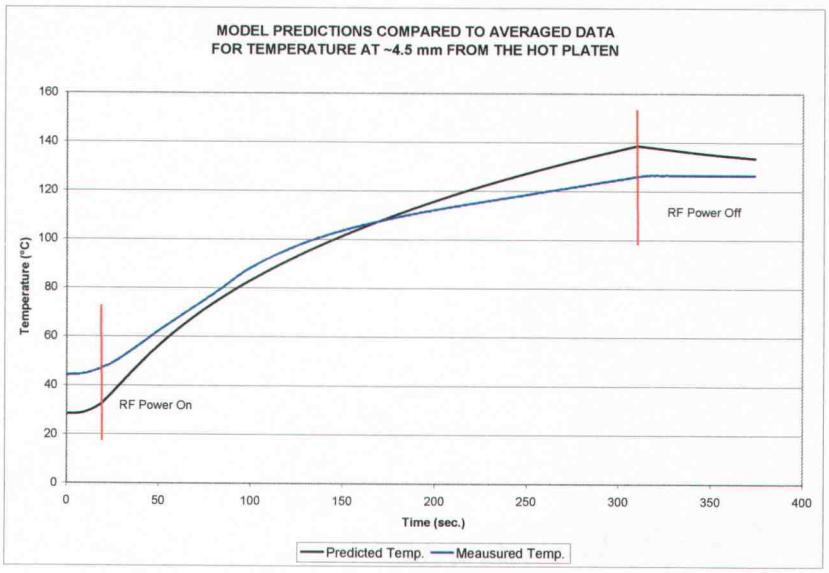

Figure 6.15- Predicted model temperature data compared to the averaged actual temperature measurements at the 2nd ply (~4.5 mm from hot platen) of the veneer assembly.

At the core, the predicted temperatures closely approximate the actual temperature measurements even though the actual temperatures are based on only two pressing cycles. There are three minor divergences that deserve some discussion.

First, there is a divergence at the beginning of the pressing cycle where the measured temperature lags the predicted temperature. This may indicate that the loss factor increases somewhat after the initial application of RF power. Since the effect it relatively minor in this study, it does not warrant further discussion here. After about 30 seconds, the actual temperature corresponds well with the predicted value. As the pressing cycle proceeds, the second divergence occurs. The measured temperature diverges from and exceeds the predicted temperature for the next 240 seconds. The greatest difference of 4.5°C comes at 160 seconds into the pressing cycle. This difference is relatively minor. A larger sampling of pressing cycles is necessary in order to determine if an adjustment should be made to the deterministic model to make it more accurate for this period of the RF pressing cycle. The third divergence noted is as at the end of the RF cycle. As discussed in Section 6.2, the measured rate of temperature rise decreases significantly after

the local region's temperature exceeds about 110°C. This is not accounted for in the current model. As a result, the predicted temperature overtakes the measured temperature at 270 seconds into the RF pressing cycle. At the conclusion of the pressing cycle the measured temperature is 3.5°C below the predicted temperature for this region. This divergence will be discussed later in conjunction with a similar divergence in the outer region.

The averaged measured temperature in the veneer assembly at about 4.5 mm from the hot platen is compared to the predicted temperature of region 4 of the deterministic model in Figure 6.15. In the outer region the measured temperature starts out higher than the predicted temperature and remains that way until the mid-point of the RF pressing cycle. The difference early in the cycle is mainly due to the fact that the press was closed and under pressure for nearly a minute before all the connections of the sensors to the data logger could be made. Therefore, the temperature at this region started out 15.5°C higher than the beginning temperature of the deterministic model. Figure 6.16 displays

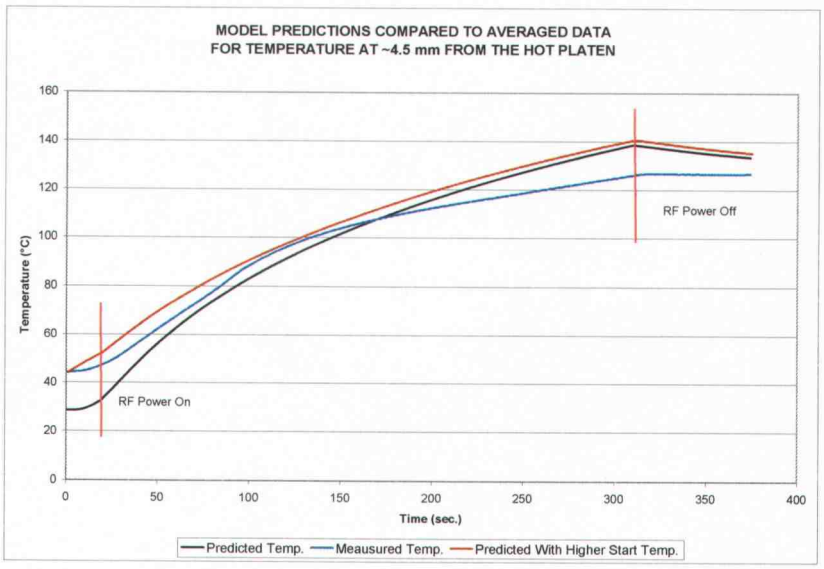

Figure 6.16 – A comparison of predicted temperatures and measured temperatures in the region of the veneer assembly ~4.5 mm from the hot platen including the initial temperature of the deterministic model adjusted for the time the assembly was pressing prior to completing the connections to the data logger.

the plot of data from the model if it is adjusted to incorporate the higher initial temperature. The main effect of making this adjustment to the deterministic model is that the predicted temperature is just shifted upwards and it starts increasing rapidly from the very beginning of the pressing cycle. Other than that, the slope of the line changes very little and does not appreciably improve the accuracy of the model.

The most significant divergence of the predicted temperatures and the measured temperatures occurs after the measured temperature rises to 100°C, at which time the slope of the line begins to flatten out. At 110°C the measured rate of temperature rise remains nearly constant until the RF power is shut off. As discussed in Section 6.2, this change in rate appears to be related to the polymerization of the adhesive in the veneer assembly. (One might think that the phase change of liquid water to vapor may also play a role in the decrease of the loss factor. However, this writer did not find anything in the literature to indicate that there is a significant shift in the loss factor due to phase change of water.) Future development of the deterministic model should be modified to account for this decline in the heating rate above 110°C.

In summary, the deterministic model generally predicts well the relative temperature gradient developed in the veneer assembly during the RF pressing cycle. Further refinement is needed to produce more accurate predictions. Still it may prove to be a useful tool for predicting the general impact of changes in the pressing material and/or pressing parameters on the temperature changes in the veneer assembly during RF pressing cycles.

6.3.2 Vapor Pressure Development

The predicted vapor pressure development plots for all regions of the model are presented in Figure 6.17. The vapor pressure development plots are based on the pressing parameters listed in Section 6.1 above. The model assumes uniform moisture content throughout the veneer assembly. Therefore, the only variable that effects vapor pressure development is temperature in the region. The model predicts that the highest vapor

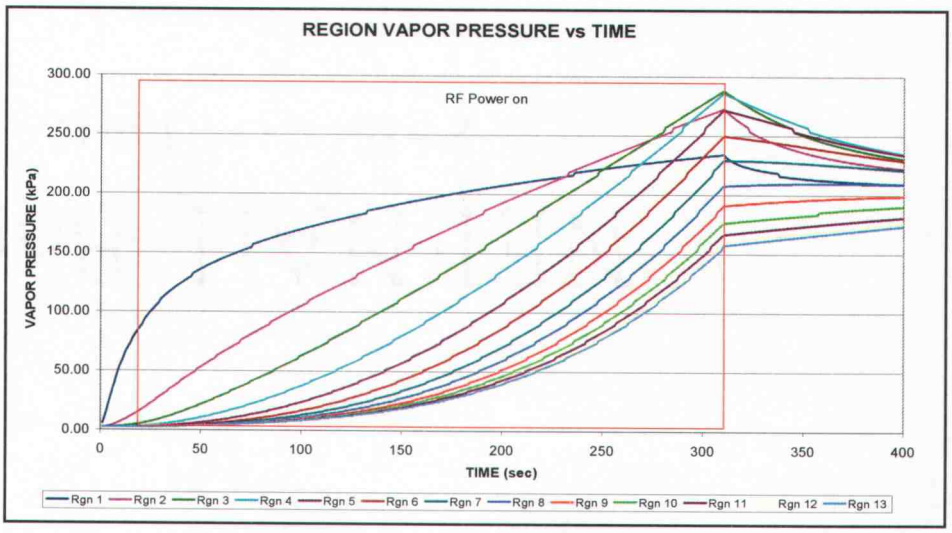

Figure 6.17 – Predicted vapor pressure developments of all regions derived from the deterministic model using the pressing parameters listed in Section 6.1.

pressure is developed in regions 3 and 4 where the greatest heat is generated in the veneer assembly. Likewise, the lowest region of vapor pressure development is region 13 at the core of the veneer assembly were the least amount heat is generated during the RF pressing cycle. By the end of the RF heating cycle, the predicted vapor pressure differential is 130 kPa between regions 3 and 13.

The difference between the predicted vapor pressures generated within the veneer assembly and the average measured vapor pressures is quite dramatic, as illustrated in Figures 6.18 and 6.19. At the end of the RF heating cycle, the difference between the predicted and measured vapor pressures at the core of the veneer assembly is 95 kPa. The difference is more than double that at the region that is ~4.5mm in from the hot platen at 218 kPa. Contrary to the predicted vapor pressure differential between the core and the outer region, the measured vapor pressures are virtually the same with a difference of only 6 kPa.

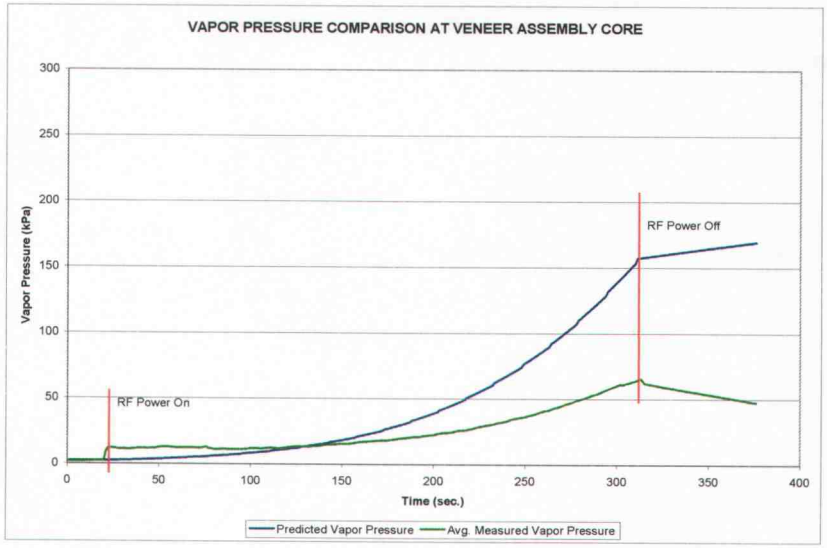

Figure 6.18 – Predicted vapor pressure development compared to the averaged measured vapor pressure development at the center of the veneer assembly. The sudden jump in measured vapor pressure at 20 seconds into the pressing cycle is the result of RF interference with the sensor. A small drop occurs when the RF power is turned off at 320 seconds into the pressing cycle.

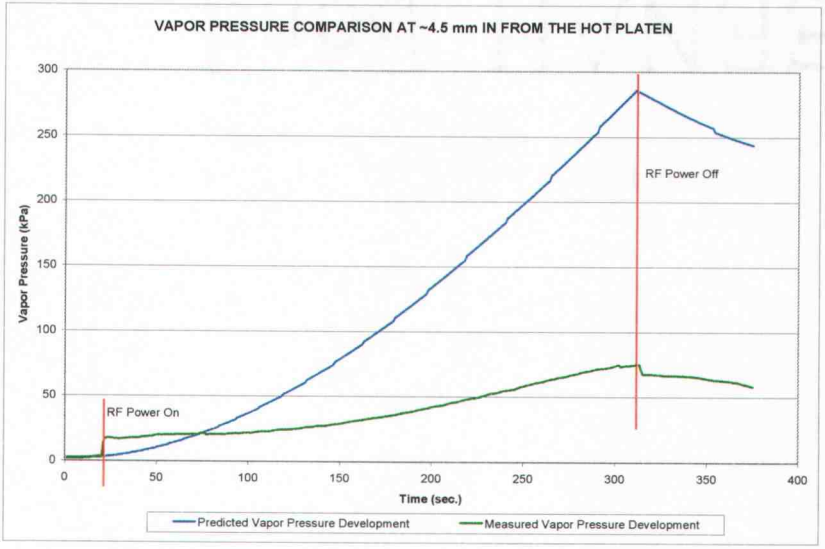

Figure 6.19 – Predicted vapor pressure development compared to the averaged measured vapor pressure development at ~4.5 mm down into veneer assembly from the hot platen. The sudden changes in the measured vapor pressure are the result of RF interface as explained in Figure 6.18.

How can these discrepancies be accounted for? Logically, either the assumptions of the deterministic model about vapor pressure are in error or the vapor pressure sensor set-up was faulty or there is an error in the mathematical formulas used in the deterministic model. It is possible that it is the result of a combination of these possible sources.

The assumption that there is little vapor migration to the exterior of the veneer assembly may not be true. The work of Zavala and Humphrey (1996) is strong evidence that this is highly improbable. Their research demonstrated that there is little vapor migration in a veneer assembly to the exterior from the position in the assembly that these measurements were taken from.

Another possible faulty assumption is that the moisture content is uniform in the veneer assembly. It is known that veneer moisture content varies from less than 1% to over 15% in extreme cases. When 4% and 12% initial moisture content are set as the fixed moisture content variable in the deterministic model, the peak predicted vapor pressure at ~4.5mm from the platen is 208 kPa and 305 kPa respectively. The variability of the veneer moisture content does not, therefore, fully explain the discrepancy.

The sensor set up may be another source that contributes to the difference between the predicted and measured vapor pressures. Since the measured pressures are all so much less than the predicted values, it would have to be a fundamental flaw in the set up. Every effort was made to ensure that there was no leakage of vapor from the connections. It is possible that there was some compression of the vapor in the Teflon® tubing but it is not likely that this compression would have such a dramatic effect on the readings. It is also possible that the adhesive failed to form a sufficient seal around the stainless steel tubing between the plies of veneer, allowing some vapor to escape along the outside of the tube to the exterior of the veneer assembly. The research of Zavala and Humphrey (1996) measured peak vapor pressure in a five ply Douglas-fir veneer assembly at 186 kPa. This study's measurement of peak vapor pressure of 105 kPa casts some suspicion that, indeed, there may have been some defect in the sensor set up. It also casts suspicion on the deterministic model which predicted a peak vapor pressure of over 280 kPa.

The final possibility is that the mathematical equation used in the deterministic model is in error. This equation has been checked over very closely and no errors were discovered.

Further research is required to determine the source of the discrepancy between measured and predicted vapor pressure values. New vapor pressure measurements could be taken using low density silicon oil in the Teflon® tubing. Also, a better method of ensuring that no vapor can escape along the outside of the stainless steel tubing should be investigated.

6.3.3 Sensitivity Studies Using the Deterministic Model

The deterministic model was never intended to precisely predict temperature, vapor pressure, or bond strength development within the LVL veneer assembly. Rather, it was intended to predict relative changes and trends based on changes in the operating parameters of the press. In this way one may gain a basic understanding of the type and comparative magnitude of the effect each of the operating parameters has on the development of temperature, vapor pressure and bond strength within the various regions of the LVL veneer assembly. Even with the obvious flaw in the model's current ability to predict vapor pressure development, sensitivity studies with the model may be helpful.

Any of the operating parameters in list below may be changed incrementally:

- RF generator plate volts
- RF efficiency factor
- Press platen temperature
- Veneer assembly density (OD)
- Veneer assembly moisture content
- Initial veneer assembly temperature

The effects of the changes on the system may then be analyzed graphically and/or numerically to understand what the contribution of that parameter is to the process of the consolidation of the LVL veneer assembly within the RF press. Changing the parameters is easily accomplished in the EXCEL® spreadsheet and the results are almost instantane-

ous. This allows a great deal of exploration of operating parameters without having to actually interrupt regular LVL production and to risk producing substandard product.

Normally, sensitivity studies involve making a number of small progressive changes in a system and observing the gradual changes. However, here for illustrative purposes, a comparison will be made with one large change to demonstrate how the deterministic model might be used to explore a change in operating the platens at ambient temperature rather than at the current operating platen temperature. If it were possible to operate the platens at ambient temperatures, energy savings could be significant. Figure 6.20 com-

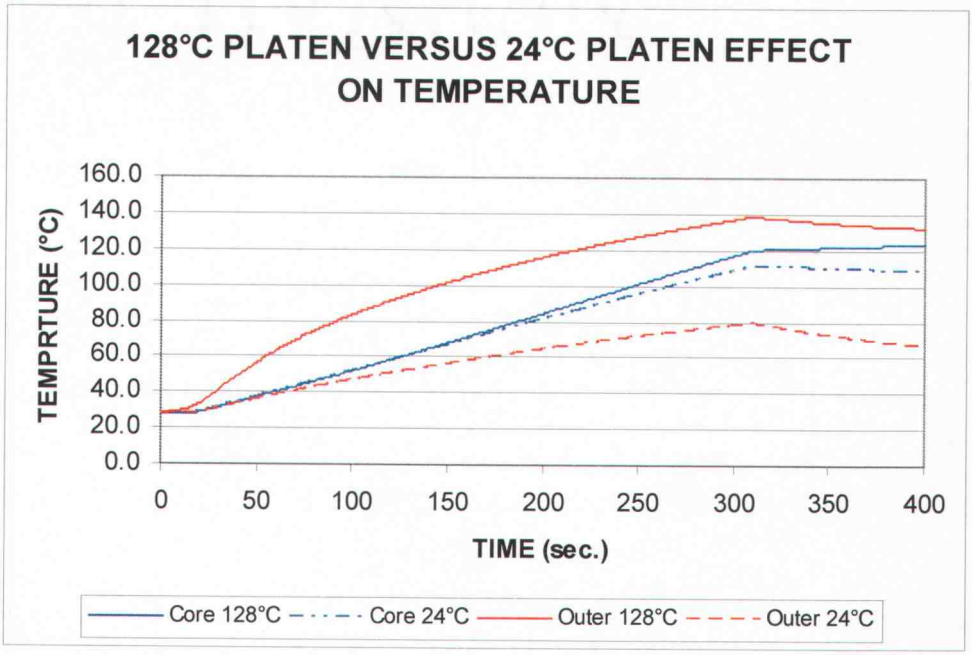

Figure 6.20 The predicted effect on temperatures within veneer assembly when operating the press platens at ambient temperature is compared to normal hot platen operation of the RF LVL press.

pares the effect of changing the temperature of the platens from 128°C to 24°C (≈ ambient) at the core of the veneer assembly and at the outer region ~4.5mm in from the platen. At the core there is only a 10°C predicted temperature reduction. However, the difference is dramatic in the outer region where the peak temperature difference is pre-

dicted to be 40°C cooler with ambient platens than with 128°C platens. With the ambient platens, the outer region is predicted to not exceed 80°C. This drop in temperature could be compensated for to some degree by extending the duration of RF energy application. However, according to the model, the RF power application would need to be extended by over 200 seconds in order for the outer region to reach 100°C. By that time the model predicts the core temperature would exceed 150°C, which is unacceptably high and would most certainly result in a rupture in the core of the veneer assembly at press opening due to extreme vapor pressure development.

Operating the platens at ambient temperature has significant implications for bond strength development as well. This is illustrated in Figure 6.21. In this graph one can see that the bond strength of the outer region is predicted to only achieve about one third

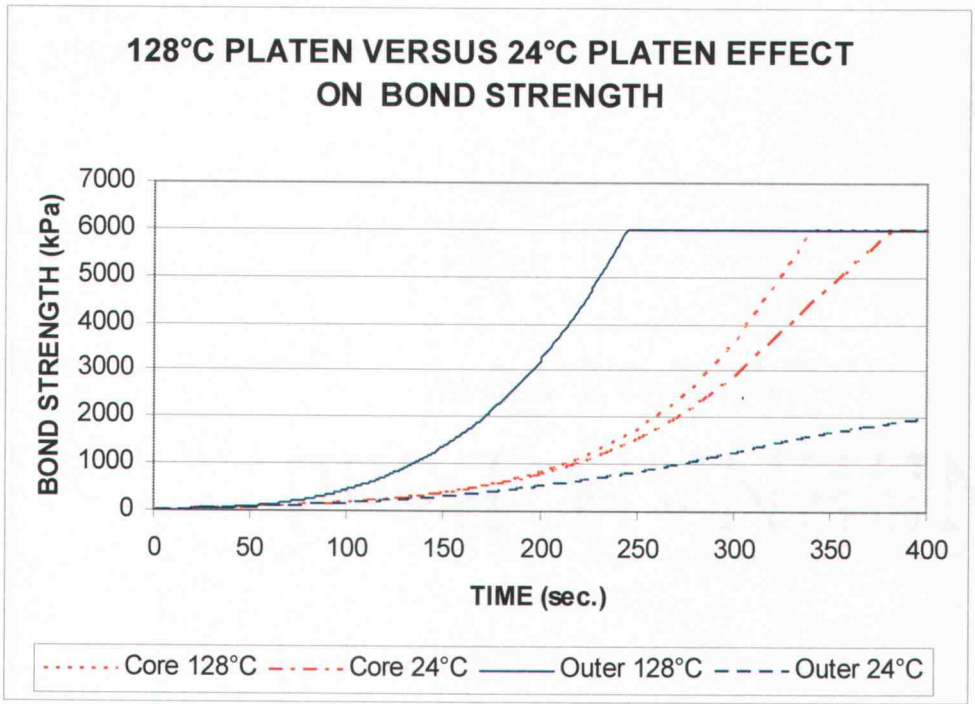

Figure 6.21 The predicted effect on temperatures within veneer assembly when operating the press platens at ambient temperature is compared to normal hot platen operation of the RF LVL press. The outer region of the veneer assembly only reaches one third of maximum bond strength while there is only a minor effect at the core.

of the maximum bond strength of 6000 kPa. This prediction, combined with a predicted maximum temperature of 80°C, would indicate that the adhesive would not achieve adequate polymerization under these conditions to provide sufficient bonding of the veneers in this area. This prediction is consistent with actual experience at the subject plant when an attempt was made to continue operation of the RF press after the hot oil system failed. Once the platen temperatures fell to a certain level, adequate bond quality could not be maintained in the outer plies even with extended RF power application.

This prediction and the actual plant experience contradict the findings of Bodenheimer's (1993) research which concluded that RF pressing would be feasible with the press platens at ambient temperature. His research was conducted in a relatively small laboratory press (1.22 m square) using an adhesive formula with an unusually high resin solid content (48%).

One way to overcome the migration of heat into the cold platens would be to use thermally insulated platens to prevent heat from migrating out of the veneer assembly. The only drawback to this platen arrangement would be if the RF generator went down for an extended period of time, there would be no back up system to heat the veneer assembly. Production would be halted until repairs to the RF generator could be completed.

A full sensitivity study of the platen temperatures in the deterministic model may prove helpful in finding the optimal platen temperature for use in RF LVL pressing for each thickness of product produced. This would help to quickly find the range of platen temperatures to begin actual pressing trials with saving time and wasted product.

Any number of sensitivity studies could be conducted using this model that may prove helpful to optimize the operation the subject RF LVL press. For example, one could study the effects of veneer moisture content on temperature, vapor pressure and bond strength development. Another study could look at variations to the application of the RF power throughout the pressing cycle. These studies may not give definitive results, but they may help to narrow scope of actual experimentation required on the press itself and point to which parameters could be changed to provide the greatest pressing benefit.

CHAPTER 7
CONCLUSIONS AND RECOMMENDATIONS FOR FURTHER STUDY

The main objective of this study was the development of a deterministic model to be used to gain insight and understanding into temperature, bond strength, and vapor pressure development within the veneer assembly of an industrial LVL RF batch press. Such a model would be useful for optimizing the pressing process and problem solving. The model proposed was a one dimensional one to allow pressing parameters to be easily manipulated and produce quick output in both graphical and numerical forms. The goal of the model was not precise accuracy, but one that would qualitatively demonstrate the impact and importance of the various pressing parameters on the development of temperature, vapor pressure, and bond strength. To a large extent, this goal has been realized.

7.1 CONCLUSIONS FROM THIS STUDY

1) One may predict the temperature gradient development in the vertical dimension through the veneer assembly from platen to platen using a spreadsheet format for a one dimensional RF LVL pressing model. These predictions appear to both qualitatively and quantitatively approximate actual temperatures during the LVL RF pressing process for nominal 38 mm thick Douglas-fir veneer assemblies.
2) Based on the temperature predictions over time during the RF pressing process, relative bond strength development within the LVL veneer assembly can be estimated using the deterministic model and the bond strength development characteristic equation determined from bonding kinetic studies using the ABES for the adhesive formula being used.
3) Both actual measurements and predicted values demonstrate that temperature and vapor pressure gradients developed within the LVL veneer assembly dur-

ing the RF pressing process are fundamentally different than those in conventional hot platen pressing.

4) Further, both actual measurements and predicted values demonstrate that temperature and vapor pressure development are not as uniform within the veneer assembly during an RF pressing cycle as some have postulated.
5) The spreadsheet format is a suitable and useful tool for one dimensional finite differencing modeling of the RF LVL pressing process. It provides a user friendly format for sensitivity studies with almost instantaneous results both graphically and numerically.

7.2 RECOMMENDATIONS FOR FURTHER RESEARCH

1) First and foremost, further research is necessary to improve the accuracy of the model in terms of the prediction of vapor pressure development within the LVL veneer assembly. The magnitude of the differences found in this study between the predicted values and the measured values, demonstrate that there are some significant flaws in the deterministic model and/or in the method of vapor pressure measurement within the LVL veneer assembly. Correct grounding of the sensors and data logging should be employed to eliminate or greatly reduce the RF interference in the data collection. It is noted that accurate vapor pressure predictions will be difficult due to the normal variation in veneer moisture content in localized areas.
2) The model could be refined to account for the change in density over time during the pressing cycle and its effect on temperature and vapor pressure development and distribution. A better means of measuring the thickness of the LVL assembly during pressing would aid in this refinement.
3) Research could be conducted comparing the cross-sectional density profiles of LVL consolidated within an RF LVL press with that of the density profile of comparable LVL consolidated in a hot platen press.

4) The model could also be improved by enabling it to account for the effect of the boundary conditions at the adhesive veneer interfaces between the plies of the veneers.
5) Additional comparisons between the predicted values of temperature and vapor pressure from the deterministic model and actual the corresponding measured values in other thicknesses of LVL veneer assemblies should be conducted to determine the robustness of the deterministic model for other thicknesses of RF LVL pressing.

END

BIBLIOGRAPHY

Annett, D. M. and C. Bowering. 1991. High frequency heating in LVL manufacturing yields significant cost reduction. *In:* Proceedings of the 25th International Particleboard/Composite Materials Symposium, Pullman, WA. pp. 109-124.

Baldwin, R. F. 1995. Plywood and veneer-based products: manufacturing practices. Miller Freeman Books, San Francisco. 388 pp.

Biryukov, V. A. 1961. Dielectric heating and drying of Wood. (Protsessy dielektricheskogo nagreva i sushki drevesiny). Translated from Russian [by R. Kondor and H. Olaru. Edited by T. Pelz] Jerusalem, Israel Program for Scientific Translations; [available from the U.S. Dept. of Commerce, Clearinghouse for Federal Scientific and Technical Information, Springfield, Va.] 1968. 117 pp.

Bodenheimer, T. W. 1992. Production of laminated veneer lumber using high frequency heating in the pressing operation. M. S. thesis, Washington State University, Pullman, WA. 53 pp.

_____. 1993. Production of laminated veneer lumber using high-frequency heating in the pressing operation. *In:* Proceedings of the 26th International Particleboard/Composite Materials Symposium, Pullman, WA. pp. 281-282.

Bohlen, J. C. 1974. Tensile strength of Douglas-fir laminated veneer lumber. For. Prod. Jour. 24(2):16-23.

_____. 1975. Shear strength of Douglas-fir laminated veneer lumber. For. Prod. Jour. 25(2):16-23.

Bolton, A. J. and P. E. Humphrey. 1988. The hot pressing of dry-formed wood-based composites. Part I. a review of the literature, identifying the primary physical processes and the nature of their interaction. Holzforschung 42(6):403-406.

_____. 1989a. The hot pressing of dry-formed wood-based composites. Part. III. Predicted vapour pressure and temperature variation with time, compared with experimental data for laboratory boards. Holzforschung 43(4):265-274.

_____. 1989b. The hot pressing of dry-formed wood-based composites. Part IV. Predicted variations of mattress moisture content with time. Holzforschung 43(5):345-350.

_____. 1994. The permeability of wood-based composite materials. Part I. A review of the literature and some unpublished work. Holzfor-

chung 48(1994) Suppl. 95-100. As quoted by D. Zavala and P. E. Humphrey. 1996. Hot pressing veneer-based products: The interaction of physical processes. For. Prod. Jour. 46(1):69-77.

Bolton, A. J. and P. K. Kavvouras. 1989. The hot pressing of dry-formed wood-based composites. Part III. Predicted vapor pressure and temperature variation with time, compared with experimental data for laboratory boards. Holzforchung 43:265-274. *As cited in*: Zavala, D. and P. E Humphrey. 1990. Hot pressing veneer-based products: The interaction of physical processes. For. Prod. Jour. 46(1):69-77.

Bowen, M. E. 1970. Heat transfer in particleboard during pressing. Ph.D. Thesis, Colorado State University, U. S. A. *As cited in:* Humphrey, P. E. and A. J. Bolton. 1989. The hot pressing of dry-formed wood-based composites.: II. A simulation model for heat and moisture transfer, and typical results. Holzforschung 43(3):199-206.

Brashaw, B. K., X. Wang, R. J. Ross and R. F. Pellerin. 2002. Relationship between stress wave velocities of green and dry veneer. For. Prod. Jour. 54(6):85-89.

Brown, G. H., C. N. Hoyler and R. A. Bierwirth. Theory and application of radio-frequency heating. D. Van Nostrand Co. Inc., New York.

Brown, J. H. 1963. Mechanism of electrical conduction in wood. For. Prod. Jour. 13(10):455-458.

Cable, J. W. 1954. Induction and dielectric heating. Reinhold Publishing Corp., New York. 576 pp.

Carruthers, J. F. S. 1959. Heat penetration in the pressing of plywood. Forest Products Res. Bull. *44*. H. M. S. O., London. *As cited in:* Bolton, A. J. and P. E. Humphrey. 1988a. The hot pressing of dry-formed wood-based composites. I. a review of the literature, identifying the primary physical processes and the nature of their interaction. Holzforschung 42(6):403-406.

Chade, J. C. and E. T. Choong. 1968. Influence of cutting velocity and log diameter on tensile strength of veneer across the grain. For. Prod. Jour. 19(7):52 & 53.

Chen, T. L. and S. W. Churchill. Heat flow through granular structures. American Inst. Chem. Eng. J. 37(4):157-161. *As cited in:* P. E. Humphrey and A. J. Bolton. 1989. The hot pressing of dry-formed wood-based composites.: II. a simulation model for heat and moisture transfer, and typical results. Holzforschung 43(3):199-206.

Chow, S. –Z. 1968. A kinetic study of the polymerization of phenol-formaldehyde resin in the presence of cellulosic materials. Wood Science 1(4):215-221.

Collett, b. M. 1972. A review of the surface and interfacial adhesion in wood science and related fields. Wood Sci. and Tech., 6:1-42.

Echols, R. M. and R. A. Currier. 1973. Comparative properties of Douglas-fir boards made from parallel-laminated veneers vs. solid wood. For. Prod. Jour. 23(2):45-47.

Engelhardt, F. 1979. Untersuchungen über die Wasserdampfsorption durch Buchenholz im Temperturbereich von 110°C bis 170°C. Holz als Roh- und Werkstoff 37:99-112.

Faust, T. D. 1983. Effects of veneer surface roughness on the glue bond quality of southern pine plywood. For. Prod. Jour. 36(4):57-62.

Feldenkirchen, W. 1994. Werner von Siemens: inventor and international entrepreneur. Ohio State University Press, Columbus, Ohio. 203 pp.

Forrer, J. B. and J. W. Funk. 1998. Dielectric properties of defects on wood surfaces. Holz als Roh- und Werkstoff 56:25-29.

Gaf, Matt. 1999. Adding value through continuous production of LVL. 33rd International Particleboard / Composite Materials Symposium, Pullman, WA. pp. 165-171.

Hartshorn, L. 1949. Radio-frequency heating. George Allen & Unwin Ltd., London. 237 pp.

Haselein, C. R. 1998. Numerical simulation of pressing wood-fiber composites. PhD. Thesis, Oregon State University, Corvallis, Oregon. 244 pp.

Haygreen, J. G. and J. L. Bowyer. 1989. Forest products and wood science. 2nd Edition. Iowa State University, Ames, 500 pp.

Humphrey, P. E. 1982. Fundamentals aspects of wood particle board manufacture. Ph. D. thesis, Univ. of Wales, Bangor, U. K. 158 pp.

_____, 1994. Engineering composites from oriented natural fibres: a strategy. *In:* J. F. Kennedy, G. O. Philips, and P. A. Williams, eds. Chemistry and processing of wood and plant fibrous materials. Wrodhead Publishing, Abington, U. K. 1994. pp 213-220.

_____, 1996. Thermoplastic characteristics of partially cured thermosetting adhesive-to-wood bonds: the significance for wood-based composites manufacture. Proceedings from the Third Pacific Rim Bio-Based Composites Symposium. 1996. Dec. Kyoto, Japan. pp. 366-373.

_____. 1997. Adhesive bond strength development in pressing operations: some considerations. Proc. First European Panel Products Symposium, Llandudno, Wales, U. K. pp. 145-155.

_____ and A. J. Bolton. 1989. The hot pressing of dry-formed wood-based composites. Part II. A simulation model for heat and moisture transfer, and typical results. Holzforschung 43(3):199-206.

_____ and D. Zavala. 1989. A technique to evaluate the bonding reactivity of thermosetting adhesives. Journal of Testing and Evaluation. JTEVA. Vol. 17(6):323-328.

James, W. L. 1977. Dielectric behavior of Douglas-fir at various combinations of temperature, frequency, and moisture content. For. Prod. Jour. 27(6):44-48.

Johnson, R. S. 2000. An overview of North American wood adhesives resins. Unpublished draft paper for Georgia Pacific Resins, Inc. Decatur, GA. 23 pp.

Jung, J. 1979. Stress-wave grading techniques on veneer sheets. USDA Forest Service General Technical Report FPL-27. 10 pp.

Kamke, F. A. and L. J. Casey. Gas pressure and temperature in the mat during flake board manufacture. For. Prod. Jour. 38(3):41-43.

Klemarewski, A. and D. M. Annett. 1995. Benefits of radio frequency gluing of laminated veneer lumber. International Particleboard/Composite Materials Symposium, Washington State University, Pullman, Washington. Pp. 143 – 150.

Kauman, W. G. 1956. Equilibrium moisture content relations and drying control in super heated steam drying. For. Prod. Jour. 6(9): 328-332. *As cited in* P.E. Humphrey and A.J. Bolton 1989. The hot pressing of dry-formed wood-based composites. Part II. A simulation model for heat and moisture transfer, and typical results. Holzforschung 43(3):199-206.

Koch, P. 1966. Super-strength beams laminated from rotary peeled southern pine veneer. For. Prod. Jour. 17(6):42-48.

_____ and Woodson, G. E. 1968. Laminating butt-jointed, log-run southern pine veneers into long beams for uniform high strength. For. Prod. Jour. 18(18):45-51.

Kröner, K. and L. Pungs. 1953. Über das Verhalten des dielektrischen Verlustfaktors von Naturholz im grossen Frequenzbereich. Holzforchung 7(1):12-18.

Kunesh, R. H. 1976. Micro=Lam: Structural laminated veneer lumber. For. Prod. Jour. 28(7):41-44.

_____. 1978. Using ultrasonic energy to grade veneer. *In*: Fourth Nondestructive Testing of Wood Symposium. Washington State University, Pullman, WA. pp. 275-278.

Langton, L. 1949. Radio frequency heating equipment. Pitman Publishing, New York. 1996 pp.

Leichti, R. J., R. H. Falk and T. L. Laufenberg. 1989. Prefabricated wood I-joists: an industry overview. For. Prod. Jour. 40(3):15-20.

Lin, R. T. 1967. Review of the dielectric properties of wood and cellulose. For. Prod. Jour. 17(7):61-66.

Logan, J. D. 2000. Machine sorting of veneer for structural LVL applications. 34th International Particleboard/Composite Materials Symposium, Pullman, WA. pp. 67-77.

MacLean, J. D. 1942. The rate of temperature change in wood panels heated between hot platens. USDA FPL report 1299. Rev. 1960. *As cited in:* Bolton, A. J. and P. E. Humphrey. 1988a. The hot pressing of dry-formed wood-based composites. I. a review of the literature, identifying the primary physical processes and the nature of their interaction. Holzforschung 42(6):403-406.

Maku, T., R. Hamada, and H. Sasaki. 1959. Studies on the particleboard. Report 4. Temperature and moisture distribution in particleboard during hot pressing. Wood Research (*Kyoto*) 21:34-46. *As cited in:* Bolton, A. J. and P. E. Humphrey. 1988a. The hot pressing of dry-formed wood-based composites. I. a review of the literature, identifying the primary physical processes and the nature of their interaction. Holzforschung 42(6):403-406.

Mark, H. F. Editor. 1986. Vol. 5. Encyclopedia of polymer science and engineering. 2nd ed. John Wiley & Sons, Inc., New York. 827 pp.

Metaxas, A. C. 1996. Foundations of electroheat: a unified approach. John Wiley & Sons, New York. 500 pp.

Moody, R. C. 1972. Tensile strength of lumber laminated from 1/8-inch-thick veneers. U.S.D.A. Forest Service Research Paper FPL 181. Madison, Wis. pp. 7.

Nelson, S. 1997. Structural composite lumber. *In:* Smulski, Stephen (Ed.): Engineered Wood Products, A Guide for Specifiers, Designers and Users. PFS Research Foundation, Madison, Wis. pp. 147-155.

Neese, J. L. 1997. Characterizing veneer roughness and glue-bond performance in Douglas-fir plywood. M. S. thesis, Oregon State University, Corvallis, OR. 68 pp.

Orfeuil, M. 1987. Electric process heating: Technologies/Equipment/Applications. Battelle Press, Columbus, Ohio. 725 pp.

Pound, J. 1959. The effect of moisture on RF heating. Wood 24(11):452-455.

Resch, H. and R. Parker. Heat conditioning of veneer blocks. Forest Research Lab. Oregon State University. Corvallis, Oregon. December 1979. Research Bulletin 29.

Resnik, J., Šernek, M.and Kamke, F. 1996. High-frequency heating of wood with moisture content gradient. Wood and Fiber Sci. 29(3):264-271.

Sasaki, H., Q. Wang, S. Kawai, and R. Kader. 1990. Utilization of thinnings from Sabah (Malaysia) hard wood plantation – properties of laminated veneer lumbers and the application to flanges of composite beams with a particle web. *In*: Proc. 1990 Int'l Conf. on Processing and Utilization of Low-Grade Hardwoods and International Trade of Forest-Related Products. Taipei, Taiwan. pp. 173-182. *In*: H. Sasaki and S. Kawai. 1993. Recent research and development work on wood composites in Japan. Wood Sci. and Tech. 28:241-248.

Schuler, A. C. and C. Adair. 2000. Ch. 11: Engineered wood products—production, trade, consumption, and outlook. *In*: Forest Products Annual Market Review. 1999-2000. pp. 131-46. Geneva, Switzerland: ECE/FAO.

Schuler, A, C. Adair and E. Elias. 2001. Engineered lumber products: taking their place in the global market. For. Prod. Jour. 99(12):28 - 35.

Shao, M. 1989. Thermal properties of wood fiber networks. Masters Thesis, Oregon State University, Corvallis, Oregon. 95 pp.

Stone, J. B. and P. Robitschek. 1977. Factors effecting the performance of plywood glue extenders. For. Prod. Jour. 28(6):32-35.

Strickler, M. D. 1959. Effect of press cycles and moisture content on properties of Douglas-fir flakeboard. For. Prod. Jour. 9(7):203-215.

Terman, F. E. 1947. Radio engineering, 3rd ed.. McGraw-Hill Book Co., New York. 969 pp.

Thömen, H. 2000. Modeling the physical processes in natural fiber composites during batch and continuous pressing. PhD. Thesis, Oregon State University, Corvallis, Oregon. 187 pp.

Thömen, H. and P. E. Humphrey. 2002. Modeling the continuous pressing process for wood-based composites. Wood and Fiber Sc. 35(3):456-468.

Tipler, P. A. 1982. Physics for scientists and engineers. vol. 2. 2rd Ed. Worth Publishers, Inc., New York.

Troughton, G. E. and C. Lum. 1999. Pilot plant evaluation of steam injection pressing for LVL and plywood products. For. Prod. Jour. 50(1):25-28.

Tsoumis, G. 1991. Science and technology of wood. Chapman & Hall, New York, 494pp.

U. S. Forest Products Laboratory. 1987. Wood handbook: wood as an engineering material. Agr. Handb. 72. rev. 1987. USDA, Washington, DC. 466 pp.

U. S. Patent Office. 1973. Patent# 3,723,230: Continuous press for pressing glue-coated consolidatable, press charges.

U. S. Product Standard. 1995. PS 1-95 for Construction and Industrial Plywood. National Bureau of Standards, Department of commerce, Government Printing Office. Washington, D. C.

Vainikainen, P. V., E. G. Nyfors and M. T. Fischer. 1987. Radio-wave senor measuring the properties of dielectric sheets: application to veneer moisture content and mass per unit area measurement. Institute of Electrical and Electronic Engineers. Transactions on Instrumentation and Measurement, IM-36(4), Piscataway, NJ.

Vermaas, H. F., J. Pound, and B. Borgin. 1974. The loss tangent of wood and its importance in dielectric heating. South African Forestry Jour. 89:5-8. (as cited in Resnik 1996).

Vlosky, R. P., Smith, P. M. and Blankenhorn, P. R. 1993. Laminated veneer lumber: a United States market overview. Wood and Fiber Sci. 26(4):456-466.

Wang, J., J. M. Biernacki and F. Lam. 1998. Nondestructive evaluation of veneer quality using acoustic wave measurements. Wood Sci. and Tech. 34:505-516.

Wangaard, F. F., 1968. Heat Transmissivity of Southern Pine wood, plywood, fiberboard and particleboard. Wood Science 2(1):54-60.

Wellons, J. D. 1979. Wettability and gluability of Douglas-fir veneer. For. Prod. Jour. 30(7): 53-55.

_____. and R. L. Krahmer, M. D. Sandoe, and R. W. Jokerst. 1982. Thickness loss in hot-pressed plywood. For. Prod. Jour. 33(1):27-34.

Whitehouse, A. A. K., E. G. K. Pritchett and G. Barnett. 1955. Phenolic rResins 2nd ed. Plastics Institute. Iliffe Books LTD, London, 149 pp.

Zavala, D. Z. 1987. Analysis of processes operative within plywood during hot pressing. Ph. D. thesis, Oregon State Univ., Corvallis, Oregon. 201 pp.

_____ and P. E Humphrey. 1996. Hot pressing veneer-based products: The interaction of physical processes. For. Prod. Jour. 46(1):69-77.

APPENDICES

APPENDIX A

Effect of Adhesive Quantity on Bond Strength Value

In order to determine if the adhesive spread rate is correlated to the resultant bond strength development of adhesive tested with the ABES testing method described in Chapter 4, tests were conducted as described below.

The ABES machine was set to a 120 °C platen temperature to give a fairly rapid cure based on prior testing experience. Pressing time was set to 75 seconds so that significant, but not maximum, bond strength would develop based on prior testing results. Pressing pressure was maintained at 0.15 MPa. The bond strength of 30 test samples were tested in shear mode, as described in Chapter 4, using the same adhesive tested for bond strength reported on there (GP 272A79).

Ten of the samples had a "normal" adhesive spread of 184 g/m^2 as described in Section 4.2.1.2. Ten samples were prepared with a "heavy" adhesive spread of approximately 370 g/m^2. On these samples, the adhesive began to run to the bottom edge when the sample was turned edgewise. Ten samples had a "light" spread of approximately 90 g/m^2. On these light samples the adhesive was just thick enough to cover the wooden sample. This was achieved by placing adhesive on the sample overlap area and then scrapping off nearly all the resin with a wooden spatula. All bonds were tested in the ABES machine immediately after the adhesive was applied.

Table A.1 contains the results of this testing. One can see from this table that there is a maximum difference of 0.13 MPa between the different adhesive spreads. It is interesting to note that the extreme adhesive spreads are very close (0.05 MPa), while it is the "normal" spread that has the lowest bond strength average. However, if the extreme high and low values are removed from the results of each of the adhesive spread levels, as in Table A.2, the bond strength averages are virtually identical. It would seem that unusually high or low results were produced about 20% of the time, perhaps from the variability of the wood samples used. It is concluded from these results that changes in the adhesive spread rate are not strongly correlated to changes in the bond strengths of the test samples for this adhesive formula.

Table A.1 Results of bond strength testing on ABES machine with 3 different spread rates.

	SPREAD RATE		
Sample Number	Heavy MPa	Light MPa	Normal MPa
1	4.63	4.62	4.48
2	5.04	4.73	5.00
3	4.77	4.97	4.69
4	4.83	4.60	4.92
5	4.57	4.74	4.62
6	4.44	4.69	5.34
7	4.55	5.85	4.69
8	4.95	5.02	4.94
9	5.51	4.65	4.11
10	4.80	4.78	4.52
Avg.	**4.81**	**4.86**	**4.73**

Table A.2 Bond strength test results from the 3 different adhesive spread rates with the highest and lowest values for each rate removed (indicated by ##).

	SPREAD RATE		
Sample Number	Heavy MPa	Light MPa	Normal MPa
1	4.63	4.62	4.48
2	5.04	4.73	5.00
3	4.77	4.97	4.69
4	4.83	##	4.92
5	4.57	4.74	4.62
6	##	4.69	##
7	4.55	##	4.69
8	4.95	5.02	4.94
9	##	4.65	##
10	4.80	4.78	4.52
Avg.	**4.77**	**4.77**	**4.73**

APPENDIX B

Table B.1 Variation of relative humidity (%) with the equilibrium moisture content (EMC) of wood and temperature. This table is based on data presented by Engelhardt (1979) with added interpolations between his data points to provide finer resolution.

TEMPERATURE (°C)

OD MOISTURE CONTENT	20	25	30	35	40	45	50	55	60	65	70	75	80	85	90
4.0	21.5	22.4	23.3	24.1	25.0	26.0	27.0	28.0	29.0	30.5	32.0	33.5	35.0	36.6	38.3
4.5	25.0	26.0	27.0	28.0	29.0	30.1	31.2	32.3	33.4	34.9	36.4	38.0	39.5	41.2	42.8
5.0	28.5	29.6	30.8	31.9	33.0	34.2	35.4	36.6	37.8	39.3	40.9	42.4	44.0	45.7	47.4
5.5	32.0	33.3	34.5	35.8	37.0	38.3	39.6	40.8	42.1	43.7	45.3	46.9	48.5	50.2	51.9
6.0	35.5	36.9	38.3	39.6	41.0	42.4	43.8	45.1	46.5	48.1	49.8	51.4	53.0	54.8	56.5
6.5	38.5	39.9	41.3	42.6	44.0	45.5	46.9	48.4	49.9	51.5	53.1	54.8	56.4	58.1	59.8
7.0	41.5	42.9	44.3	45.6	47.0	48.6	50.1	51.7	53.3	54.9	56.5	58.1	59.8	61.4	63.0
7.5	44.5	45.9	47.3	48.6	50.0	51.7	53.3	55.0	56.6	58.3	59.9	61.5	63.1	64.7	66.3
8.0	47.5	48.9	50.3	51.6	53.0	54.8	56.5	58.3	60.0	61.6	63.3	64.9	66.5	68.0	69.5
8.5	49.9	51.3	52.8	54.3	55.8	57.5	59.3	61.0	62.8	64.3	65.9	67.4	69.0	70.4	71.8
9.0	52.3	53.8	55.4	56.9	58.5	60.3	62.0	63.8	65.5	67.0	68.5	70.0	71.5	72.8	74.1
9.5	54.6	56.3	57.9	59.6	61.3	63.0	64.8	66.5	68.3	69.7	71.1	72.6	74.0	75.2	76.4
10.0	57.0	58.8	60.5	62.3	64.0	65.8	67.5	69.3	71.0	72.4	73.8	75.1	76.5	77.6	78.8
10.5	59.3	61.0	62.8	64.5	66.3	67.9	69.6	71.3	73.0	74.3	75.6	76.9	78.3	79.3	80.3
11.0	61.5	63.3	65.0	66.8	68.5	70.1	71.8	73.4	75.0	76.3	77.5	78.8	80.0	80.9	81.9
11.5	63.8	65.5	67.3	69.0	70.8	72.3	73.9	75.4	77.0	78.2	79.4	80.6	81.8	82.6	83.4
12.0	66.0	67.8	69.5	71.3	73.0	74.5	76.0	77.5	79.0	80.1	81.3	82.4	83.5	84.3	85.0

TEMPERATURE (°C)

OD MOISTURE CONTENT	95	100	105	110	115	120	125	130	135	140	145	150	155	160
4.0	39.9	41.5	43.1	44.8	46.4	48.0	49.5	51.0	52.5	54.0	55.3	56.5	57.8	59.0
4.5	44.5	46.1	47.7	49.3	50.8	52.4	53.8	55.3	56.7	58.1	59.3	60.4	61.6	62.8
5.0	49.1	50.8	52.3	53.8	55.3	56.8	58.1	59.5	60.9	62.3	63.3	64.4	65.4	66.5
5.5	53.7	55.4	56.8	58.3	59.7	61.1	62.4	63.8	65.1	66.4	67.3	68.3	69.3	70.3
6.0	58.3	60.0	61.4	62.8	64.1	65.5	66.8	68.0	69.3	70.5	71.4	72.3	73.1	74.0
6.5	61.4	63.1	64.4	65.8	67.1	68.4	69.5	70.7	71.8	73.0	73.8	74.6	75.4	76.3
7.0	64.6	66.3	67.5	68.8	70.0	71.3	72.3	73.4	74.4	75.5	76.3	77.0	77.8	78.5
7.5	67.8	69.4	70.6	71.8	72.9	74.1	75.1	76.1	77.0	78.0	78.7	79.4	80.1	80.8
8.0	71.0	72.5	73.6	74.8	75.9	77.0	77.9	78.8	79.6	80.5	81.1	81.8	82.4	83.0
8.5	73.2	74.6	75.7	76.8	77.8	78.9	79.7	80.5	81.3	82.1	82.7	83.3	83.9	84.5
9.0	75.4	76.8	77.8	78.8	79.8	80.8	81.5	82.3	83.0	83.8	84.3	84.9	85.4	86.0
9.5	77.7	78.9	79.8	80.8	81.7	82.6	83.3	84.0	84.7	85.4	85.9	86.4	87.0	87.5
10.0	79.9	81.0	81.9	82.8	83.6	84.5	85.1	85.8	86.4	87.0	87.5	88.0	88.5	89.0
10.5	81.3	82.4	83.2	84.0	84.8	85.6	86.2	86.8	87.4	88.0	88.5	89.0	89.5	90.0
11.0	82.8	83.8	84.5	85.3	86.0	86.8	87.3	87.9	88.4	89.0	89.5	90.0	90.5	91.0
11.5	84.3	85.1	85.8	86.5	87.2	87.9	88.4	88.9	89.5	90.0	90.5	91.0	91.5	92.0
12.0	85.8	86.5	87.1	87.8	88.4	89.0	89.5	90.0	90.5	91.0	91.5	92.0	92.5	93.0